



Multifocal VEP and ganglion cell damage: applications and limitations for the study of glaucoma

Donald C. Hood^{a,*}, Vivienne C. Greenstein^b

^aDepartment of Psychology, Columbia University, New York, NY 10027-7004, USA

^bDepartment of Ophthalmology, Columbia University, New York, NY 10032, USA

Abstract

With the multifocal technique, visual evoked potentials (VEPs) can be recorded simultaneously from many regions of the visual field in a matter of minutes. Recently, the multifocal visual evoked potential technique (mfVEP) has generated considerable interest, especially among those seeking objective measures of glaucomatous damage. It is well accepted that significant ganglion cell damage can occur before functional deficits are detected with static automated achromatic perimetry, the “gold standard” for detecting and monitoring glaucomatous damage. In this article, we ask the following questions: What are the potential applications of the mfVEP technique? What are its limitations? To what extent will it replace or augment static automated achromatic perimetry? To answer these questions requires an understanding of the mfVEP technique, as well as techniques needed to relate its results to those of automated perimetry. Section 2 describes how the mfVEP is elicited, recorded, derived and displayed. If both eyes of an individual are normal, then mfVEPs recorded for monocular stimulation of each eye are essentially identical. However, the amplitude and waveform of the mfVEP responses vary across individuals, as well as across the visual field within an individual. These variations in the normal mfVEPs are described in Section 3. In Section 4, these variations are related to cortical anatomy, and to the cortical sources contributing to the mfVEP. The mfVEP is predominantly generated in V1. Although there are undoubtedly extrastriate contributions, these contributions are probably smaller for the mfVEP than for the conventional VEP. The mfVEP is not a small version of the conventional VEP. To detect ganglion cell damage with the mfVEP requires methods for analyzing the responses and for displaying the results. In Section 5, a method for detecting ganglion cell damage is described. This method compares the monocular responses from the two eyes of an individual and produces a map of the defects. This map is in the form of a probability plot similar to the one used to display visual field defects measured with automated perimetry. Procedures are described for directly comparing these mfVEP probability plots to the probability plots for Humphrey visual fields (HVF). The interocular mfVEP test described in Section 5 will not be sensitive to bilateral damage. Section 6 describes a test based upon monocular mfVEPs. The statistical basis of the monocular mfVEP test is relatively complex (see Section 9). In any case, under many conditions the interocular test will be more sensitive and this is discussed in Section 7. Section 8 summarizes a number of clinical applications of the mfVEP and concludes that the mfVEP has a place in the clinical management of glaucoma. To understand the limitations of the mfVEP, a signal-to-noise ratio (SNR) approach is described in Section 9. Using the techniques described in Section 9, the relationship between the amplitude of the mfVEP and the sensitivity loss of the HVF is discussed in Section 10. The evidence supports a simple model in which the amplitude of the signal portion, but not the noise portion, of the mfVEP response is proportional to HVF loss where HVF loss is expressed in linear, not dB, units. It is hypothesized that both the signal in the mfVEP, and the sensitivity of the HVF, are linearly related to ganglion cell loss. A theoretical approach, developed in Section 11, allows a direct comparison of the efficacy of the mfVEP and HVF in detecting glaucomatous damage. In short, when the mfVEP has a large SNR it will often be superior to the HVF in detecting damage. On the other hand, when the mfVEP has a small SNR, the HVF will probably be superior. Section 12 summarizes the relative advantages of the HVF and the mfVEP. In summary, the mfVEP does have a place in the clinical management of glaucoma, although it is not likely to replace static automated achromatic perimetry in the near future. However, this is an evolving technology and the future will undoubtedly see major improvements in the mfVEP technique. © 2003 Elsevier Science Ltd. All rights reserved.

*Corresponding author. Tel.: +1-212-222-7984.

E-mail addresses: dch3@columbia.edu (D.C. Hood).

Contents

1.	Introduction	203
1.1.	Background	203
1.2.	A guide to this article	203
2.	Recording mfVEPs	204
2.1.	Stimulus display	204
2.2.	Displaying the responses	204
2.3.	Placement of electrodes	204
2.3.1.	Single channel recording	204
2.3.2.	Multiple channel recording	206
2.4.	Single vs. multiple channel recording	206
2.5.	Choice of amplifier cutoffs	209
2.6.	How are the mfVEP responses derived?	209
2.7.	Spatial resolution	209
3.	Variations in the normal mfVEP	211
3.1.	Variations between eyes	211
3.2.	Variations across individuals	211
3.3.	Variations across the field	211
4.	Relating mfVEPs to traditional VEPs and cortical anatomy	212
4.1.	Are the mfVEPs “little” VEPs?	212
4.2.	Where is the mfVEP generated?	214
5.	Detecting ganglion cell damage with the mfVEP	214
5.1.	Humphrey visual field	214
5.2.	Qualitative comparisons of mfVEP and HVF topographies	215
5.3.	Two eyes can be better than one	217
5.4.	Measuring the amplitude or size of the response	217
5.5.	mfVEP probability plot: interocular comparisons	217
5.6.	Comparing HVF and mfVEP probability plots	217
5.7.	Interocular HVF	218
6.	Bilateral damage and the need for a monocular test	218
6.1.	Need for a monocular test: bilateral damage	218
6.2.	Monocular mfVEP test	219
7.	Need for both interocular and monocular tests	221
8.	mfVEP in the clinical management of glaucoma: possible applications	221
8.1.	Unreliable HVFs	221
8.2.	Questionable or inconsistent HVFs	222
8.3.	Confirmation of HVF results	224
8.4.	Detecting early damage and progression	225
9.	Understanding the monocular mfVEP test (advanced topic)	227
9.1.	How can a monocular test work?	227
9.2.	Need for a signal-to-noise ratio	227
9.3.	Noise window as a proxy for a total defect	229
9.4.	Individual variations in SNR: distinguishing false positives from true defects	230
9.5.	Test of the monocular test	232
10.	Relationship between mfVEP amplitudes and HVF sensitivities (advanced topic)	234
10.1.	Need for a theoretical understanding	234
10.2.	Interpolated field	235
10.3.	Monocular amplitudes as a function of HVF defects	235
10.4.	Detecting unreliable visual fields with large mfVEP responses	235
10.5.	Interocular mfVEP ratios as a function of HVF defects	237
10.6.	mfVEP signal is proportional to HVF loss: a simple model	237
10.7.	Are mfVEP signals and HVF sensitivity losses proportional to ganglion cell loss?	239

11. Will the mfVEP or the HVF be better at detecting damage? A theoretical approach (advanced topic) . . .	240
11.1. Detecting damage with interocular mfVEP comparisons	240
11.2. Detecting damage with monocular mfVEP comparisons	241
11.3. Comparison of the efficacy of the monocular and interocular mfVEP tests	243
11.4. Detecting progression and the repeat reliability of the mfVEP	243
12. Summary of the relative advantages of the mfVEP and HVF	244
12.1. Confidence in test	245
12.1.1. Unreliable or questionable HVFs.	245
12.1.2. Poor mfVEP producers	245
12.2. Size of mfVEP signal	245
12.3. Type of damage	245
12.4. Size and location of defect	246
12.5. Latency	246
12.6. Testing time	246
12.7. Problems in common	247
12.7.1. Poor fixation	247
12.7.2. Pupil size, refractive error and cataracts	248
12.7.3. “Reliability” indices	248
13. Conclusion and future directions.	249
Acknowledgements	249
References	249

1. Introduction

1.1. Background

The visual evoked potential (VEP) is a gross electrical potential generated by the cells in the occipital cortex. It is easily recorded with scalp electrodes and provides an objective and reproducible measure of the function of the visual pathways up to and including the visual cortex (see Regan, 1989 for a review). For over 40 yr, the VEP has been used to diagnose and study diseases of the visual system (see Sokol, 1976; Brigell, 2001 for a review). However, it has been of limited use in the study of glaucoma. The reason is simple. The VEP does not provide a topographical measure and glaucomatous damage often involves localized regions of the retina. In principle, this limitation could be overcome by obtaining VEPs at different retinal locations but this would be too time consuming. A new VEP method (Baseler et al., 1994), based upon multifocal technology (Sutter, 1991), circumvents this problem. With the multifocal VEP (mfVEP) technique, many (typically 60) spatially local VEP responses can be recorded simultaneously allowing spatially localized damage to be identified.

Although the mfVEP has been used to study a variety of diseases of the optic nerve/ganglion cells including optic neuritis/multiple sclerosis (e.g. Hood et al., 2000a; Kardon et al., 2001; Betsuin et al., 2001; see Hood et al., 2003a for a review), the clinical focus of this review is the detection of ganglion cell damage secondary to glaucoma. Automated achromatic perimetry is generally accepted as the “gold standard” for detecting glauco-

matous damage. However, there are problems with this visual field technique. For some patients it is very difficult, or even impossible, to obtain reliable visual field measures. In addition, significant loss of ganglion cells can occur prior to the development of visual field loss (e.g. Quigley et al., 1982, 1989; Kerrigan-Baumrind et al., 2000; see review by Quigley, 1999). The multifocal electroretinogram (mfERG) has failed thus far to reliably detect local ganglion cell damage (see Hood, 2000; Hood et al., 2003b for a review of the mfERG). On the other hand, the mfVEP has been proposed as a solution to these problems. Local damage can be visualized in mfVEP recordings (e.g. Klistorner et al., 1998; Graham et al., 2000; Hood et al., 2000b; Hood and Zhang, 2000; Betsuin et al., 2001; Hasegawa and Abe, 2001), but it is not yet clear to what extent the mfVEP will either replace or augment the information obtained with static automated perimetry.

In this article, we ask the following questions: What are the potential applications of the mfVEP technique? What are its limitations? To what extent will it replace or augment automated perimetry? To answer these questions requires information not only about the mfVEP technique but also about the techniques needed to relate its results to those of automated perimetry. The purpose here is to supply this information and then to consider the potential applications and limitations of the mfVEP.

1.2. A guide to this article

This article contains elementary and introductory material as well as a discussion of advanced, and

technically more challenging topics. Those seeking an introduction to the use of the mfVEP in the clinic should read Sections 2, 5–8 and 12. Those interested in a deeper understanding of the issues underlying the relative advantages of the mfVEP and automated perimetry should read all sections, including the basic material in Section 2 as it provides some of the details needed to understand the advanced topics. It is important to note that most of the problems involved in validating the usefulness of the mfVEP are inherent to all tests, including the new structural measurements of nerve fiber thickness (e.g. OCT and HRT). In this context, this article provides a general methodology for validating new techniques as well as comparing their results to standard automated perimetry.

2. Recording mfVEPs

2.1. Stimulus display

Currently there is no standard display for the mfVEP technique. However, most of the mfVEP recordings to date have been obtained with a dartboard pattern like the one shown in Fig. 1A. This pattern is a standard option (Dart Board 60 With Patterns) of the VERIS software (EDI, San Mateo, CA). A modified version of this pattern has recently been introduced as part of the AccuMap system (ObjectiVision Pty, Ltd., Sydney, Australia). The modification was based upon the work of Graham, Klistorner and colleagues (e.g. Goldberg et al., 2002). For the work from our group reviewed in this article, the dartboard pattern was presented on a monitor viewed at a distance of 32 cm; the diameter of the display subtended 44.5° . As can be seen in Fig. 1A, there are 60 sectors in this display and each sector contains 16 checks, 8 black and 8 white. The sectors, and the checks, are scaled to be of approximately equal effectiveness, based upon cortical magnification factors (Baseler et al., 1994). For example, the inner-most sectors are about 1.2° in width while the outer-most sectors exceed 7° in width. Our display is viewed through an optical system with a camera (EDI, San Mateo, CA), which allows for the monitoring of eye position and the correction of spherical refractive errors (about ± 5 diopters). Some investigators have recorded mfVEPs with the display used for mfERG recordings (e.g. Hasegawa and Abe, 2001). This is not a good idea as the sectors in this stimulus are optimized for retinal cell density rather than cortical scaling. The peripheral sectors will produce very small responses. In addition, in this display, there are sectors that cross the horizontal midline. These sectors produce responses of opposite polarity which cancel yielding a small response (see Section 3.3 and Figs. 1B, D and E).

2.2. Displaying the responses

The mfVEPs in Fig. 1B are the averaged responses from 30 normal subjects. The color here, and in subsequent figures, indicates the mfVEP responses from monocular stimulation of the left (red) and right (blue) eyes. The pairs of responses are associated with the 60 locations in the visual field. It is important to note, however, that the 60 pairs of responses are arbitrarily placed in this figure. This is a common practice as linear coordinates would lead to considerable overlap of the responses from the central regions. The colored “circles” in Fig. 1B represent circles with radii of 2.6° (red), 9.8° (blue) and 22.25° (green). The need for the arbitrary scaling in Fig. 1B is obvious. Note, for example, that the center 12 responses come from an area subtending 5.2° in diameter or 2.6° in radius. [In this article, the phrase “central X° ” will mean the central region with a radius of X° (a diameter of $2X^\circ$).].

The 60 mfVEP responses can be grouped and summed both for display purposes and to improve the signal-to-noise of the records, provided the loss of spatial resolution can be tolerated. Fig. 1C shows the display divided into 16 groups. Each group consists of 4 sectors except for the center 4 groups where each is made up of 3 sectors. [On average, the waveforms within each of these groups are similar (Hood and Zhang, 2000; Klistorner and Graham, 2000).] The grouped responses from the same 30 normals as in Fig. 1B are shown in Fig. 1D.

2.3. Placement of electrodes

2.3.1. Single channel recording

Typically, the mfVEP is recorded with two midline electrodes (the so-called bipolar recording) serving as the active and reference with a third electrode, the ground, on the forehead or ear. A variety of midline placements have been used. The lower electrode has been placed anywhere from 1 cm above the inion (i) to 6 cm below the inion (e.g. Baseler et al., 1994; Graham et al., 2000). In our recordings, electrodes are placed on the inion (reference) and 4 cm above the inion (active) with a forehead electrode as the ground. The position of our active electrode was chosen based upon mfVEP recordings (e.g. Hood et al., 2000b and unpublished observations) as well as upon anatomical considerations (Hood and Zhang, 2000). In a study of 50 normal MRI scans we found that a line through the calcarine fissure intersected the skin anywhere from 1.5 cm below the inion to 3.5 cm above (see Figs. 8 and 9 in Hood and Zhang, 2000). Fig. 2A shows the positions of the two midline electrodes marked on an MRI as A (active) and R (reference). In this individual, a line through the calcarine fissure intersected the skin approximately at the electrode placed at the inion i. The dashed lines show

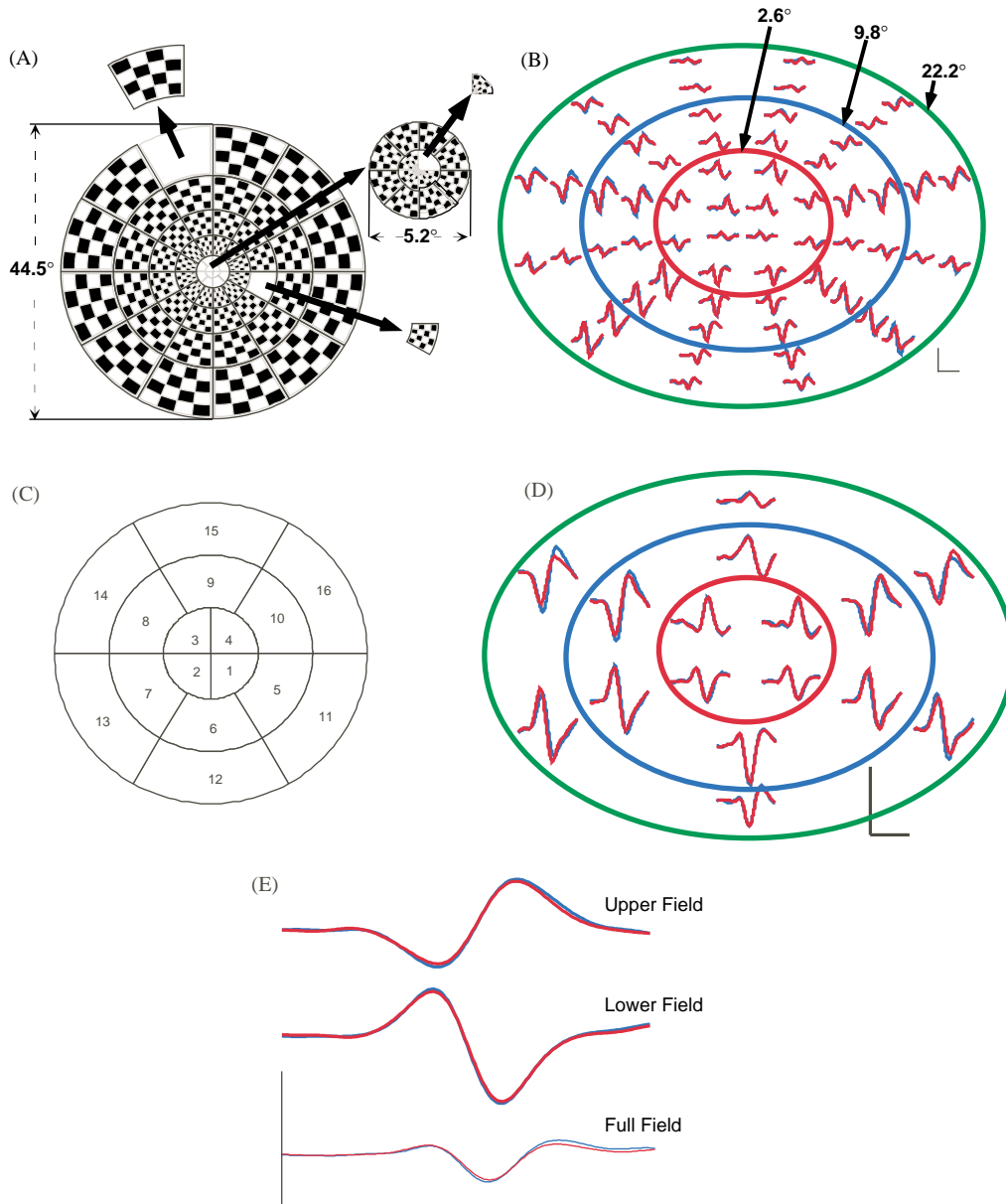


Fig. 1. (A) The mfVEP display with 60 scaled sectors. (B) The averaged mfVEP responses from the right (blue) and left (red) eyes of 30 control subjects for 60 sectors. The colored circles have radii of 2.6° (red), 9.8° (blue), and 22.2° (green). (C) The mfVEP display divided into 16 groups. Each group includes 4 sectors, except for the center 4 groups which include 3 sectors. (D) The averaged mfVEP responses from the 30 controls summed by the 16 groups shown in panel C. (E) The responses from panel B summed and averaged separately for the upper and lower field and summed and averaged for the entire field. The calibration bars in panels B, D, and E indicate 200 nV and 100 ms.

the range of calcarine locations for all 50 subjects (see also Steinmetz et al., 1989). There is substantial variation among individuals in the location of the inion with respect to the calcarine fissure. Placing the upper electrode at 4 cm above the inion assures that it is above the calcarine in nearly all individuals. The lower electrode is placed at the inion, the lowest point at which we can get stable electrode placement while minimizing electrical noise from movement of the neck muscles.

In their most recent work, Graham and Klistorner place their midline electrodes 3 cm above, and 4.5 cm below, the inion. They built a special holder to maintain the electrodes in position (Klistorner and Graham, 2000). In a recent study, we compared our electrode placements to theirs in 10 normal control subjects (Gallagher et al., 2002) and found, on average, that our configuration produced better records (higher signal-to-noise ratios). Their placement of the upper electrode, at 3 cm, is probably too low to obtain optimal recordings

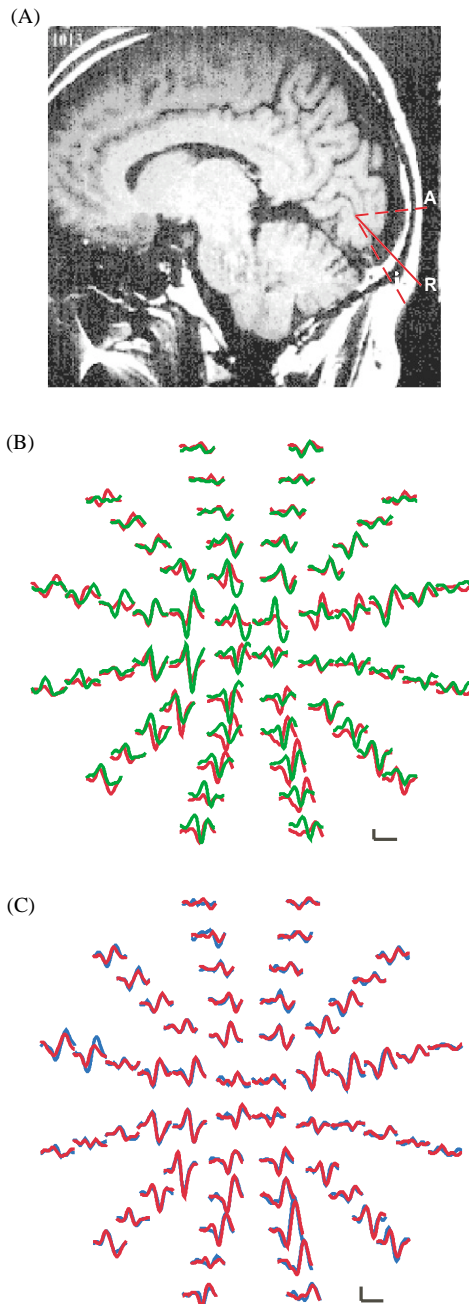


Fig. 2. (A) Mid-sagittal MRI showing the placement of the two midline electrodes for the mfVEP. The dashed lines represent the range of calcarine locations for 50 subjects. (B) mfVEP responses obtained from the left eye of two control subjects. (C) mfVEP responses obtained from the left (red) and right (blue) eyes of the control subject whose responses for the left eye are shown in red in panel B. The calibration bars in panels B and C indicate 200 nV and 100 ms.

from an individual with a relatively high calcarine fissure. In addition, the placement of the lower electrode on the nape of the neck makes it more difficult to avoid noise from neck muscles. Turning their holder upside down so that the upper electrode is now 4.5 cm above the inion produces results very similar to ours. In summary, we recommend either using our method or

their holder turned upside down. Regardless of the method used, as with all EEG recordings, it is very important to assure that the electrode placement is stable and that the resistance is low. Further, if you intend to follow patients over time, then it is critical to place the electrodes in the same position each time you test the patient (see Section 11.4).

2.3.2. Multiple channel recording

Klistorner and Graham (2000) were the first to point out that the mfVEP responses can be small in the center of the field as well as along the midline. This can be seen in the averaged records in Fig. 1B as well as in some of the subsequent figures. In the averaged responses of Fig. 1B, the responses just below the horizontal meridian are considerably smaller than those above. Klistorner and Graham (2000) found that electrodes placed lateral to the inion often improved the signal in these regions (see also Hood et al., 2002a). Fig. 3A shows the 4 channels employed by Klistorner and Graham. Following their example, we placed additional electrodes 4 cm lateral to the midline. We record from 3 channels and, with software, derive the recordings that would result from three other channels, including the channels used by Klistorner and Graham. This technique effectively produces 6 channels of recording. Fig. 3B shows the 3 channels we record (black arrows) and the three that we derive (gray arrows) from the records of channels 1–3.

2.4. Single vs. multiple channel recording

Fig. 4 (modified from Hood et al., 2002a) shows the records from an individual whose responses showed improvement with multi-channel recording. The three recorded channels are shown in panel A with the midline channel (channel 1) in the leftmost panel. Fig. 4B shows the responses for the three derived channels. It is clear that the responses for many sectors are smaller in the midline channel than in one or more of the other channels.

The advantage of the multi-electrode recording for this subject is easier to see in Fig. 5A where the responses from the midline channel are compared to the array of “best responses”. To obtain an array of the best responses one needs a definition of “best”. Klistorner and Graham selected the largest response based on a measurement of peak-to-trough amplitude. We define the best response as the response with the largest signal-to-noise ratio (SNR). The SNR of the “best response” has certain advantages (Zhang et al., 2002), which will be explained in Section 9. [Note: As described below, when the responses from the two eyes are compared, they are always from the same channel. In this case, the “best” channel is the channel at each

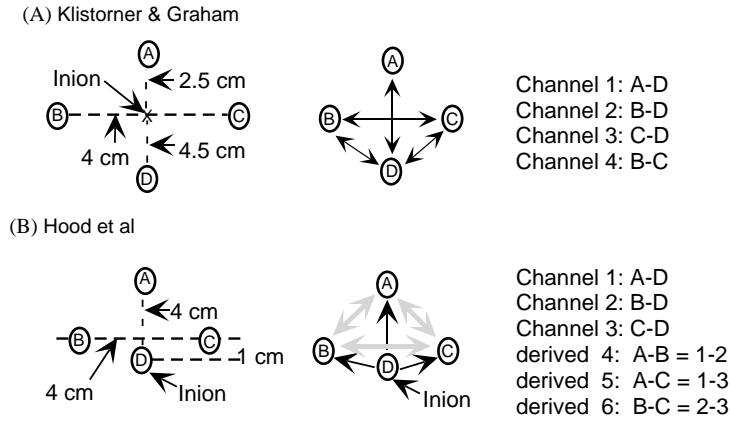


Fig. 3. (A) The 4 channels recorded by Klistorner and Graham (2000). (B) The 3 channels recorded by Hood et al. (2002a). The black arrows indicate the 3 channels that are recorded, and the gray arrows indicate three additional channels derived with software.

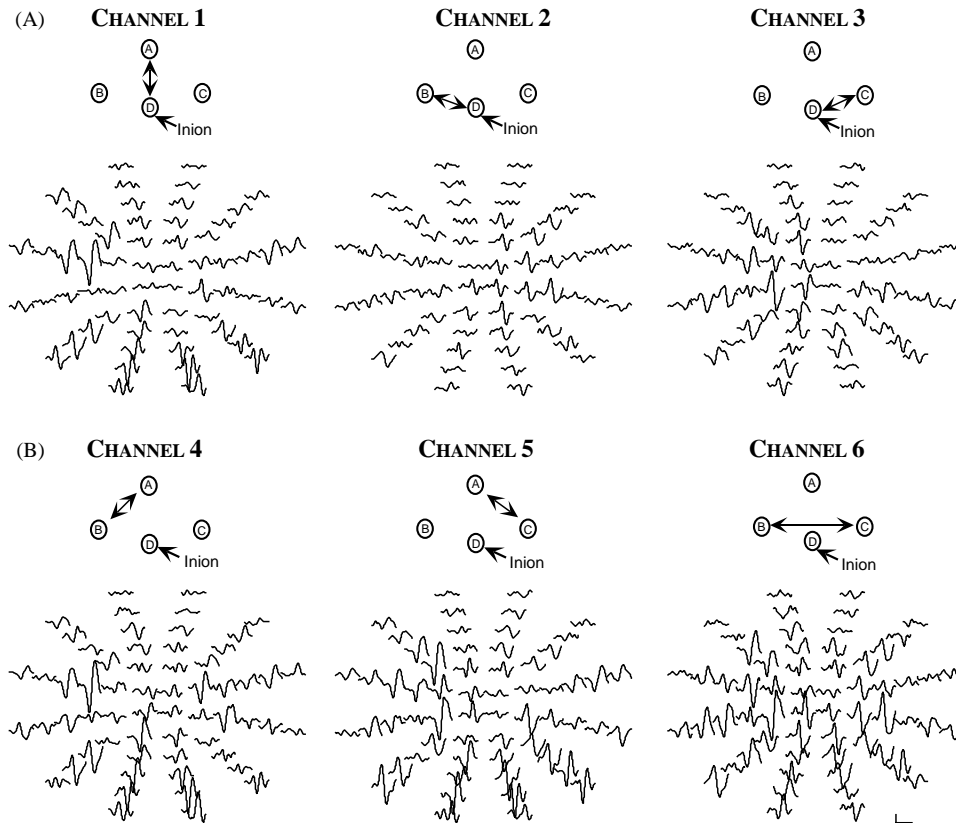


Fig. 4. (A) mfVEP responses of a control subject for the 3 channels that are recorded. (B) mfVEP responses for the three derived channels. The calibration bar indicates 200 nV and 100 ms.

location that produces the largest SNR of the 12 responses (2 eyes \times 6 channels).]

For subject C1, Fig. 5A (left panel) shows the response array from the midline channel (channel 1 from Fig. 4A) and the response array from the “best of channels”(right panel). As noted by Klistorner and Graham (2000), the responses from the midline channel can be small along the lower horizontal meridian and

multi-electrode recording can improve the amplitude of these responses. For C1, the best response is clearly larger than the midline response in the center (gray ellipse) and along the horizontal meridian (e.g. black ellipses). Figs. 5B and C show the arrays for two other control subjects. In these subjects, the additional channels produced less impressive improvements. In the case of C2 (Fig. 5B), the midline channel already

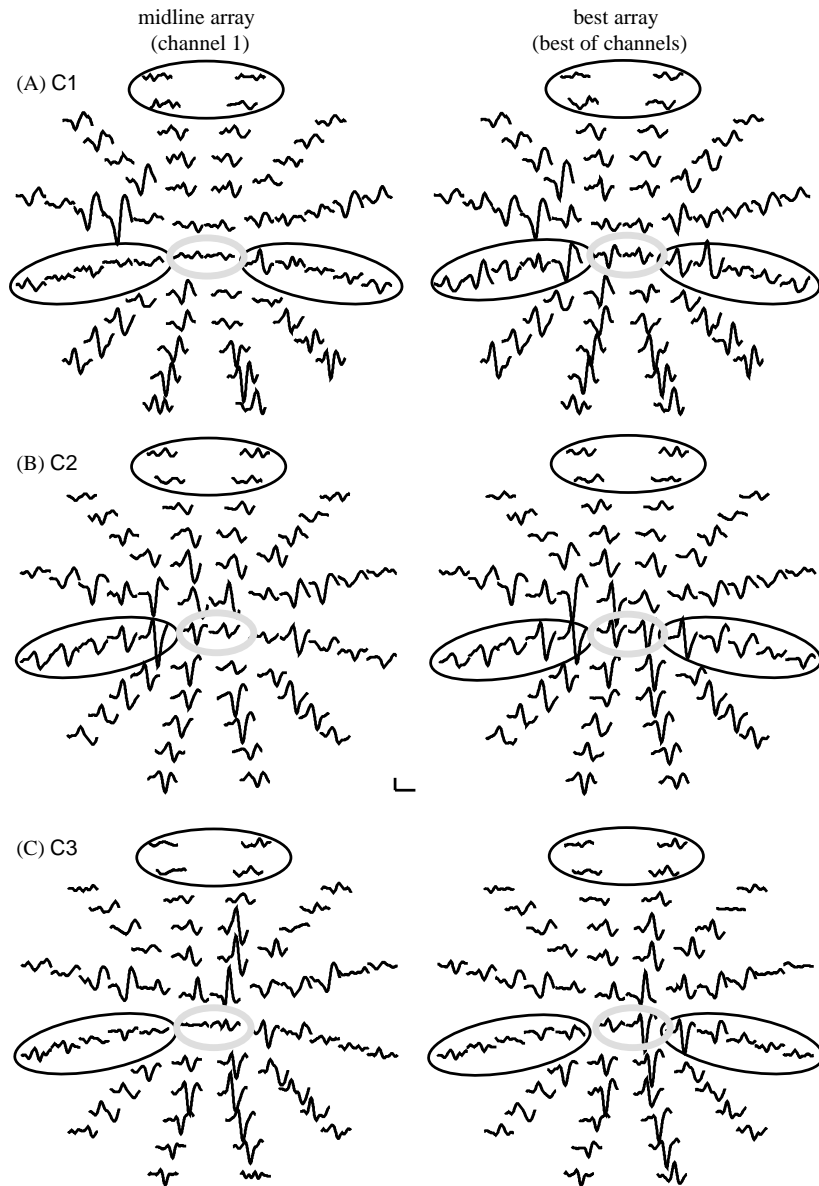


Fig. 5. (A) A comparison of the mfVEP response array from the midline channel (left-hand panel) to the best response array (right-hand panel) for a control subject (C1). (B and C) As above for two other control subjects (C2, C3). The calibration bar indicates 200 nV and 100 ms.

yielded reasonable responses. Although the best array shows larger responses (see central gray ellipse) in some locations, the improvement is less prominent than in the case of C1. Subject C3 (Fig. 5C) also showed less improvement than C1, but in this case the responses are small along the horizontal meridian even in the best array. In sum, for many individuals, multi-channel recording can improve the amplitude of the responses recorded from the lower horizontal meridian including those in the center (gray ellipses). However, the responses in the midline of the upper field (upper ellipses) are small for both the midline channel and the best channel. As we will see, this finding makes it

difficult to detect defects in this region of the superior visual field.

Is it worth the time and trouble of recording multiple channels? This is a cost benefit analysis. The costs involve the time in placing extra electrodes (a few minutes) and the time and software needed to analyze the additional data. A quantitative evaluation of the benefits of added electrodes is provided in Hood et al. (2002a). This study concluded that if two additional electrodes are added it is worth obtaining 6 channels of data. This can be done with 6 amplifiers, if available, or with 3 amplifiers and offline analysis as described above and in Hood et al. (2002a). Further, the results in Fig. 5

suggest that the configuration employed by Klistorner and Graham would be improved by obtaining the equivalent to our channels 4 and 5 offline.

2.5. Choice of amplifier cutoffs

Most mfVEP recordings to date have been made with the high and low pass filters set to 3 and 100 Hz, the settings generally used for the full-field VEP. In their most recent work, Klistorner and Graham (2001) employed a low pass setting of 30 Hz. This is a hardware filter so it is actually reducing the signal at 30 Hz by 3 dB and, of course, passing some signal above 30 Hz as well as reducing the signals below 30 Hz. They point out that a 30 Hz cutoff is below the ISCEV recommendation of 100 Hz (Harding et al., 1996), but in their experience this cutoff has a minimal effect on the responses, increasing latencies by 2–3 ms while leaving amplitude unchanged. We have used a software filter (fast Fourier transform technique) that provides a sharp cutoff. We find that a sharp cutoff at 35 Hz provides the best results and has relatively little effect on amplitude or latency. Fig. 6A shows mfVEP responses, grouped as in Fig. 1C, from a patient with a considerable amount of noise presumably due to muscle tension since the electrode resistance was low (i.e. below 2 k Ω). This patient with glaucoma had deficits mainly in the left eye. Notice that after filtering (Fig. 6B), it is easier to see that the responses (red) from the left eye are smaller than those (blue) from the right. The low pass filter will, however, change the waveforms. Fig. 6C shows the same averaged responses from the 30 normal subjects as in Fig. 1D but without the 35 Hz filter. The high frequency detail seen on the leading edge of the first prominent component is lost when filtered at 35 Hz. This is easier to see in Fig. 6D (arrow) where the hemifield responses from the right eye (green) without filtering are shown together with those filtered at 35 Hz (black) from Fig. 1E. If high frequency information is of interest, the low pass filter should be set to 100 Hz.

2.6. How are the mfVEP responses derived?

Although the recording of the mfVEP is the same as for the traditional VEP, both the stimulus and the method of deriving the responses are different. In the typical mfVEP technique, each sector is an independent stimulus. It goes through a random sequence where on every frame change (13.3 ms) it can reverse contrast or stay the same (see Fig. 7A). In the traditional pattern reversal VEP, the pattern is reversed, typically 2 times/s, and the VEP response is obtained by averaging the records time-locked to the stimulus reversals (Harding et al., 1996). For the mfVEP, each record is not a response in the traditional sense. It is a mathematical abstraction, the result of a correlation between the reversal sequence of each sector and the continuous

record. Another way to think of this is shown in Fig. 7B. For a particular sector, if you sum the first 200 ms of all the records immediately following the frame change in which the sector reverses contrast, the response resembles R . If you sum the first 200 ms of all the records immediately following the frame change in which there is no contrast reversal for that sector, the response resembles NR . The records following the reversals will contain the response to this particular sector while the records following the non-reversals will not. The mfVEP for this particular sector is the difference between these two sums (i.e. $\text{mfVEP} = R - NR$).

Technically the response, derived as shown in Fig. 7B, is called the first slice of the second-order kernel. Those new to the mfVEP often ask: “Why isn’t there a first-order kernel?” Fig. 7C illustrates why the first-order kernel, by definition, should not contain a response. To obtain the first-order kernel, we sum all the records following the presentation of a checkerboard sector when it is in one of its two phases and subtract all the records following the presentation of the sector when it is in the reversed phase. The response to a particular sector should be the same for both phases of the checkerboard. Thus, the first-order kernel should be “flat” and contain only noise.

2.7. Spatial resolution

Roughly speaking, scotomas less than 1° or 2° can be detected in the central portion of the field while scotomas exceeding 5° or more can be missed in the peripheral regions of the field (see Section 12.4). However, precisely determining the spatial resolution of the mfVEP is not a trivial matter. Those new to the multifocal technique sometimes mistakenly believe that the spatial resolution can be simply determined by occluding portions of the display. This is false. If a sector of the display is occluded, then there can be no responses from that sector since there is no stimulus. If there is a response, then the software is not working correctly. Thus, no matter how small the sector is, the result will be the same, i.e. no response.

To correctly determine the spatial resolution in a region of the field, the response amplitude, as well as the noise level, must be taken into consideration. If the response from a region is much larger than the noise level, then the resolution will be better than the size of the stimulated region. On the other hand, if the response amplitude is close to the noise level, then the resolution will be poorer than the size of the stimulated region. Since the response per unit area decreases with eccentricity, the spatial resolution will decrease with eccentricity. However, since the response amplitude varies among individuals, the resolution will not be the same for everyone. To precisely determine the spatial resolution requires a signal-to-noise analysis and a

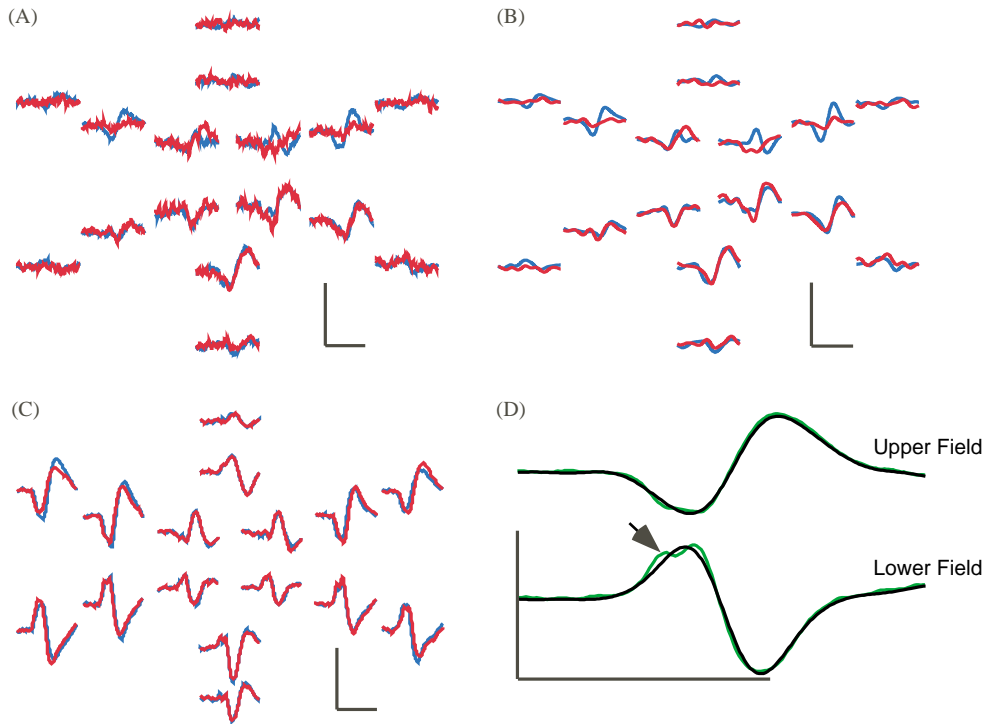


Fig. 6. (A and B) mfVEP responses, grouped as in Fig. 1C, for the right (blue) and left eyes (red) of a patient with glaucoma before (A) and after (B) filtering. (C) Averaged mfVEP responses from the 30 normal subjects as in Figs. 1D and E but without filtering to remove frequencies above 35 Hz. (D) Summed and averaged responses, as in Fig. 1E, for the hemifields of the 30 control subjects for the filtered (black) and unfiltered (green) responses. The calibration bars in panels A–D indicate 200 nV and 100 ms.

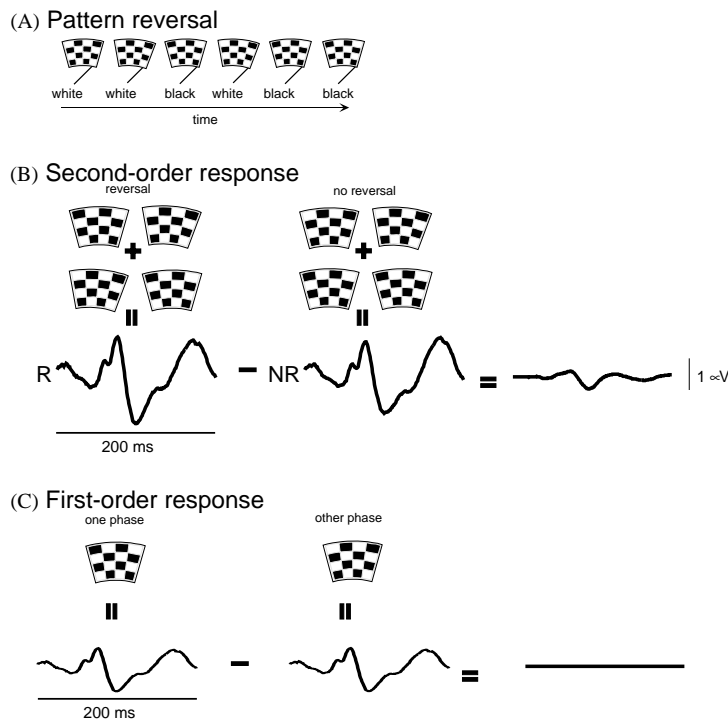


Fig. 7. (A) An example of a random sequence of pattern reversal of a single sector of the mfVEP display. (B) An illustration of how the second-order response is derived. (C) An illustration of how the first-order response is derived. There is no first-order response to pattern reversal.

calculation of sensitivity and specificity. Sections 9.2–9.4 provide a technical basis for determining the spatial resolution.

3. Variations in the normal mfVEP

3.1. Variations between eyes

Corresponding points in the visual fields of the two eyes project to the same region of the brain. Thus, variations in folding and positioning of the brain in relation to the electrodes are the same for the representations of the two eyes. Consequently, the mfVEPs recorded from monocular stimulation of each eye are essentially identical for subjects without visual defects (Hood et al., 2000b; Hood and Zhang, 2000; Graham et al., 2000). This can be seen in Fig. 1B in the responses averaged across 30 individuals. An example for a single individual is provided in Fig. 2C where the responses from the left (red) and right (blue) eyes are shown together for the control subject whose records are shown in red in Fig. 2B. There are two minor qualifications. First, there is a small amplitude asymmetry along the horizontal meridian. Second, there is a small interocular latency difference of about 4 or 5 ms across the midline with the left eye leading in the left visual field and the right eye leading in the right visual field. These differences between the mfVEPs of the two eyes will be discussed in Section 3.3.

3.2. Variations across individuals

Variations in the amplitude and waveform of the mfVEP can be seen across individuals as well. Fig. 2B shows the mfVEP records from the left eye of two normal controls. Local waveforms can be very different and the parts of the field producing the largest or smallest responses differ as well (see also below). These differences are undoubtedly due to two primary factors, the location of the calcarine fissure relative to the external electrodes and the differences in the local folding of the primary visual area (a.k.a. V1, striate cortex). As mentioned above (Section 2.3 and Fig. 2A), there is a wide variation in the location of the calcarine fissure in relation to the external landmarks. The relative amplitudes of the upper vs. lower field responses are roughly correlated with the position of the calcarine fissure (see Fig. 9D in Hood and Zhang, 2000). Local cortical folding is probably an even greater determinant of individual differences. Individuals differ in the way the V1 region is folded, and this will affect the amplitude of the mfVEP. For example, Brindley (1972) showed that there was a wide variation among individuals in the amount of the central 2° represented on the occipital pole (see also Rademacher et al., 1993). Thus, the cells in

the central 2° can have very different orientations with respect to the recording electrodes in different individuals.

3.3. Variations across the field

Not only are there variations in amplitude and waveform across individuals, but there are also variations across the field within an individual. The mfVEP waveform and amplitude varies across the field in at least 5 ways. First, as Baseler et al. (1994) pointed out, the responses from the upper and lower field are reversed in polarity in most subjects (see also Baseler and Sutter, 1997; Klistorner et al., 1998; Hood and Zhang, 2000). This is easier to see in Fig. 1E where the responses from the upper and lower fields for 30 normal subjects are summed separately. This reversal in polarity is consistent with the known anatomy of V1. Most of V1 lies within the calcarine fissure with the upper and lower banks of the calcarine representing the lower and upper visual fields, respectively. Thus, in the calcarine fissure the cells generating the mfVEP are oriented in opposite directions and, consequently, the recorded responses are reversed in polarity.

Second, the responses vary in amplitude even from regions at the same eccentricity. As expected, cortical magnification is only one factor determining the size of the response. The location of the cortical region in relation to the recording electrodes is a crucial factor. Interestingly, the responses, on average, are smaller just below the horizontal meridian than just above (Fig. 1B). One possible explanation comes from a study by Aine et al. (1996). They recorded magnetic evoked potentials to focal stimuli and localized the sources of the responses with dipole modeling. If, as they suggest, the field just below the horizontal meridian projects to the lower bank of the calcarine cortex in many individuals, then the mfVEPs from the region below the horizontal meridian would be in the fold of the calcarine. Consequently, the associated cells would be oriented more perpendicular to the recording electrodes of the midline channel and thus a smaller response would be recorded. Consistent with this explanation, larger responses are recorded from below the horizontal meridian with the lateral electrodes (compare channels 1 and 6 in Fig. 4).

Third, in many subjects the waveform of the responses along the vertical meridian differs from the waveform of the other responses (Klistorner et al., 1998; Hood and Zhang, 2000; Klistorner and Graham, 2000). This can be seen best in the averaged data in Fig. 1D. This variation in waveform indicates that there must be more than one source generating the mfVEP. Responses generated by a single localized source will produce responses that vary in amplitude but not in waveform. This second source may be in the extrastriate cortex or

in V1, but oriented perpendicular to the first source. On one hand, it is likely that the responses along the vertical meridian have a greater contribution from extrastriate regions. The cells in V1 that receive input from the vertical, but not the horizontal, meridian are in close proximity to those in V2 representing the same region (e.g. see Fig. 11 in Horton and Hoyt, 1991). On the other hand, the vertical meridian is represented on the medial surface of the cortex (Horton and Hoyt, 1991) and, like the bend in the calcarine, is not optimally oriented for the midline channel.

Fourth, along the upper horizontal meridian in Fig. 1B, the responses from the right eye (blue) are larger than those from the left eye (red) for the leftmost four sectors while the reverse is true for the corresponding sectors of the right visual field. Thus, along the upper horizontal meridian the responses from the temporal retina are larger, on average, than the responses from the nasal retina (see also James, 2003). This naso-temporal difference has little to do with the blind spot per se as it is occurring for regions far removed from the blind spot (compare Fig. 1B and the location of the blind spot in Fig. 35). Others (Brad Fortune, pers. comm.) have confirmed this small naso-temporal difference. It may reflect the small naso-temporal difference in sensitivity (approximately 1 dB or less) that has been reported for visual field measurements (Brenton and Phelps, 1986; Heijl et al., 1987).

Finally, there is a small latency difference between the eyes that can be seen along the midline where the responses for the left eye lead those for the right in the left visual field while the reverse is true for the right visual field (Hood et al., 2000b). These latency differences are in the range of about 5 ms and probably reflect a small difference in the time it takes signals to arrive at V1 from the nasal as opposed to temporal retina. Most likely, this small difference is due to the conduction time of the unmyelinated ganglion cell axons on the retinal surface (see references in Sutter and Bearnse, 1999). In particular, the action potentials from the ganglion cells in the temporal retina travel further to the optic disc than do the action potentials from corresponding points on the nasal retina.

4. Relating mfVEPs to traditional VEPs and cortical anatomy

4.1. Are the mfVEPs “little” VEPs?

Like the conventional VEP, the mfVEP can be recorded to flash, pattern onset or pattern reversal stimuli. Barber (1998) used pattern onset stimuli and reported a qualitative resemblance between the mfVEP and VEP waveforms. However, most of the work with the mfVEP thus far has been done using the pattern

reversal paradigm described above. Recently, Fortune and Hood (2002) compared the waveforms of the mfVEP to those of the conventional, pattern VEP (PVEP) after modifying aspects of the PVEP and mfVEP paradigms to make the conditions more comparable. Fig. 8A shows a subset of the spatial conditions employed. For the PVEP, the field was 20° in diameter and the checks were all the same size, 50 min wide (about the average width of the check size in the central 10° of the mfVEP display). (Note that the checks in the two displays of Fig. 8A are not drawn to scale.) The mfVEP display was the same as the one shown in Fig. 1A. The PVEP responses were compared to the sum of the mfVEP responses from the central 10° (20° diameter) (lower part of Fig. 8A).

The conditions chosen for the PVEP are relatively standard (Harding et al., 1996). The PVEP was recorded with a 20° wide field or with the upper or lower hemifield covered (see Fig. 8A). The active electrode was placed at Oz (approximately 3.5 cm above the inion for these subjects), the reference at Fz (approximately 12 cm posterior to the nasion), and the ground on the left earlobe. Although not technically correct, this configuration is usually referred to as monopolar (MP) recording. Records were simultaneously obtained using the electrode at Oz as the active and the electrode at the inion as the reference. This electrode configuration, referred to as bipolar (BP) recording, is similar to that for the midline channel used in the mfVEP studies (see Fig. 3B).

Fig. 8B (top row) shows the PVEP response (average of 12 subjects) to the full, 20° field. The major components, N75, P100, and N135, are apparent (see Harding et al., 1996). For comparison, the mfVEP responses to the 20° diameter display (Fig. 8A), summed separately for upper and lower hemifields, are shown in the second (BP) and third (MP) rows of Fig. 8B. The mfVEP from the lower field is reversed in polarity so that the component near 100 ms is positive. The two early components, referred to as C1 and C2, are apparent in both the BP and MP recordings of the mfVEP and approximately correspond to N75 and P100, although C1 and C2 occur slightly earlier than the N75 and P100 components in the PVEP (Fortune and Hood, 2002).

While the waveforms of the mfVEP to pattern reversal stimuli, recorded with either MP or BP configurations, bear a qualitative resemblance to the PVEP, there are four significant differences. These can be seen in Fig. 8C where the PVEPs recorded to the 20° diameter hemifield stimuli are shown together with the mfVEP responses summed across hemifields. [These are the same responses as in Fig. 8B but with both upper and lower waveforms reversed in polarity. The multifocal software (VERIS) reverses the polarity (Sutter, 2001).] First, the mfVEP, as described above (Fig. 1E), exhibits

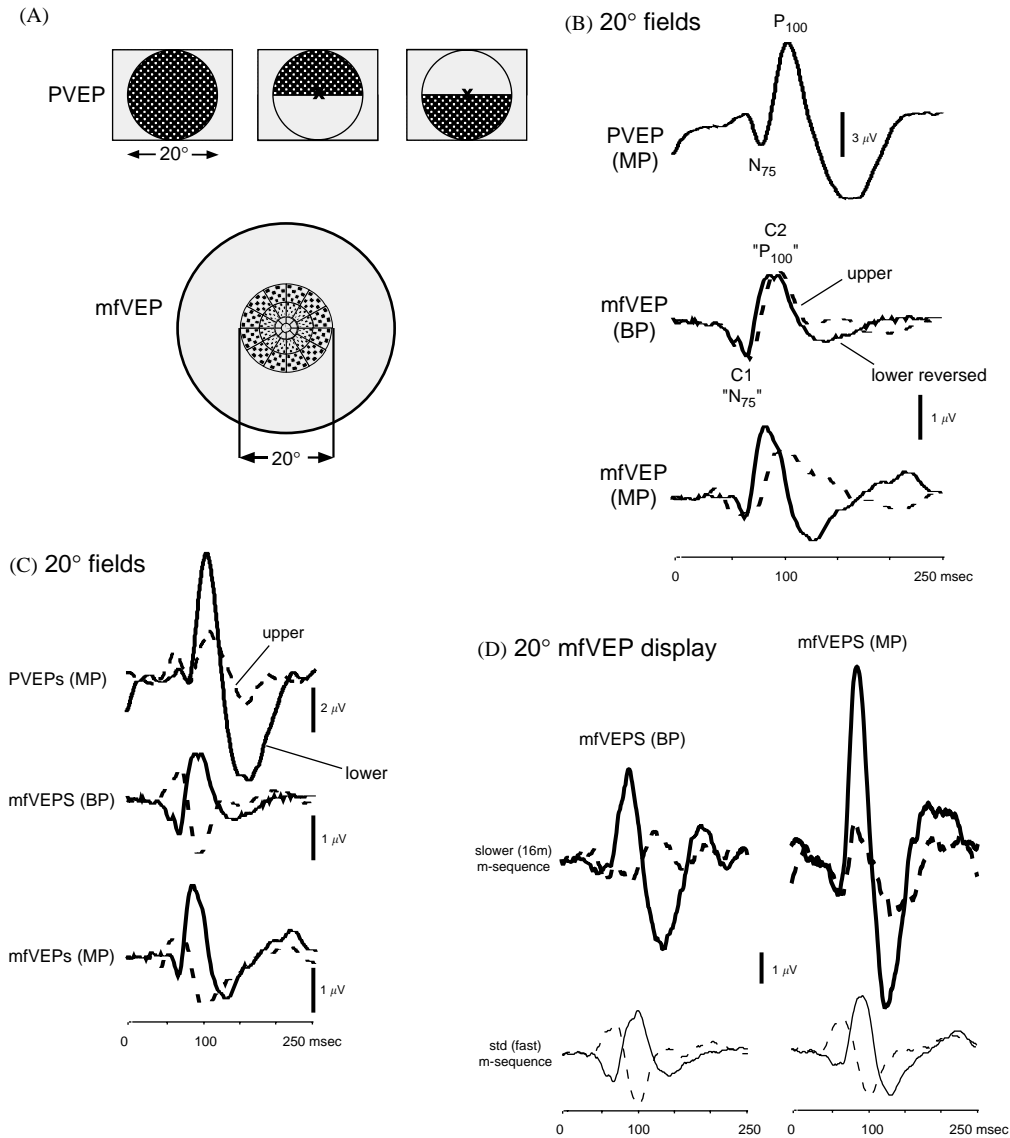


Fig. 8. (A) The spatial conditions of the conventional pattern reversal VEP (PVEP) display (upper) used by Fortune and Hood (2003). The PVEP responses were compared to the sum of the mfVEP responses from the central 10° of the mfVEP display (lower). (B) The averaged VEP responses for 12 control subjects for the 20° diameter field compared to the summed mfVEP responses to the upper (dashed line) and lower (solid line) hemifields of the mfVEP display. (The polarity was reversed for the lower hemifield.) The mfVEP results were obtained with two electrode configurations, MP and BP. (C) The PVEP response to the upper (dashed line) and lower (solid line) hemifield of the PVEP display compared to the mfVEP responses summed across hemifields. The mfVEP responses are the same as in B except that the waveforms to both the upper and lower hemifields are reversed in polarity. [The VERIS software reverses the polarity of these responses.] (D) The effect of slowing the mfVEP stimulation rate on the averaged hemifield responses. The hemifield responses are shown for a slow sequence (top row) and the standard (fast) sequence (bottom row). Modified with permission from figures and data from Fortune and Hood (2003).

a polarity reversal for upper vs. lower field stimulation. The PVEP does not. The mfVEP and PVEP responses from the lower field, but not the upper field, have the same polarity. Second, the mfVEP is smaller than the PVEP, on average about one-third the size. (Note that the scales differ in Fig. 8C for the PVEP and mfVEP responses.) Third, as mentioned above, the latency of "P100" is shorter for the mfVEP than it is for the PVEP. And, fourth, although both the PVEP and mfVEP responses to the lower field are larger than the responses

to the upper field, this amplitude asymmetry is far more extreme in the case of the PVEP.

To conclude, the mfVEP is not strictly speaking a "little PVEP". In some sense, this is hardly surprising, as the stimulus and recording conditions are different. The electrode configuration, the spatial display and the pattern of temporal stimulation all differ. However, it appears that the rate of stimulation accounts for most of the differences between the PVEP and the mfVEP. As Fig. 8D indicates, slowing the stimulation rate of the

mfVEP, such that successive pattern reversals can be no closer in time than 213 ms, produces responses that more closely resemble the waveform of the PVEP. For comparison, Fig. 8D also shows the response to the standard mfVEP sequence. By slowing the rate of stimulation, the response becomes larger, especially from the lower field, and the response from the upper field loses the clear polarity reversal seen with the standard (fast) sequence. Fortune and Hood (2003) speculate that the fast mfVEP sequence decreases the contribution of extrastriate regions thus producing the differences between the mfVEP and the PVEP.

4.2. Where is the mfVEP generated?

Two lines of evidence suggest that the mfVEPs are largely, but not entirely, generated in V1 or striate cortex (Fortune and Hood, 2003). First, to a remarkable extent, the polarity of the mfVEP reverses as we move across the horizontal midline. This can be seen in Figs. 1 and 8. This polarity reversal provides strong evidence for local generators in V1, or at least in the calcarine fissure. In the calcarine fissure, the cells generating the responses to upper and lower field stimulation will be reversed in orientation. The second line of evidence comes from dipole analysis. Based upon an analysis of PVEPs with multiple electrodes and a mathematical source model (dipoles), a number of studies have concluded that there is a large contribution of extrastriate cortex to the PVEP (see Di Russo et al., 2002 for references). Using the same techniques, Slotnick et al. (1999) concluded that the source of the mfVEP was primarily V1.

On the other hand, since the mfVEP responses do not all have the same waveform, other sources must be contributing. Note the difference between the responses from the vertical midline and the more lateral responses in Fig. 1D. As mentioned above (Section 3.3), the additional dipole(s) could represent an extrastriate signal or a second signal generated within V1 but with a different orientation than the primary signal.

In sum, it is likely that the mfVEP, like the PVEP, has both striate and extrastriate contributions although the extrastriate contribution is probably smaller in the case of the mfVEP (Fortune and Hood, 2003).

5. Detecting ganglion cell damage with the mfVEP

Once an mfVEP has been recorded from a patient, the next problem is interpretation. Here we consider two related questions. How do we compare the mfVEP array to the results from static automated perimetry, in particular to the Humphrey visual field (HVF)? How do we know if an mfVEP result is abnormal? Before

answering these questions, a brief introduction to the HVF follows.

5.1. Humphrey visual field

As mentioned in the Introduction, the “clinical standard” for detecting and monitoring glaucoma is static automated achromatic perimetry, which was introduced to the clinic in the early 1980s. In this article, by “static automated achromatic perimetry” we mean visual fields obtained with the HVF Analyzer using the 24-2 program. In case the reader is not familiar with the technique, a short review is provided here. The subject’s task is to press a button when he or she detects the presence of a small (0.43°), brief (200 ms) test light presented on a dim background (10 candelas/m^2). During this task, the patient maintains the same eye position by fixating on a small centrally located circle. For the 24-2 program, the test light is randomly presented to 54 locations within the central 24° of the visual field. These locations are spaced 6° apart. The tester has the option of including a test spot in the center (fovea) bringing the total to 55 locations. Fig. 9 shows a sample HVF report for the left eye of a patient with glaucoma. Unless otherwise noted, the information used in this article is contained within the large rectangle of Fig. 9 (“Total Deviation”). The upper display in the rectangle shows the difference in dB ($1 \text{ dB} = 0.1 \log \text{ unit}$) between the patient’s sensitivity and the sensitivity of an age-matched control group. So -10 means that sensitivity is decreased by $-1 \log \text{ unit}$ or that it is decreased by a factor of 10 compared to the sensitivity of the age-matched control group, while -3 means it is decreased by $-0.3 \log \text{ unit}$ or a factor of 2. The lower display in the rectangle codes these sensitivity differences in the form of a probability plot where the significance level is coded from 5% (square of 4 dots) to 0.5% (filled black square).

In addition to the 24-2 program, other test strategies used by the clinician include the 30-2 and 10-2 programs. The 30-2 program tests more locations, a total of 76 out to 30° . As in the case of the 24-2 program, the locations are spaced 6° apart. The 10-2 program tests 68 locations spaced 2° apart out to 10° . The 2° spacing allows for greater spatial resolution. Until recently, a full threshold algorithm was used to obtain HVFs. This staircase procedure took 10–20 min/eye to complete. To reduce the duration of the test, the Swedish Interactive Threshold Algorithm (SITA) was developed. The SITA standard procedure approximately halves the testing time, and the SITA fast procedure results in an additional decrease in time. However, with the SITA algorithm, particularly the SITA fast, the region of abnormal vision may be over estimated as compared to the full threshold algorithm (Wild et al., 1999).

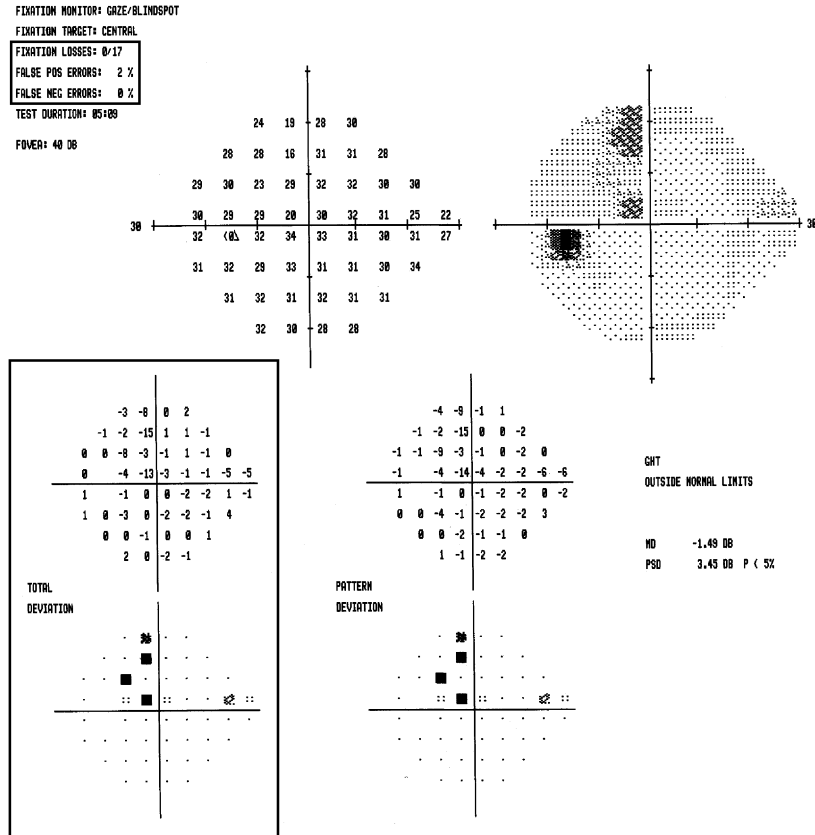


Fig. 9. Sample 24-2 HVF report for the left eye of a patient with glaucoma. The reliability indices are shown within the small rectangle. The differences in dB between the patient’s sensitivity and that of the age-matched control group, i.e. “Total Deviation”, are shown within the large rectangle. The lower display in the large rectangle is a probability plot for the “Total Deviation”, where the significance level is coded from 5% (square of 4 dots) to 0.5% (filled black square).

5.2. Qualitative comparisons of mfVEP and HVF topographies

How can we compare mfVEP arrays to HVF results? To illustrate the problems involved in comparing mfVEP arrays and HVFs, consider the following patient referred for mfVEP testing. This patient, whose HVF results are shown in Fig. 10B, has unilateral glaucomatous damage documented on the HVF. The probability plots in Fig. 10B, and in all subsequent figures, are the total deviation plots from the 24-2 HVF (see Fig. 9). The defect circled in gray had been observed on earlier 24-2 HVF tests performed by this patient. The perifoveal defect circled in black was new. The glaucoma specialist (Dr. R. Ritch) requested an mfVEP test to determine if the mfVEP would confirm this perifoveal defect.

The mfVEP responses obtained from the patient’s left eye are shown in Fig. 10A. As mentioned above, these responses are arbitrarily spaced so that the records do not overlap. Therefore, care must be exercised in comparing visual fields to mfVEP arrays. While the test spots in the 24-2 HVF are of equal size and spaced by 6°, the sectors in the mfVEP vary in size and thus in spacing. Fig. 10D shows the 24-2 test points for the left

eye superimposed upon the sectors of the mfVEP display from Fig. 1A. The field is sampled in a very different way by the two techniques. For example, within the central 2.6° (5.2° diameter) there are 12 mfVEP responses but only one HVF test point (see red circles Figs. 10A and D). In the outer ring, three or four HVF test points fall within each of the sectors.

Do this patient’s mfVEP records show a defect in the same region as the HVF field? A qualitative comparison between the HVF and mfVEP topographies can be made by drawing iso-degree contours (Hood et al., 2000a). (See Klistorner et al., 1998 for the first qualitative comparisons of mfVEP and HVF defects in a patient with glaucoma.) The red, blue and green “circles” in Fig. 10A denote radii of 2.6°, 9.8° and 22.2°, and the corresponding loci for the 24-2 HVF are shown in Fig. 10B. The gray records in Fig. 10A indicate the responses for sectors falling approximately within the area of the defect circled in gray in Fig. 10B. The black records in Fig. 10A are responses for sectors falling within the area of the defect circled in black in Fig. 10B. Decisions made with this type of comparison are somewhat arbitrary. It is difficult to be sure what constitutes a corresponding region on the two tests.

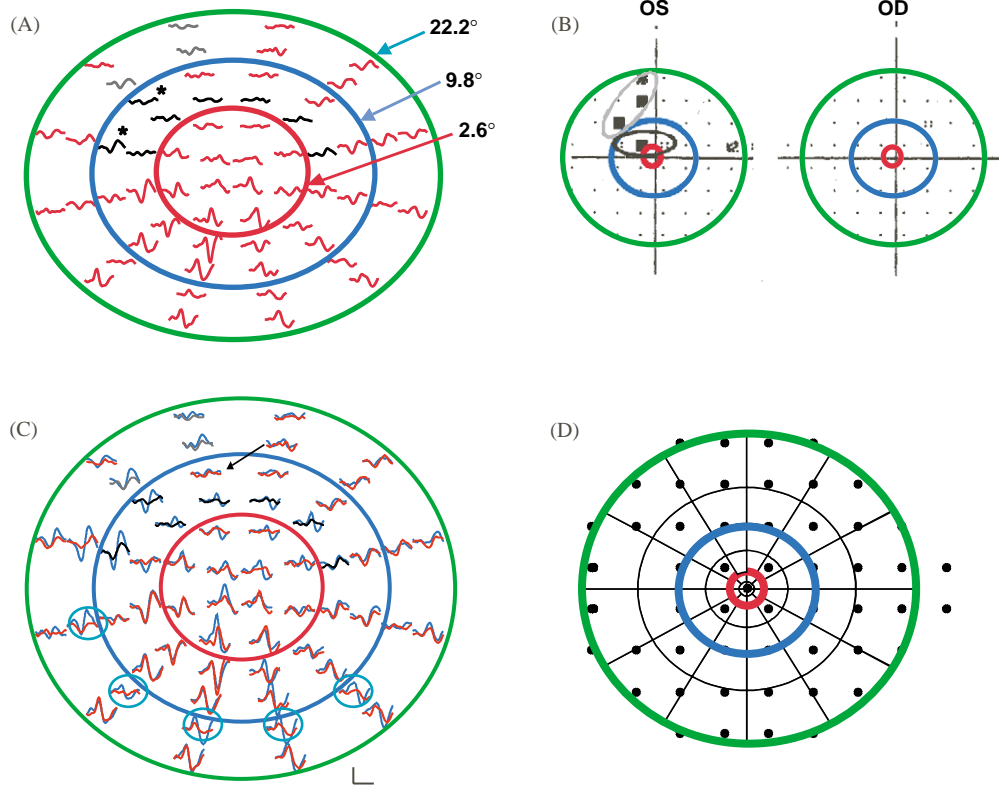


Fig. 10. (A) The mfVEP responses obtained from the left eye of a patient with glaucoma. The red, blue, and green circles have radii of 2.6°, 9.8°, and 22.2°, respectively. (B) HVF 24-2 probability plots for the patient's left and right eyes. These are derived from the total deviation plots (see Fig. 9). The red, blue, and green circles have the same radii as in panel A (2.6°, 9.8°, and 22.2°). The defect within the gray ellipse was observed on previous 24-2 HVF tests, but the defect within the black ellipse was new. (C) The mfVEP responses obtained from the left (red) and the right (blue) eyes of the patient. The green ellipses surround five contiguous locations in which responses from the left eye are reduced compared to the right eye. (D) The 24-2 HVF test points for the left eye superimposed upon the sectors of the mfVEP display from Fig. 1A. The calibration bar in panel C indicates 200 nV and 100 ms.

Further, deciding what constitutes an abnormal response is even more difficult. Some of the responses coded as black or gray appear smaller than their "normal" neighbors (upper asterisk) while others (lower asterisk) appear as large or larger than those in the supposedly unaffected regions. On the other hand, some of the responses that are not coded as either gray or black appear small as well.

To complicate matters further, many normal controls have small responses in various parts of their fields. For example, notice the small responses in the upper field within the ellipses in Fig. 5 and in some of the locations along the lower horizontal meridian. The problem posed by the range of normal responses is illustrated in Fig. 11. The records in Fig. 11 show the responses with the next to smallest amplitude (gray) and next to largest amplitude (black) from among 30 control subjects' best mfVEPs arrays for the left eye. (The second smallest and largest were chosen, instead of the smallest and largest, to avoid an abnormally small or large response that might occur once by chance.) There is clearly a large range of amplitudes for the normal controls. More to the point, the normal range includes very small

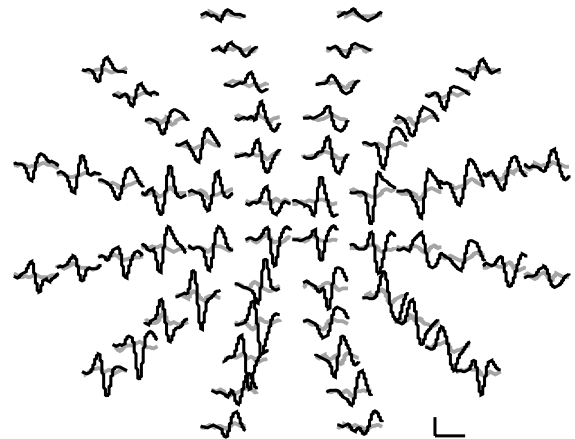


Fig. 11. A comparison between the mfVEP best channel responses for the next to smallest amplitudes (gray records) and the next to largest amplitudes (black records) of the responses from the left eyes of the 30 control subjects.

responses in some locations. Thus, it can often be difficult to discern what is normal or abnormal with these qualitative comparisons.

5.3. Two eyes can be better than one

Often localized damage can be more readily detected by comparing the mfVEPs generated by monocular stimulation of each eye (Zhang et al., 1999; Hood et al., 2000b; Hood and Zhang, 2000). Although there are large differences in amplitude and waveform among individuals (see Figs. 2B and 5), the mfVEP from the two eyes of the same individual are, for our purposes, identical if there are no defects in either eye (see Section 3.1 and Figs. 1B and 2C). In Fig. 10C, the records in blue from the right eye are superimposed on those from the left eye (from panel A). In a number of locations, including some in the region of interest in the perifovea (black records in panel A), the responses from the right eye are larger. In other locations, the responses from both eyes are small and approximately of equal size. Further, in a number of locations in which the HVF field does not show a defect, the mfVEP responses from the left eye appear smaller than those from the right eye. Of particular interest are five contiguous locations in the lower field (green ellipses) that resemble an arcuate defect. This arcuate defect is not apparent on the 24-2 HVF.

This example raises two questions: First, how do we know which of the responses from the affected left eye is significantly smaller? Second, can we improve on the rather crude method described above for comparing the HVF data to the mfVEP results? In Section 10.2, we describe a method of estimating (interpolating) the HVF loss associated with each of the sectors of the mfVEP display. In the following section we describe a method for deriving a probability plot for the mfVEP that addresses both questions. The first step in deriving a probability plot is to measure the amplitude of the mfVEP responses.

5.4. Measuring the amplitude or size of the response

The size or amplitude of a VEP response can be measured in a number of ways. We use the root-mean square (RMS) amplitude calculated over a time interval of 45–150 ms. RMS amplitude is a common measure of the “amplitude” of a VEP response. (The details are not important for our purposes, but the RMS is obtained by taking the difference between the voltage at each point in time and the mean voltage. These differences are first squared and then averaged. The square root of this average is the RMS value.) For the mfVEP, the RMS has advantages over other commonly used measures of amplitude. For example, the RMS measure does not depend on a particular aspect of the response waveform, as does the peak-to-trough measure (Zhang et al., 2002).

5.5. mfVEP probability plot: interocular comparisons

To see if the mfVEP is significantly smaller in one eye than the other, the ratios of the RMS amplitudes for the

responses from each eye are calculated. By comparing these ratios to the mean and standard deviation (SD) of the ratios for a group of normal subjects, the significance level can be obtained. The technique is illustrated in Fig. 12 where the records from the patient in Fig. 10C are presented again in Fig. 12A. As an example, consider the two pairs of responses in the inset of Fig. 12A. The ratios of the RMS(OD) to RMS(OS) are 1.1 (upper pair) and 2.3 (lower pair). When compared to a group of normals, the upper pair of responses was not significantly different than normal while the other pair was highly significant (> 4.5 SDs). [Note: the actual comparisons are performed on the log of the ratio RMS(OD)/RMS(OS) so that a ratio of 0.5 and 2.0 represent equivalent differences (i.e. -0.3 and 0.3). With this log transformation, the measure approximates a normal distribution (Hood et al., 2003d).]

Fig. 12B shows the results displayed in a manner similar to the HVF probability plots. Each symbol is in the center of a sector of the mfVEP display (see Fig. 1A). If the symbol is black, then it signifies that the two eyes are not significantly different. A desaturated color denotes significance at the 5% level (> 1.96 SD) and a saturated color significance at the 1% level (> 2.58 SD). The color indicates whether the left (red) or right (blue) eye had significantly smaller responses. The gray square indicates that the responses were too small in both eyes to allow for a meaningful comparison between eyes. [Technical note: The SNR (described in Section 9.2) is obtained for the responses from both eyes at each location. If the larger of the two SNRs is less than a criterion value (1.7), then the location is coded gray. The criterion value of the SNR was chosen such that records without any signal present would have an SNR above this value in less than 2.5% of the cases.]

5.6. Comparing HVF and mfVEP probability plots

If the mfVEP probability plot (Fig. 12B) and the HVF probability plot are scaled in the same way, they can be compared directly to each other. Fig. 12C is the HVF from Fig. 10B scaled to have the same dimensions as the mfVEP plot in Fig. 12B. The probability plots in Figs. 12B and C can be overlaid to compare the defects detected by each. In this case, both plots show a perifoveal defect (black ellipses) in the left visual field. That is, the mfVEP is confirming the perifoveal defect seen on the HVF. However, it fails to detect the long-standing defect circled in gray in Figs. 10B and 12C. As will be discussed in Section 12.4, defects are difficult to detect in this upper region, as the responses from normal controls are so small. On the other hand, an arcuate defect in the lower field appears in the mfVEP plot of Fig. 12B, but not in the HVF 24-2. Fig. 12D shows a 10-2 HVF for this patient's left eye. Remember that the 10-2 HVF samples the central 10° (radius) with test points

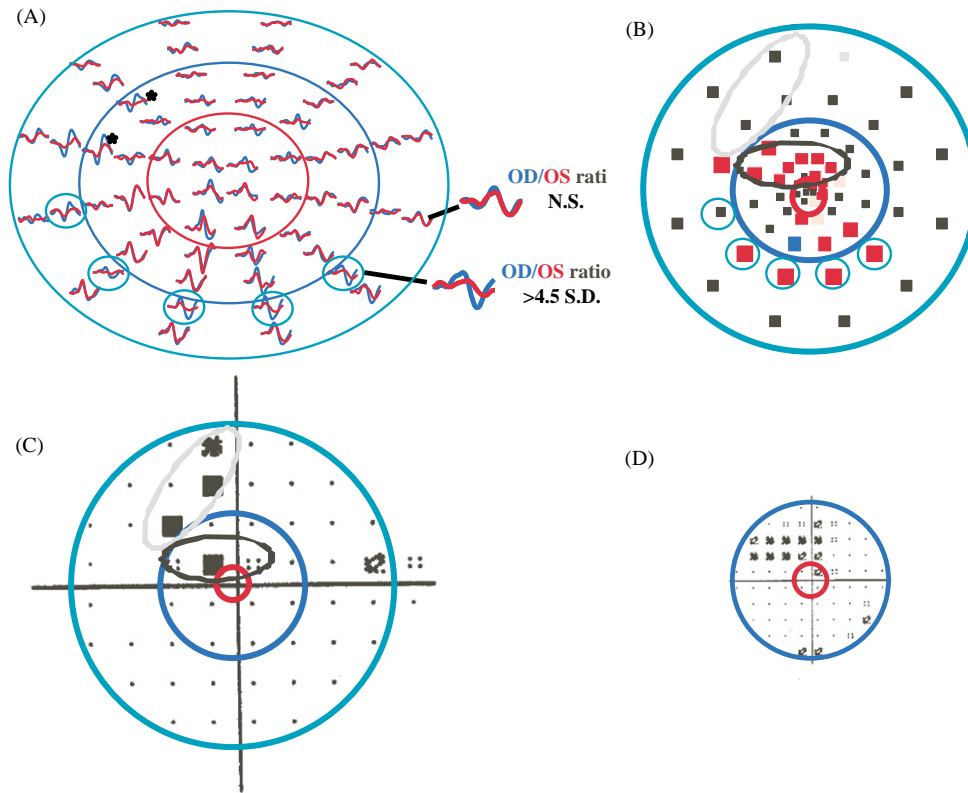


Fig. 12. (A) mfVEP responses shown in Fig. 10C. The inset shows the results of comparing the RMS ratios of two pairs of responses to those from a group of control subjects. N.S. means that the ratio of amplitudes is not significantly different from normal. (B) An interocular mfVEP probability plot. Each symbol is in the center of a sector of the mfVEP display. A black square indicates that there is no significant difference between the two eyes. The colored squares indicate that there is a significant difference at greater than the 5% (desaturated) or 1% (saturated) level. The color denotes whether the right (blue) or left (red) eye had the smaller response. A gray square indicates that the responses from both eyes were too small to allow for a comparison. (C) The 24-2 HVF for the patient's left eye from Fig. 10B but scaled to have the same dimensions as the mfVEP probability plot. (D) The 10-2 HVF for the left eye of the patient.

spaced every 2° . Note that there is a hint of the arcuate defect in the patient's 10-2 HVF field (see Fig. 12D).

5.7. Interocular HVF

In many cases, the “better” eye can have abnormal HVF points as well. A comparison to the monocular HVF, as in Figs. 12B and C, fails to take this into account. To take this into consideration, we can derive an HVF probability plot for the difference between the 24-2 HVFs of the two eyes. The method for deriving this interocular HVF comparison is shown in Fig. 13. Panel C is the difference between the 24-2 absolute deviation values (OD-OS) from each eye shown in panel A. [Since the HVF values are in log units (dB), this difference is equivalent to taking the ratio of the antilog of the HVF dB values. Thus, this measure is comparable to the ratio measure of response amplitude employed for the mfVEP probability plot.] Fig. 13B shows the values from Fig. 13C coded for significance level using the same code as in Fig. 12B for the mfVEP. (The norms employed for this comparison come from Johnson and Spry, 1999.) This interocular HVF probability plot is

also shown in Fig. 14A (upper left panel) along with the monocular HVFs coded in the same way as the mfVEP plots to show the 5% and 1% points. These plots can be compared directly to the mfVEP plots in the lower panel since they are on the same scale. Patients with unilateral damage will tend to show similar interocular and monocular HVF plots. However, we occasionally find that the interocular HVF shows up defects better than the traditional monocular HVF (e.g. see Fig. 20). In the case of the patients with bilateral damage, the interocular and monocular HVFs will differ.

6. Bilateral damage and the need for a monocular test

6.1. Need for a monocular test: bilateral damage

The obvious shortcoming of an interocular comparison for the mfVEP test is the possibility that bilateral damage will be missed. The interocular comparison test can miss bilateral damage located in corresponding field locations. In other words, defects in the same part of the visual field in both eyes (e.g. inferotemporal in one eye

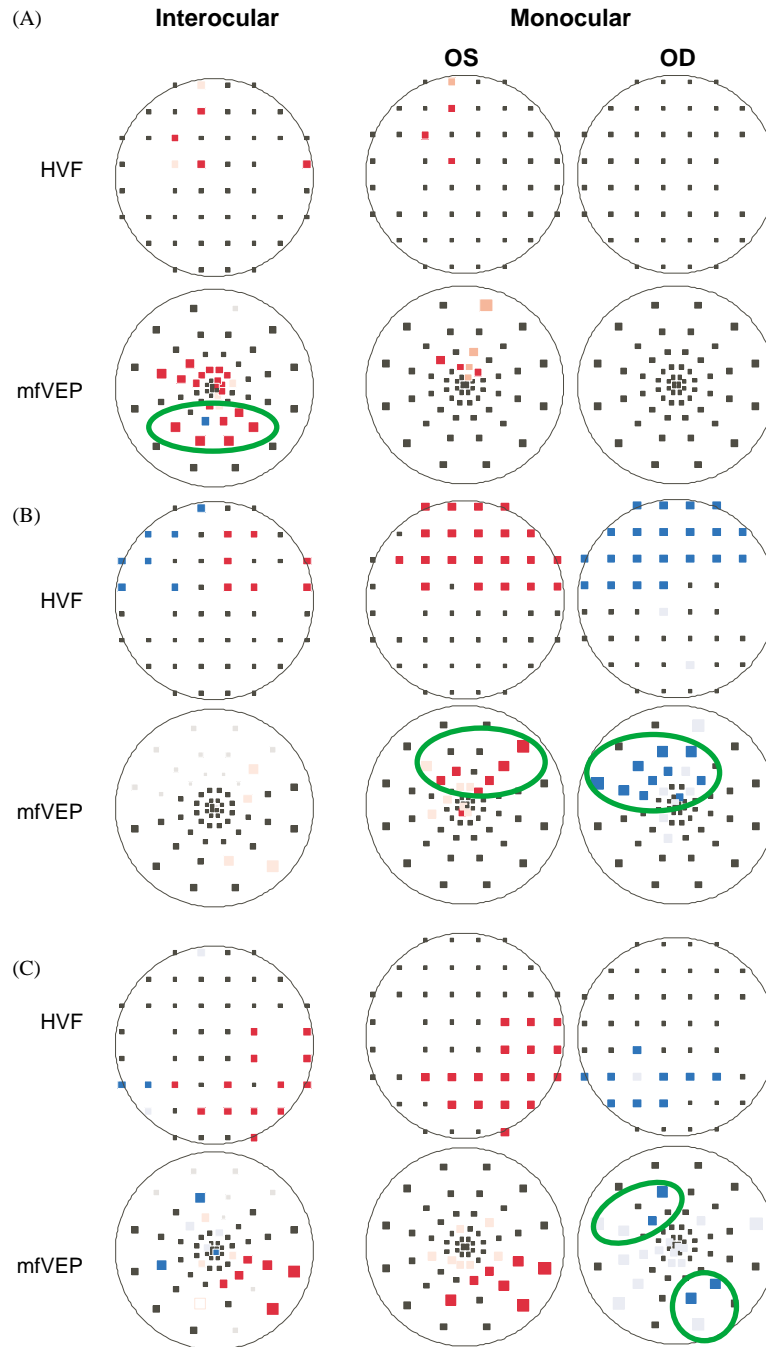


Fig. 14. Probability plots for interocular (column 1) and monocular (columns 2 and 3) comparisons of HVF (upper row) and mfVEP (lower row) results obtained from three patients (A–C) with glaucoma. For the monocular mfVEP plots, the colored squares indicate the locations with SNR values that are significant at greater than the 5% (desaturated) or 1% (saturated) level. The green ellipses enclose defects picked up by either a monocular or an interocular mfVEP test, but not by both tests.

stimulus display. The colored squares indicate the locations with SNR values that fell more than 1.96 (desaturated color) or 2.58 (saturated color) SDs below the mean values. Blue indicates that the right eye, while red indicates the left eye, had significantly smaller SNRs. On average 2.5% and 0.5% of the points of each eye should fall below 1.96 and 2.58 SD, respectively. Thus, on average, the sum of the number of abnormal points

in the two monocular plots should equal the number of abnormal points in the interocular plot.

The reader is warned that the statistics underlying the monocular plots are not simple and that the monocular plots need to be interpreted with care. For example, normal controls with noisy records will tend to have more “defects” (i.e. more false positives) than expected by chance. These problems are detailed in Section 9 and

in Hood et al. (2003c). For now, we note that these problems can be circumvented to some extent by defining a defect in terms of a cluster of points.

The problem of deciding what constitutes a local defect is not unique to the mfVEP. The HVF test has a similar problem. With the 24-2 HVF, it is common to define a “cluster” of points as abnormal if they collectively meet some criterion (e.g. Chauhan et al., 1988; Katz et al., 1991). For example, 3 or more adjacent points exceeding the 5% level or 2 or more adjacent points exceeding the 2%, or 1%, level have been used as criteria (e.g. Wu et al., 2001; Reyes et al., 1998; Kook et al., 2001). Typically for these criteria, points have to be within a hemifield (i.e. the cluster cannot cross the horizontal midline). To solve the problem of excessive false positives in the monocular plots, Goldberg et al. (2002) suggested a similar cluster approach. They labeled the mfVEP probability plot abnormal if 3 contiguous points exceeded 5% with at least one of the points exceeding 2%. Further, only one of the three points could appear among the sectors of the outer ring. Our criteria differ from the Goldberg et al. criteria in two ways: (i) we do not exclude the points falling in the peripheral ring and (ii) we do not allow the cluster to cross the midline based upon the same logic used for the analysis of HVFs. With these criteria in mind, significant clusters are defined as follows: 2 points exceeding 1% or 3 points exceeding 5% with one of the three contiguous points exceeding 1%. For our 30 controls, three eyes (i.e. 5% of the 60 eyes) satisfied the three point criteria while no eye satisfied the two point criteria (Hood et al., 2003c).

7. Need for both interocular and monocular tests

The green ellipses in Fig. 14 show the regions with significant defects on either the interocular or the monocular mfVEP fields but not on both. Defects are defined, based upon the cluster criteria (see Section 6.2), for upper and lower hemifields. In Figs. 14B and C, where the HVFs show bilateral damage, the monocular mfVEP test is detecting more defects than the interocular mfVEP test. In Fig. 14B, the monocular mfVEP test is detecting the upper field defects seen in both eyes on the HVF. These defects were missed by the interocular mfVEP. In Fig. 14C, the interocular mfVEP is detecting the damage in the left eye but missing the damage in the right. In this case, the monocular mfVEP detects the lower field damage in the right eye as well as the damage in the upper field of the right eye which is not apparent on either the interocular mfVEP or the HVF. On the other hand, for the patient with the unilateral damage in Fig. 14A, the interocular test is detecting damage missed on both the monocular mfVEP and the HVF. We will see below that under many

circumstances the interocular mfVEP will do better than the monocular mfVEP. The circumstances under which each test will detect damage will be explored in Sections 11 and 12. For now, Fig. 14 illustrates the need for both interocular and monocular mfVEP tests.

8. mfVEP in the clinical management of glaucoma: possible applications

The mfVEP is a relatively new technique that has yet to find its place in the clinic. We have recorded mfVEPs from about 500 patients. Of these, approximately 300 were patients with glaucoma or glaucoma suspects studied in conjunction with Drs. Ritch, Liebmann, and Thienprasiddhi. The others were patients referred by neuro-ophthalmologists Drs. Behrens and Odel and are discussed elsewhere (Hood et al., 2000a; Miele et al., 2000; see Hood et al., 2003a). In this section, we summarize our experience focusing on the potential clinical uses of the mfVEP in the management of glaucoma.

8.1. Unreliable HVFs

It is well known that many patients cannot, or will not, produce reliable HVFs. For most of these patients, the mfVEP provides an alternative. Fig. 15 shows an example of a 43yr old male with a family history of glaucoma. While playing golf, this patient noticed he had some trouble seeing with his left eye. His visual acuity was 20/20 (OD) and 20/40 (OS). His 24-2 HVF for the left eye showed significant defects (Fig. 15B), but false negative errors of 50% were recorded. Since the rest of the examination, including his cup-to-disc ratios, was normal, the visual field was assumed to be unreliable. The mfVEP confirms this. There is little indication of unilateral damage in either the trace arrays (Figs. 15A) or the interocular mfVEP probability plots (Fig. 15C). In addition, as we will see below (Section 10.4), the responses from the left eye in the regions with poor 24-2 HVF sensitivity are too large given the extent and depth of the field defect.

We usually find that reliable mfVEP records can be obtained from patients with unreliable HVFs. There are however, patients who are uncooperative or difficult to test, and the very reasons that make them poor or questionable HVF takers can make them poor mfVEP candidates. For example, we tested a 75yr old woman who had produced unreliable fields for over 5yr. The only consistent finding was a profound and generalized loss in sensitivity OD and reasonably good sensitivity (on some days) OS. She complained before, during and after the mfVEP test and refused to finish the second run of the mfVEP test. The mfVEP records, however, were of help as they confirmed the general impression

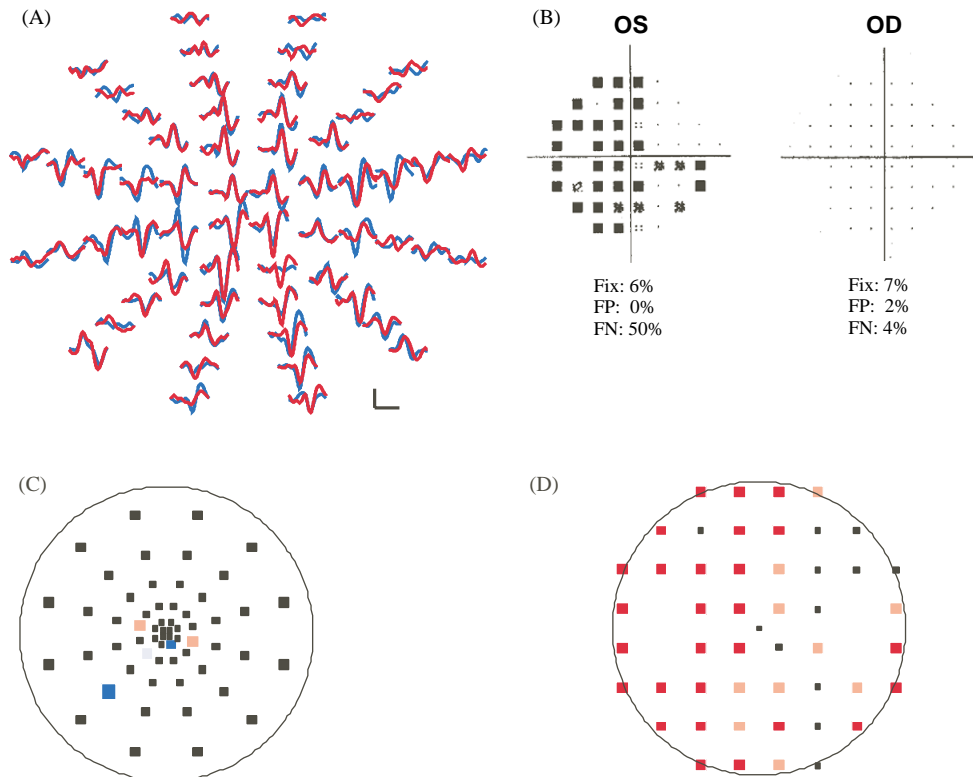


Fig. 15. Results obtained from a patient with unreliable HVFs. (A) The mfVEP responses for the right (blue) and left (red) eyes. (B) The 24-2 HVFs for the right and left eyes and the reliability indices. (C) The interocular mfVEP probability plot. (D) The interocular HVF probability plot. The calibration bar in panel A indicates 200 nV and 100ms.

obtained from the HVFs. In particular, there was little or no response OD and reasonably good signals OS.

Another example of an “uncooperative or difficult” patient is provided in Fig. 16. The patient’s HVF could be classified as borderline unreliable OD (36% false negative errors) and “fairly reliable” OS. (No index was in the unreliable range, but there were 18% false negative errors and 17% false positive errors.) In addition, there were a few fixation losses for each eye, and the technician noted that the patient was sleepy. The HVF total deviation numbers, rather than the probability plots, are shown in Fig. 16B so that the depth of the defects can be appreciated. The HVF showed deep “defects” in both eyes with losses ranging from -6 to -28 dB (Fig. 16B). The HVFs for the difference between the two eyes is shown in Fig. 16D. When we obtained mfVEPs from this patient, he was also sleepy, which was not surprising given the variety of drugs he was taking for asthma, depression and anxiety. Because he had to be kept awake and because he complained of neck pain and tension, it took much longer than usual to obtain mfVEP records. Although his records were noisy due to muscle tension, useable records were obtained, and the responses are shown in Fig. 16A after being combined into 16 groups and averaged. The interocular mfVEP probability plot in Fig. 16C confirmed that the defect in

the nasal visual field of the right eye was significantly worse than in the left eye (see blue squares in Fig. 16C). The relative defect in the lower nasal visual field of the left eye seen in Fig. 16D was not confirmed. The monocular mfVEP fields (Fig. 16E) showed little evidence of a defect. Further, the responses from both eyes are far too large given the size and depth of the HVF defect. As will be seen in Section 10.4, there should be essentially no response in regions of the field with field losses greater than about 10 dB. This patient is showing sizable visual field losses in both eyes in such regions. Thus, although a field defect is probably present in the right eye, it is relatively minor. Further, there is far less damage in both eyes than suggested by the HVFs.

Our experience thus far is that most unreliable field takers can stay awake and perform well on the mfVEP test. Occasionally poor visual field takers, such as the patient in Fig. 16, will produce poor, though often usable, mfVEP records either because of poor fixation or because they are too sleepy, too tense, or too uncooperative.

8.2. Questionable or inconsistent HVFs

A related category of patients are those whose HVF field results are questionable even though the reliability

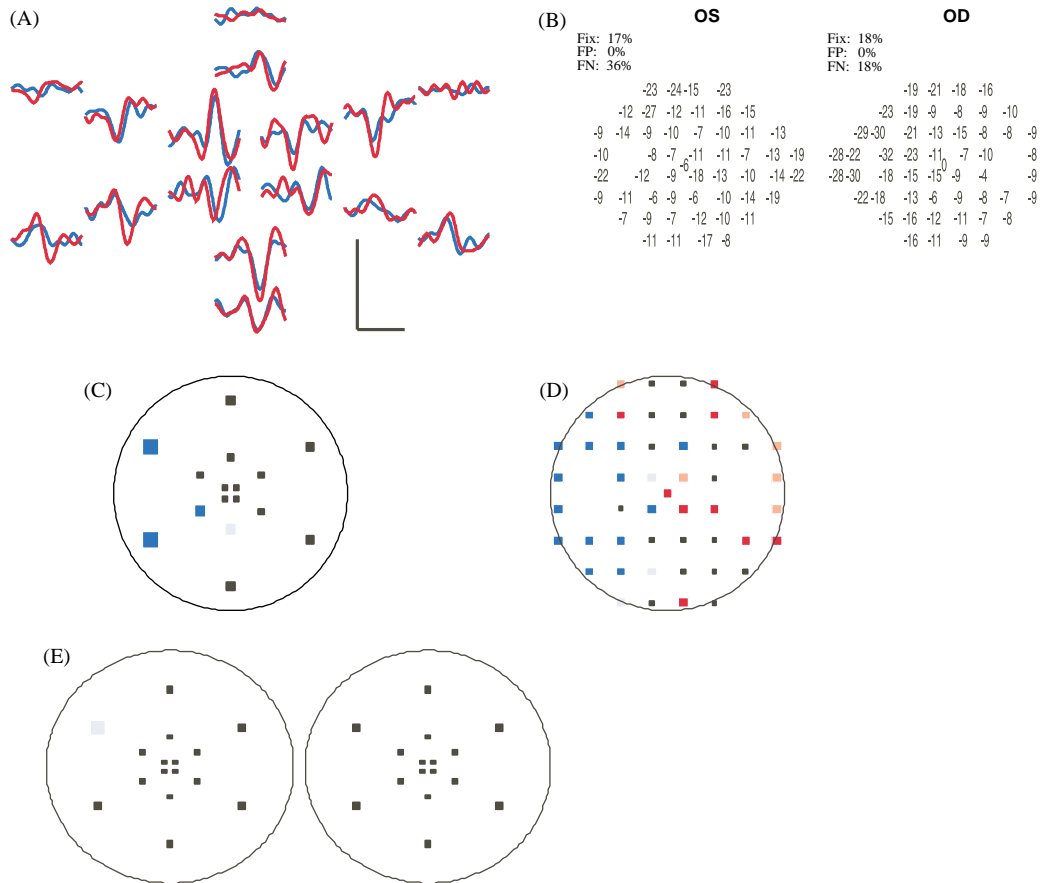


Fig. 16. Results obtained from a patient with unreliable HVFs. (A) The mfVEP responses for the right (blue) and left (red) eyes combined into 16 groups and averaged. (B) The 24-2 HVFs for the right and left eyes and the reliability indices. (C) The interocular mfVEP probability plot. (D) The interocular HVF probability plot. (E) The monocular mfVEP probability plots. The calibration bar in panel A indicates 200 nV and 100 ms.

indices are within the normal ranges; they are questionable to the ophthalmologist as they do not appear to reflect the other clinical findings. Fig. 17 shows one example. This 74 yr old female had abnormal HVFs that would not be classified as unreliable based upon standard statistics. (In fact, the reliability indices were good, 0%/0%/0% (OS) and 0%/0%/25% (OD) for percent of fixation losses/false positive errors/false negative errors, respectively.) These fields replicated 10 months later, although at this time the reliability indices for the right eye showed a 43% false positive error rate. The HVFs for both eyes had regions of sensitivity loss that exceeded -20 dB (see total deviation HVFs in Fig. 17B). Her ophthalmologist questioned the fields because they were too poor given her cup-to-disc ratios [0.6 (OD) and 0.5 (OS)]. The mfVEPs we obtained were inconsistent with her visual fields in two ways. First, the responses from both eyes (Fig. 17A) were too large given the depth of the defect. As we will see in Section 10.4 when we discuss Figs. 17E and F, responses of this size are never associated with “true” pathologic visual field defects of this magnitude. Second, the interocular mfVEP field (Fig. 17C) did not match the interocular

HVF plot (Fig. 17D). In fact, the mfVEP probability plot indicated that there was little difference between the two eyes while the HVF probability plot showed a significant difference. The monocular plots (not shown) also failed to show any abnormalities. The abnormalities seen on the HVF (Fig. 17B) are undoubtedly due to a conservative response criterion (Kutzko et al., 2000) rather than to glaucomatous damage.

Fig. 18 provides another example in which the ophthalmologist questioned the extent of the visual field damage, although the reliability indices of the HVF were good. In this case, the fields seemed very poor given the patient’s age (52 yr) and cup-to-disc ratios. In addition, there was a question of a lower visual field defect that appeared in some of the earlier fields including those seen 10 months earlier (Fig. 18B). In this patient, the mfVEP generally confirmed the defects seen in the 24-2 HVFs obtained 2 months earlier. (Compare the probability plots in Figs. 18C and D.) Note, however, there was no indication in the mfVEPs of a defect in the lower field. The monocular mfVEP plots (Fig. 18E) show good agreement with the interocular mfVEP plots (Fig. 18C).

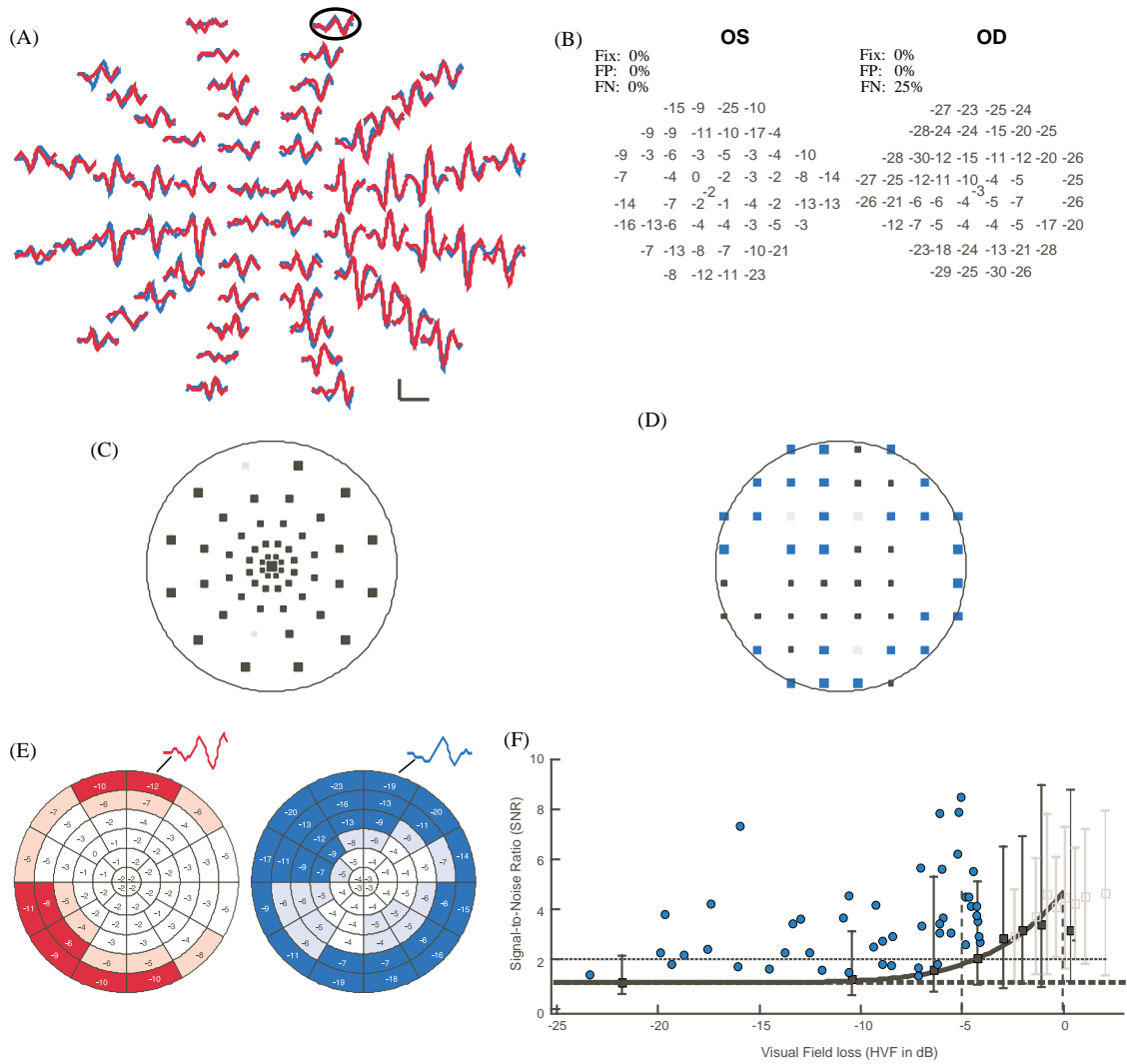


Fig. 17. Results from a patient with questionable HVFs. (A) The mfVEP responses for the right (blue) and left (red) eyes. (B) The 24-2 HVFs for the right and left eyes and the reliability indices. (C) The interocular mfVEP probability plot. (D) The interocular HVF probability plot. (E) The interpolated HVF plots shown for both eyes. (F) The blue symbols are the SNRs of the mfVEP responses, shown as a function of the interpolated HVF value for each sector, from the right eye of the patient. The black and gray symbols are the summary data for the 20 patients from Fig. 27B. The vertical lines indicate the 95% confidence intervals. The calibration bar in panel A indicates 200 nV and 100 ms.

In sum, there are patients with reliable fields as defined by the HVF indices, but whose fields are questioned by the ophthalmologist for one reason or another. In our experience, these patients are excellent candidates for the mfVEP test.

8.3. Confirmation of HVF results

There are also situations where the glaucoma specialist may be reasonably sure of an HVF defect but would like additional evidence because a decision regarding clinical management may depend upon it. The patient whose records appear in Figs. 10 and 12 is one such example. For this patient, it was important to establish the existence of a new visual field defect just outside the fovea.

Another example is presented in Fig. 19. This patient had normal tension glaucoma and was a candidate for surgery on her left eye if her visual field defect showed signs of progressing. The region of interest is outlined by the black square on the 10-2 HVF probability plot (Fig. 19B) and on the interocular HVF (Fig. 19E). This region appeared to be less affected on earlier tests. The mfVEP (Fig. 19A) performed within 1 month of the HVF showed a defect in the upper left quadrant but minimal signs (1 point) of damage in the region of interest (square in Fig. 19C). The mfVEP was repeated 3.5 months later with similar findings (Fig. 19D). The repeat reliability was good. The patient is being followed with both the mfVEP and HVF. The surprising finding here is in the lower field. The interocular mfVEP plots (Figs. 19C and D) show a defect in the lower field of the

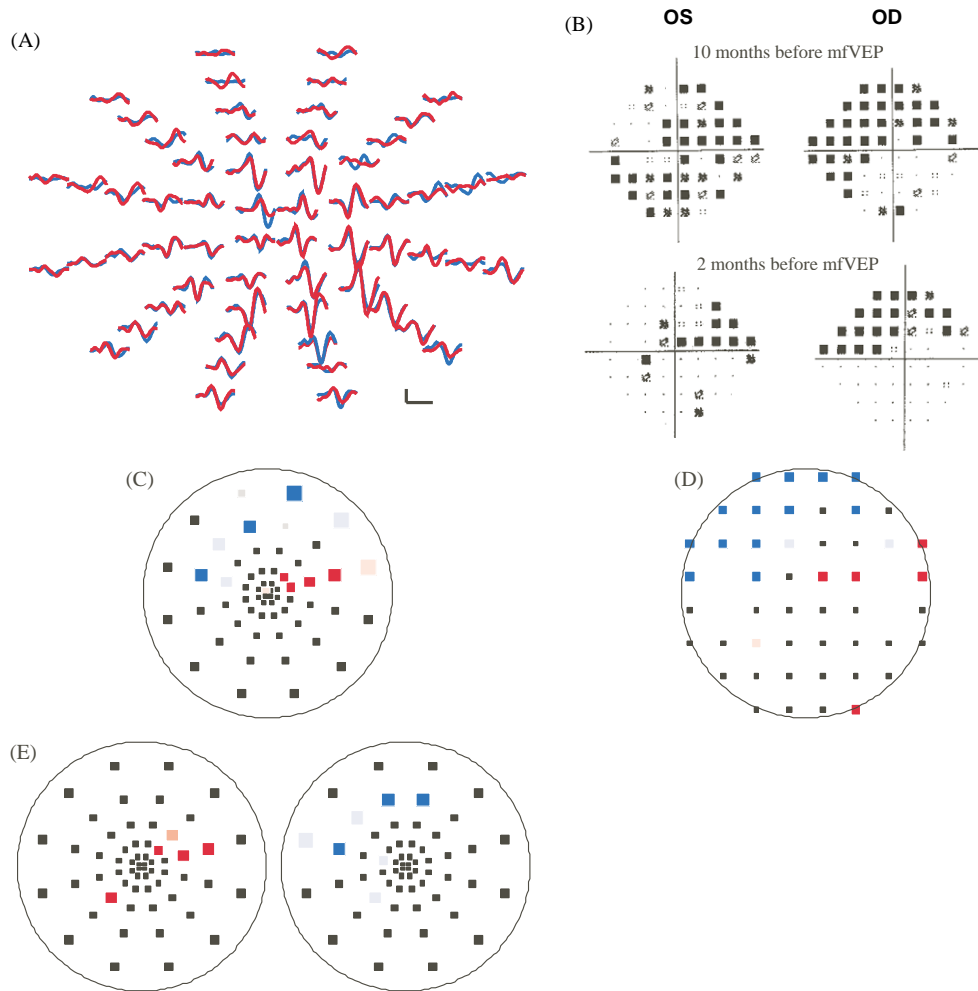


Fig. 18. Results from a patient with questionable HVFs. (A) The mfVEP responses for the right (blue) and left (red) eyes. (B) The 24-2 HVFs for the right and left eyes recorded 10 months before the mfVEP test (upper panel) and 2 months before the mfVEP test (lower panel). (C) The interocular mfVEP probability plot. (D) The interocular HVF probability plot. (E) The monocular probability plots. The calibration bar in panel A indicates 200 nV and 100 ms.

right eye. This has not been found on the HVF, but it was found with frequency doubling perimetry. Notice that the monocular mfVEP plots (Fig. 19F) show the upper defect in the left eye but not the lower defect in the right.

It is well known that optic disk changes can precede HVF damage. A recent study using scanning laser polarimetry has shown that patients with visual field defects confined to one hemifield have damage in the retinal nerve fiber layer in the presumably intact hemifield (Reyes et al., 1998). If the mfVEP technique can detect functional deficits in this hemifield, this would affect the prognosis and subsequent management of the patient. Fig. 20 illustrates an example where the ophthalmologist suspected that damage had crossed the midline but wanted confirmation because the defect in the upper fields was somewhat equivocal (Thienprasiddhi et al., 2002). In particular, on repeated HVF tests over a 2 yr period, abnormal field values were seen in the

region shown with the rectangle in Fig. 20B. However, the pattern and the extent of these defects were quite variable. The mfVEP plot in Fig. 20C shows evidence of a defect in this region. In addition, the mfVEP reveals a defect in the upper left quadrant (black oval) in a region that appeared normal on the HVF test. Interestingly, the HVF difference field (Fig. 20D) shows this defect, suggesting that the interocular comparison of HVFs may be of value. Again the monocular mfVEP plot (Fig. 20E) confirms the deep scotoma in the lower field, but misses the more subtle damage in the upper field.

8.4. Detecting early damage and progression

Detecting glaucomatous damage early and documenting its progression are keys to the successful management of glaucoma. The HVF is less than optimal in both cases. As summarized below (Section 10.7), it is well

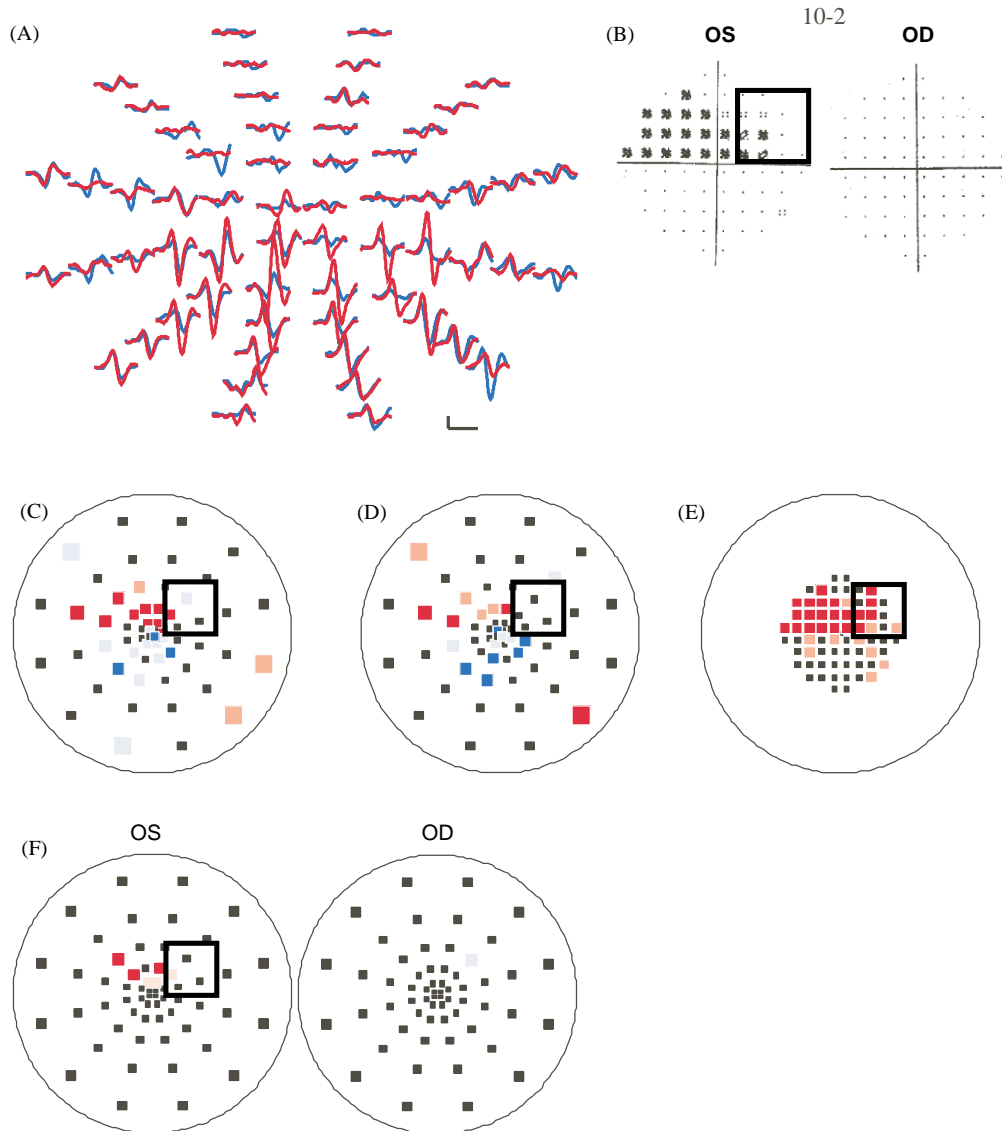


Fig. 19. (A) The mfVEP responses from a patient with normal tension glaucoma. (B) The 10-2 HVFs for the right and left eyes. The black square indicates the area of interest. (C) The interocular mfVEP probability plot recorded within 1 month of the HVF. (D) The interocular mfVEP probability plot recorded 3.5 months later. (E) The interocular HVF probability plot. (F) The monocular mfVEP probability plots. The calibration bar in panel A indicates 200 nV and 100 ms.

documented that substantial ganglion cell death can occur before abnormalities appear in the HVF. Can the mfVEP detect damage earlier than the HVF? Will the mfVEP be useful in tracking progression? These important questions have yet to be answered.

Concerning the tracking of progression, to date, nothing has been published regarding whether or not the technique will be useful. However, the ability of the mfVEP to detect progression will be limited by its repeat reliability. Recent evidence suggests that the repeat reliability is very good and the information on this topic is summarized in Section 11.4.

The important issue of early detection has yet to be thoroughly explored, although the general answer seems clear. In some patients, the mfVEP will do better than

the HVF in detecting early damage. In other patients, the reverse will be true. We have already seen examples in this article of abnormal mfVEP responses in regions of normal HVFs. The arcuate defect in Fig. 12, the lower field defect in Fig. 19, and the defect in the upper left quadrant in Fig. 20 are three examples of the mfVEP detecting damage missed by the 24-2 HVF. Further, abnormal mfVEPs have been reported in patients with normal HVFs (Goldberg et al., 2002; Greenstein et al., 2000). On the other hand, the defect marked with the black oval in Fig. 12 was well documented on the HVF but missed with the mfVEP. The defect was in a region of the upper field where mfVEP responses are small even for normal controls. Similarly, subtle defects occurring in both eyes may be hard to detect. Furthermore, in the

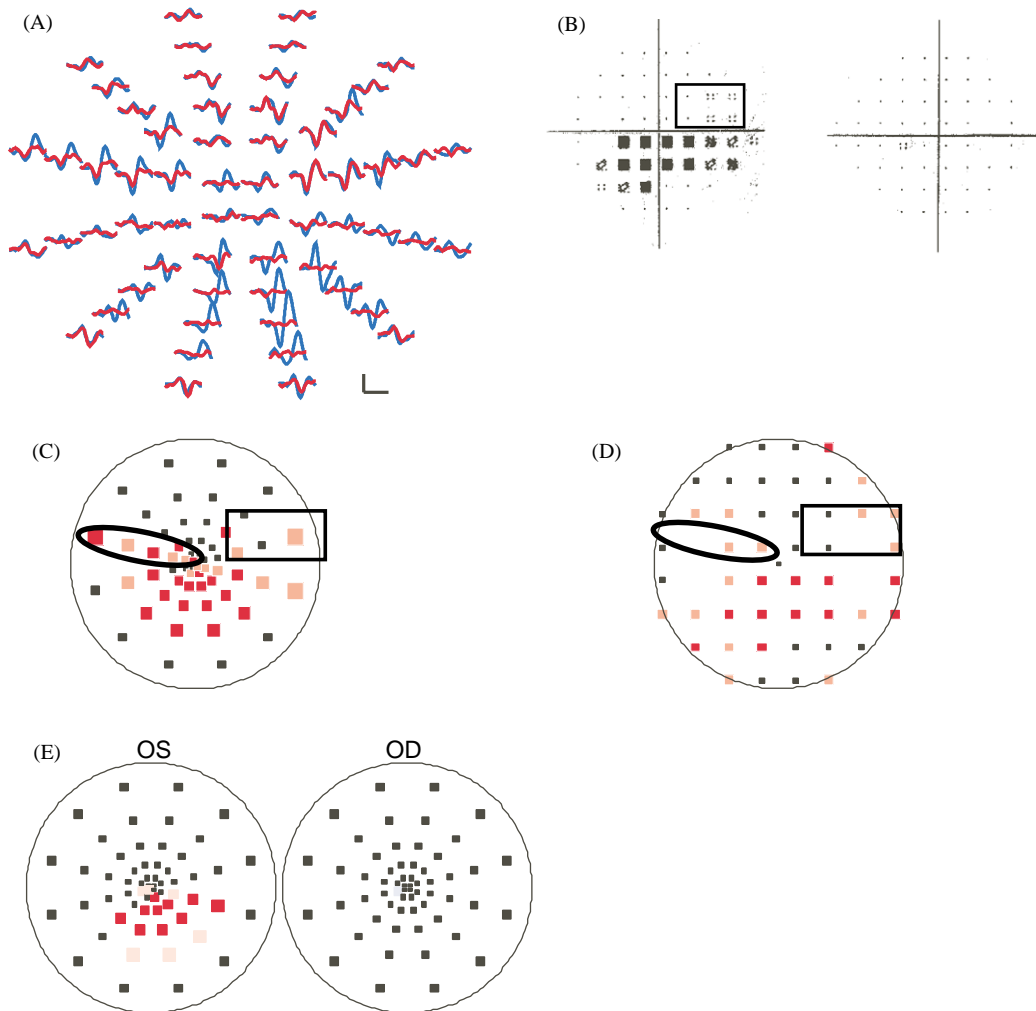


Fig. 20. (A) The mfVEP responses for the right (blue) and left (red) eyes of a patient with a unilateral hemifield defect. (B) The 24-2 HVFs for the right and left eyes. (C) The interoocular mfVEP probability plot. (D) The interoocular HVF probability plot. (E) The monocular mfVEP probability plots. The calibration bar in panel A indicates 200 nV and 100 ms.

case of those unable to perform the HVF test, obviously the mfVEP will be better. However, there are also patients who are poor mfVEP producers (see Section 12.1.2). Thus, the question is not which technique is better at detecting damage, but rather under which conditions will one technique be superior to the other. By answering this question, we hope to improve both techniques. We return to this question of which test will do better in Section 12 after introducing a signal-to-noise technique essential for this analysis.

9. Understanding the monocular mfVEP test (advanced topic)

9.1. How can a monocular test work?

We have discussed the need for a monocular mfVEP test and introduced our approach in Sections 6 and 7. The monocular test involves detecting abnormally small

signals, but some individuals with normal vision have small signals. Will the mfVEPs of these individuals be classified as abnormal (i.e. false positives)? In addition, the range of mfVEP amplitudes at any location is very large (Fig. 11). How can the monocular test detect damage if the normal range appears in some cases to include responses that approach noise level? These questions will be addressed below after our method for obtaining an SNR is presented.

9.2. Need for a signal-to-noise ratio

The mfVEP records, like all electrophysiological recordings, contain the signal of interest embedded in noise. Fig. 21A illustrates how the relative amplitudes of the signal and the noise can affect the amplitude of the record. In the first row a hypothetical signal (first column) is added to a hypothetical noise (second column) to produce a simulated mfVEP record (third column). In the second row, the same signal is combined

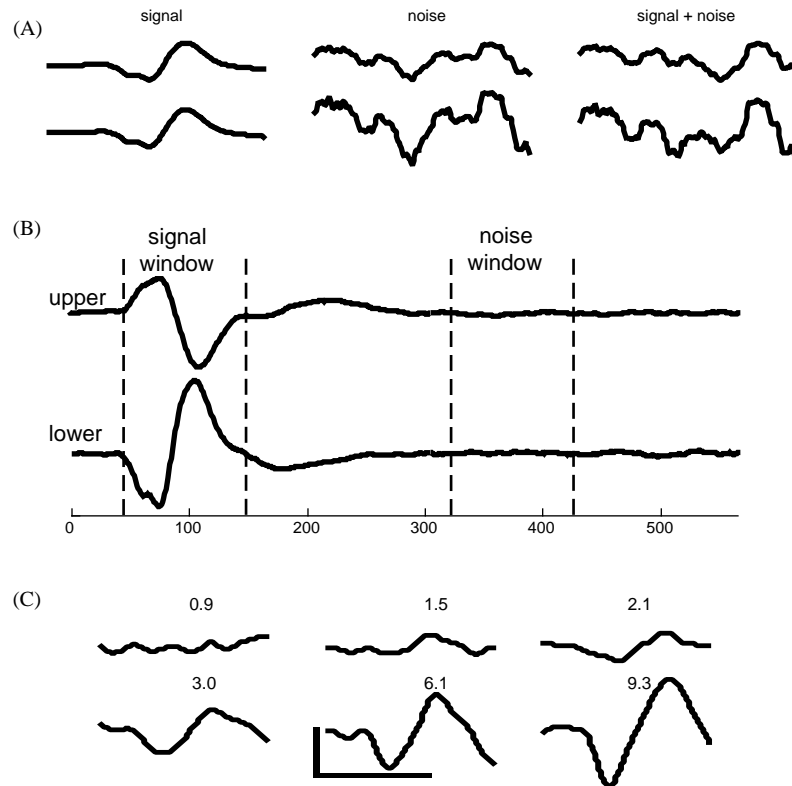


Fig. 21. (A) In the first row, a hypothetical signal is shown in the first column, hypothetical noise in the second column, and a simulated mfVEP record, the result of adding the signal to the noise, in the third column. In the second row the mfVEP record in the third column is a result of adding the same hypothetical signal to the same noise but at twice the amplitude of the noise in the first row. (B) The signal and noise windows used in the calculation of the SNR. The SNR is the amplitude (RMS) of the signal window divided by the mean RMS of the 60 noise windows. (C) Sample responses from a control subject showing a range of SNR values.

with the same noise component, but at twice the amplitude. (That is, the amplitude of the noise in the first row is multiplied by two at each point in time to produce the noise component in the second row.) The result is a record (third column) with a larger amplitude than the one in the first row, although the signal contributions are identical. If we had a measure of the noise (column 2) in the record, then we could take the level of noise into consideration.

Taking noise into consideration is particularly important for a monocular test. Individuals can vary in how noisy their records are and noise can be confused for a response. There are various approaches to this problem and some of these have been applied to the mfVEP (Zhang et al., 2002; Hood et al., 2002a; Klistorner and Graham, 2001; Hasegawa and Abe, 2001). Zhang et al. (2002) compared several methods and decided upon the one illustrated in Fig. 21B. To obtain a record with only noise, they chose a part of the record (“noise window” in Fig. 21B) that appeared free of the response and that was of equal length to the period within which the response was analyzed. Confirmation that this window contains relatively little signal can be found in the mfVEP responses in Fig. 21B, which are the averaged responses from 14 control

subjects for the responses to the 30 sectors above (upper field) and 30 sectors below (lower field) the midline of the display. Notice that there is little indication of a signal in the “noise window” (i.e. the period from 325 to 430 ms) in Fig. 21B. (There is probably some signal present in this window, but it is very small relative to the signal in the signal window.)

To obtain an SNR, the amplitude (RMS) of the “signal window”, which contains both signal and noise, is divided by an estimate of the amplitude (RMS) of the “noise window”, which to a first approximation contains only noise. To obtain the best estimate of noise for each eye, the mean RMS amplitude of the noise window of all 60 responses is obtained. The SNR of an individual record is defined as the RMS of the signal window divided by the mean RMS of the 60 noise windows.

It is important to note that the SNR is actually not a measure of signal divided by noise. Rather, the SNR is a measure of the signal plus noise of a given record divided by a measure of the average noise level. So, for example, if there were no signal present, then, on average, the SNR would equal 1.0. Of course, under these conditions individual SNRs could be greater or less than 1.0 depending upon the noise in the individual record.

Fig. 21C shows sample responses from a control subject chosen to show a range of SNR values. [Note the SNR defined here is equal to the one defined in Zhang et al., 2002 plus 1.0.] Since the mean SNR of a record with only noise is 1.0, it is not surprising that it is difficult to discern a signal in the record with an SNR of 0.9. In the record with an SNR of 1.5, the signal is barely discernible. With further increases in SNR, the signals become larger, the waveforms more consistent and one can be more confident that the response represents the signal.

9.3. Noise window as a proxy for a total defect

One of the problems that a monocular test has to overcome is the variation in the SNR within and across normal subjects. To illustrate this problem, we will make use of the fact that the “noise window” contains essentially no signal. Thus, the SNRs for the noise-only window provide a distribution of SNRs for records without a signal (Hood et al., 2002a; Zhang et al., 2002). The dashed curve in Fig. 22A is the frequency distribution of the SNRs for 3600 noise windows (30 normal individuals \times 2 eyes \times 60 mfVEP records from the best channel). The solid curve is the distribution of SNRs for the signal windows of the same records. [The x -axis is the logged (SNR) since this yields a distribution that is well approximated by the normal distribution.] Notice that the peak of the noise distribution is at 1.0. The noise and signal distributions overlap indicating that some of the mfVEP responses from the signal window cannot be distinguished from noise. For example, suppose the criterion for detecting a response in the signal window was set at the vertical line (-1.96 SD). The area under the solid curve (signal window) to the left of the vertical line comprises 2.5% of the total responses. Thus, one would conclude incorrectly that there was no signal present for 2.5% of the normal mfVEPs. This is a false alarm (or false positive) rate of 2.5%. (Note that the definitions of false alarms, false positives, etc. used here are consistent with their use in the medical literature and are opposite to those used in the literature on Signal Detection Theory.) The area under the dashed curve (noise window) to the right of the vertical line comprises 6.4% of the total noise windows. Under these conditions, one would conclude that there was a signal present when in fact there was no signal present. Consequently, even when a defect is so extreme that there is no signal, a monocular test will miss a significant proportion of the abnormal responses, on average a 6.4% false negative (or miss) rate. [It is important to keep in mind that these calculations apply to the particular recording parameters (e.g. 14 min records per eye) employed.]

Fig. 22B contains the same analysis for two of the control subjects. These individuals have reasonably

similar noise distributions (dashed curves), but the SNR is, on average 2 times larger for one (black curves) as compared to the other (gray curves). Suppose we were try to detect the difference between noise and a signal in these individuals using the -1.96 SD cutoff (vertical line) from the group data in Fig. 22A. For the group data, 2.5% of the SNRs fall to the left of this line, which indicates a false positive rate of 2.5%. For these two controls, this rate is 0.8% vs. 4.2%. In short, this supplies quantitative evidence that a monocular test will have different a priori false positive rates for different individuals.

We saw earlier that the response amplitude, and consequently the SNR, varied across the field (e.g. Figs. 1 and 5). Thus, the signal window distributions in Fig. 22A for a group of 30 control subjects will vary across the field. The local mean will depend upon the size of the signals, and the SD will depend upon the consistency in size across individuals. Fig. 23A summarizes this variation by showing the -1.96 SD points (the location of the vertical line in Fig. 22A) for all 60 responses for the 30 subjects. The cutoff values vary from SNR values of 1.0, the mean of the noise distribution, to 3.0, well outside the noise distribution. This suggests that if a patient had no signal present in a particular location, then the false negative rate (i.e. concluding there is no defect when in fact there is one) would be essentially zero in many locations, but could be as large as 50% in others. Fig. 23B shows the false negative rate by field location for the noise window of our 30 normal subjects. They vary from 0% to 53%. (In other words, sensitivity varies from 100% to less than 50% while specificity is held fixed at 97.5%.) The two right-hand curves in Fig. 22C are the frequency distributions of SNR values for the regions with the 6 highest (squares in Fig. 23A) and 6 lowest (ellipses in Fig. 23A) -1.96 SD cutoffs. The vertical lines show the two -1.96 SD cutoffs for the two groups. In each case, by definition, 2.5% of the points from the signal window fall to the left of this line. The false negative rates (area of the noise curve to the right of the dashed line) are 34% and 0%, respectively. Thus, for the regions with the 6 lowest SNR cutoffs, 34% of the responses with no signal present will be classified as “normal”, while for the regions with the 6 highest cutoffs this value approaches zero.

This analysis provides a quantification of the two concerns expressed in the preceding section. First, for a monocular test to work, it has to overcome the variation in SNR among normal individuals (Fig. 22B). Second, the 95% confidence interval at some places in the field approaches the level of noise. This implies that glaucoma has to reduce the size of the signal to below the noise level for the monocular test to detect damage in some locations. We will argue in Section 10 that this is

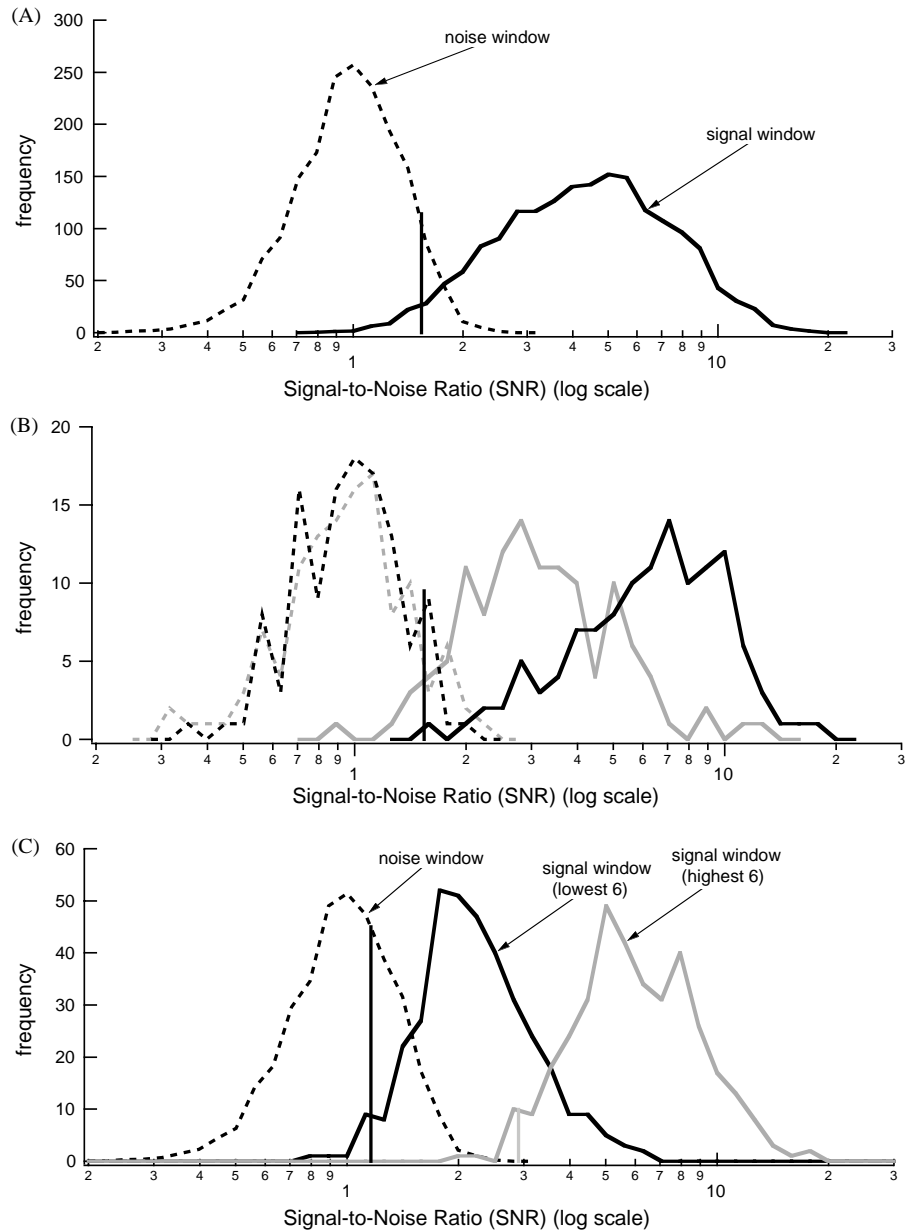


Fig. 22. (A) The frequency distributions of 1800 SNRs from 30 control subjects. The dashed curve is the distribution of SNRs for the noise window, the solid curve the distribution of SNRs for the signal window. The vertical line represents -1.96 SD for the signal window distribution. (B) As in A, but for two of the control subjects. (The black curves are for one subject, and the light gray curves are for the second subject). The vertical line (-1.96 SD for the entire group) is the same as in panel A. (C) The two curves on the right-hand side are frequency distributions of SNRs for mfVEP locations with the highest and lowest values. The vertical lines are the two -1.96 SD cutoffs for the two signal windows. Modified and reproduced with permission from Hood et al. (2003c).

indeed the case. First, the problem of the variation in SNR among individuals will be considered.

9.4. Individual variations in SNR: distinguishing false positives from true defects

There is a wide range of SNRs among normal individuals. In our control group of 30 subjects, the mean SNR varied by a factor of about 3, from about 2.0–6.0. The relatively small SNRs in a few individuals

can be traced, in part, to high noise levels. However, by and large, the variation in SNR among controls is attributable to a variation in the size of the signals. It is this range of SNR values that creates a problem for tests of significance, especially those based upon analyses of monocular mfVEPs. Individuals with small SNRs show many more significant points on the monocular mfVEP probability plots than do individuals with large SNRs (Hood et al., 2003c). Fig. 24 shows the probability plots for the six controls with the lowest SNRs out of the

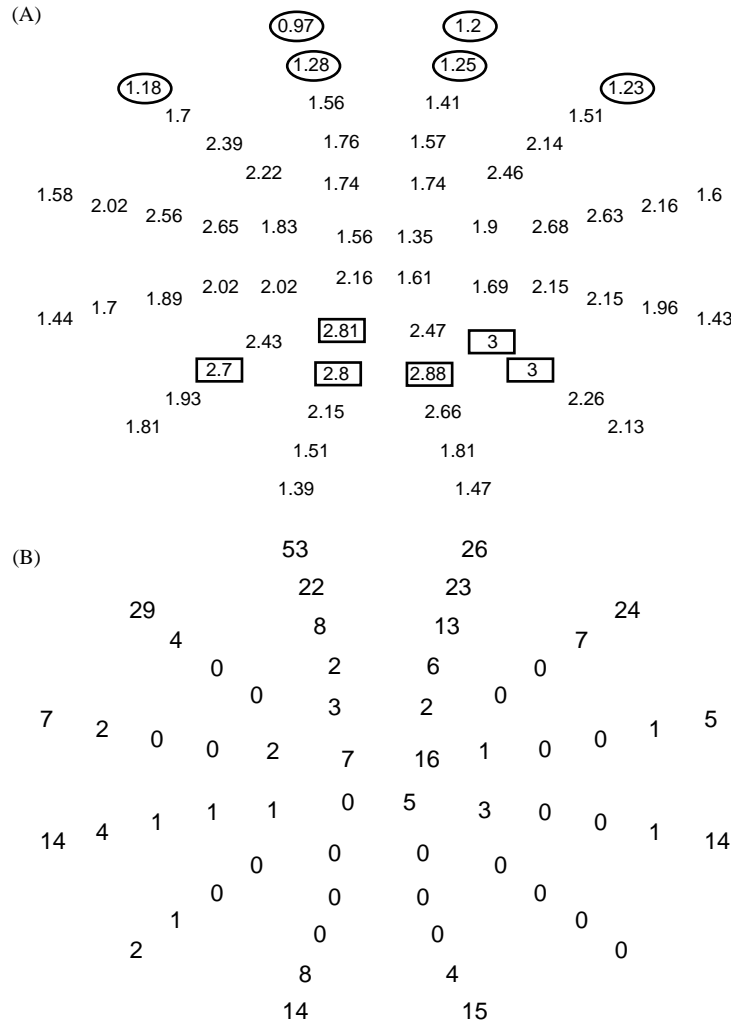


Fig. 23. (A) The -1.96 SD points (the location of the vertical dashed line in Fig. 22A) for all 60 locations for the 30 control subjects. The SNR values range from 0.97 to 3.0. The regions with the highest (squares) and lowest (circles) cutoffs (-1.96 SD) are indicated. (B) The false negative rate by field location for the 30 control subjects. They range from 0% to 53%. Reproduced with permission from Hood et al. (2003c).

group of 30. These six controls had a large number of significant points (15, 11, 11, 9, 9, and 7) on the monocular plots, far exceeding the expected number of 3 per eye. The six controls with the highest SNRs (not shown) had no significant points on the monocular plots. The wide range of significant points among normal controls presents a problem for a monocular test.

Clearly the 5% criterion does not have the same meaning for every individual. Thus, there is no simple theoretical approach to deciding what constitutes a defect (Hood et al., 2003c). As described in Section 6.1, defining a defect in terms of a cluster of abnormal points circumvents this problem to some extent. The clusters satisfying our criteria (see Section 6.1) are circled in green in Fig. 24. These six individuals with the lowest SNRs show significant clusters in 3 of the eyes. In fact, this represents the total number (i.e. 3) of false positives

out of the 60 normal eyes. Thus, individuals with relatively small SNRs will be more likely to produce false positives on the monocular test even when a cluster criterion is used. Since the number of significant points in the interocular test is not correlated with the SNR, the interocular plots in Fig. 24 show fewer significant points than on the monocular plots, ranging from 1 to 3 points (the expected number is 3). More importantly, there are no abnormal clusters in these interocular plots. Thus, for the control individuals, the interocular plots do not confirm the abnormal points found in the monocular plots.

In sum, an individual with normal vision and small SNRs will be more likely to be classified as abnormal than an individual with large SNRs. The cluster criteria helps to overcome this problem, although the false positives will still be seen among those individuals with small SNRs (Hood et al., 2003c). Further, it appears

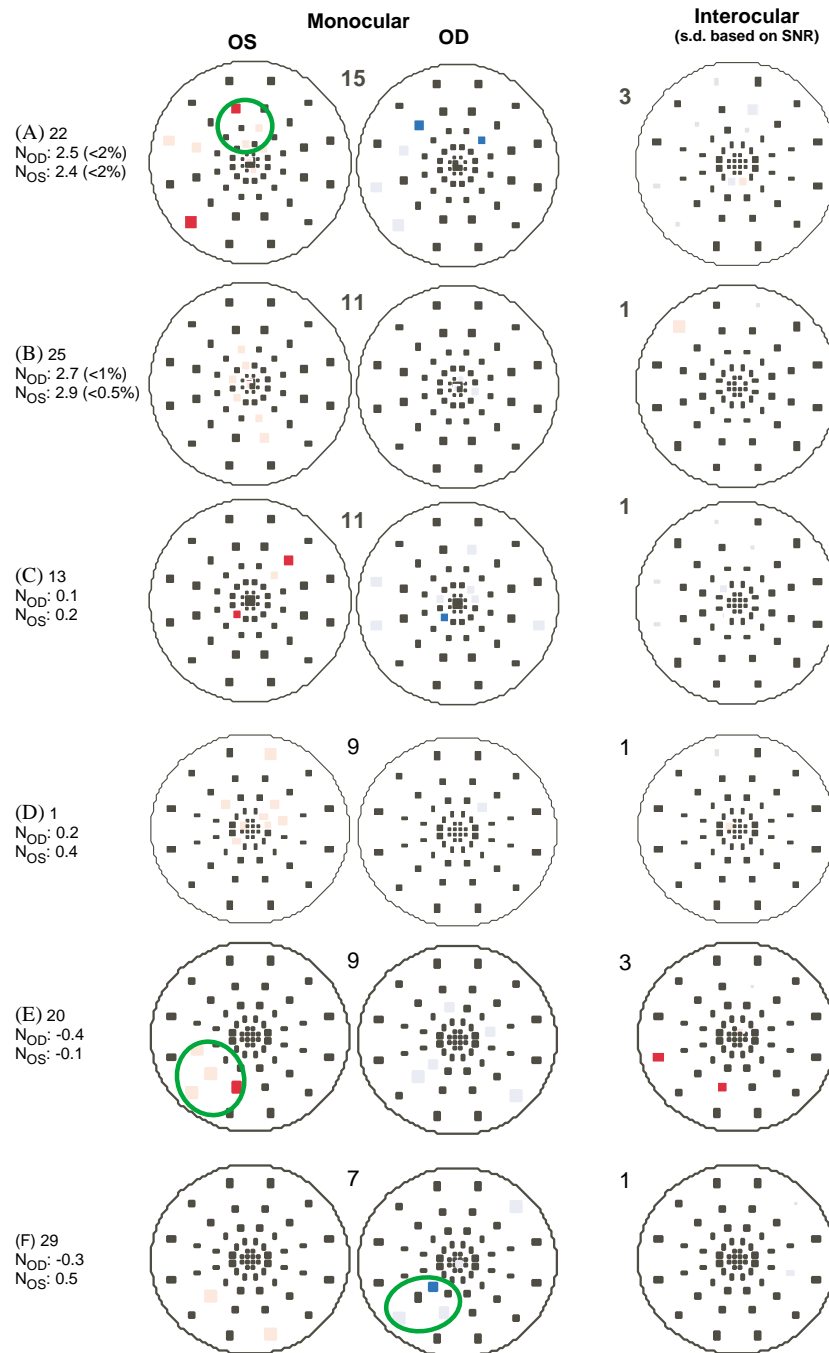


Fig. 24. Monocular and interocular mfVEP probability plots for the six control subjects with the lowest SNRs. Significant clusters of abnormal points are circled in green. The noise index is given for each eye in z -scores (see Section 12.7.3 for details). Modified and reproduced with permission from Hood et al. (2003c).

that the cluster criteria can improve specificity (i.e. decrease false positives) without substantially decreasing sensitivity (i.e. increasing false negatives or misses) (Goldberg et al., 2002; Fortune et al., 2003). One factor that makes the monocular test viable is that the significant points for the controls have a relatively low tendency to cluster, while in the case of glaucomatous damage neighboring regions are more likely to be affected (Fortune et al., 2003).

9.5. Test of the monocular test

To evaluate the viability of a monocular test, the monocular and interocular mfVEP plots from patients with unilateral damage can be compared. Figs. 25 and 26 show the monocular and interocular probability plots for 10 patients with glaucoma. These 10 patients, whose data were presented as part of a study comparing HVFs and mfVEPs (Hood et al., 2002b), had one eye with an

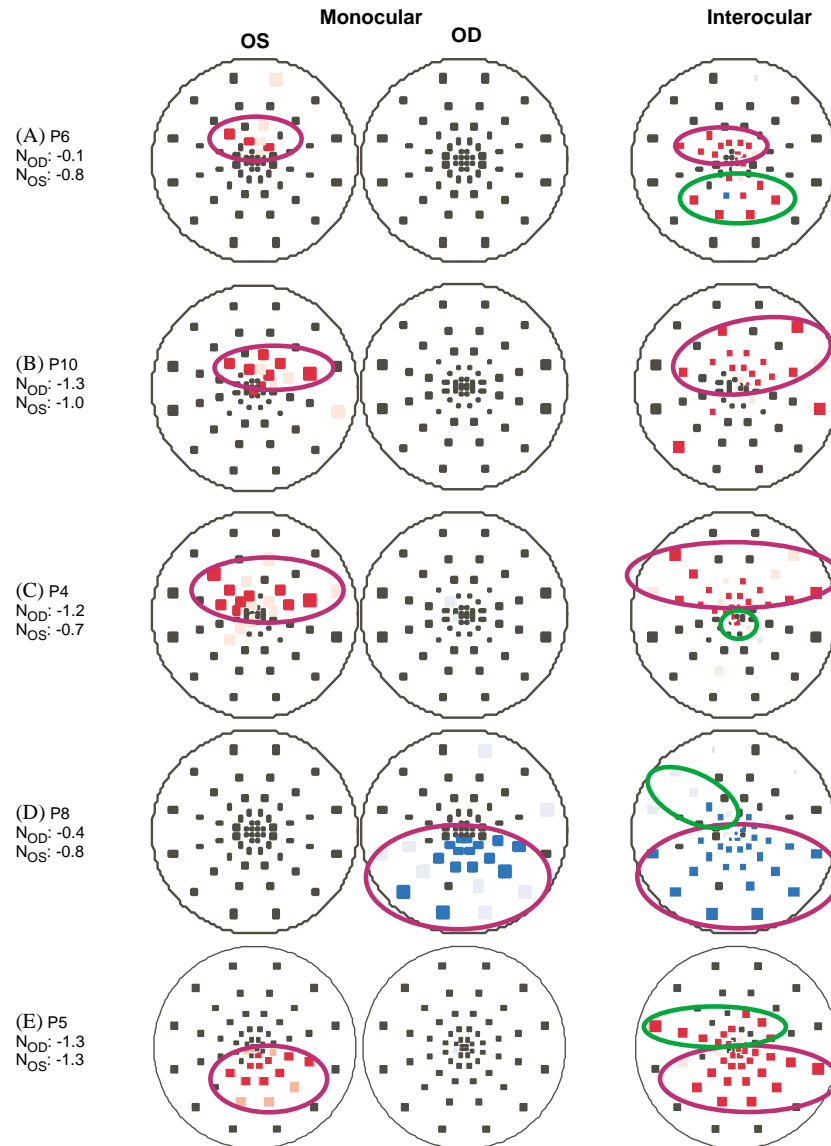


Fig. 25. Monocular and interocular mfVEP probability plots for the five patients with glaucoma (P6, P10, P4, P8, P5) who have the highest median SNR in the better eye. Significant clusters of abnormal points detected by both the monocular and interocular tests are circled in purple. Significant clusters detected only by the interocular test are circled in green. The noise index is given for each eye in z-scores (see Section 12.7.3 for details).

abnormal HVF and one with a normal HVF. The plots for the patients with the 5 highest median SNRs in the better eye are shown in Fig. 25 and those with the 5 lowest median SNRs in Fig. 26.

When compared to the interocular test, the monocular test does reasonably well. The regions circled in purple show the significant clusters detected by both tests. Those circled in green show a cluster detected in one test but not the other. For this analysis, each hemifield was considered separately. The monocular test coupled with the cluster criteria appears to detect similar defects to those detected by the interocular test. However, the discrepancies highlight important differences between the tests. There were two clusters detected

on the monocular but not on the interocular test (P7 and P3 in Fig. 26). These two defects appeared to be in regions of bilateral damage. It seems that the monocular test is capable of detecting bilateral damage missed on the interocular test. Other examples can be found in Figs. 14B and C.

While there were two clusters detected on the monocular but not on the interocular test, there were five clusters for which the converse was true (P4, P6, P8 and P5 in Fig. 25 and P3 in Fig. 26). Four of these five clusters were seen in patients with relatively high SNRs in their better eye. To explain why the interocular, but not the monocular test, detects these defects requires a better understanding of the relationship between the

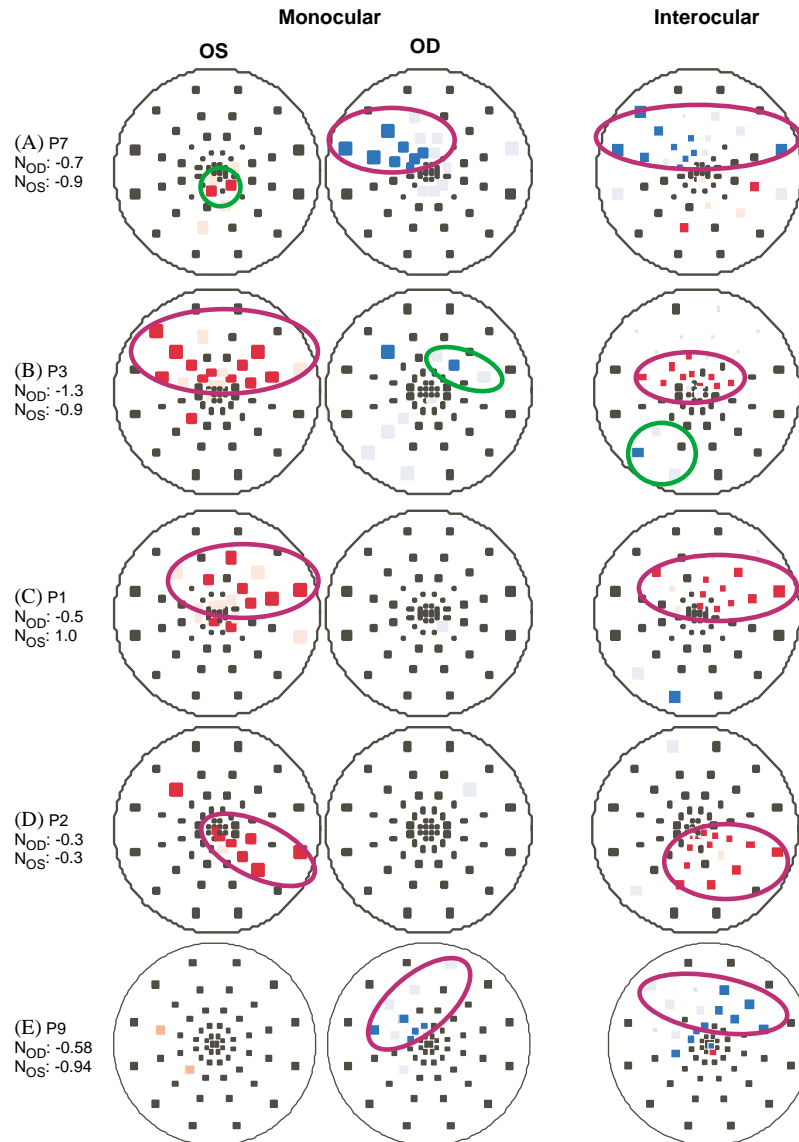


Fig. 26. Monocular and interocular mfVEP probability plots for the five patients with glaucoma (P7, P3, P1, P2, P9) who have the lowest median SNR in the better eye. Significant clusters of abnormal points detected by both the monocular and interocular tests are circled in purple. Significant clusters detected by either the monocular or the interocular test are circled in green. The noise index is given for each eye in z-scores (see Section 12.7.3 for details).

mfVEP amplitude and HVF loss. This is discussed in Section 10. For now, we can say that the interocular test will detect damage missed on the monocular test particularly when the SNR in the better eye is high.

10. Relationship between mfVEP amplitudes and HVF sensitivities (advanced topic)

10.1. Need for a theoretical understanding

It has been suggested that the mfVEP may be more sensitive in detecting glaucomatous damage than the HVF (Graham et al., 2000; Goldberg et al., 2002). We

have already seen that while the mfVEP can detect defects missed on the HVF, the converse can also be true. For example, consider the results obtained from patient P6 shown in Fig. 12. There is an arcuate defect on the mfVEP interocular plot that is missed on the 24-2 HVF. On the other hand, the HVF shows a defect in the upper portion of the superior field that is missed with the mfVEP (gray ellipse in Fig. 12C). To determine the conditions under which either test may be more sensitive to glaucomatous damage requires a better theoretical understanding of the relationship between the amplitude of the mfVEP and the depth of the HVF defect. Hood et al. (2002b) studied patients with unilateral visual field damage in an attempt to discover the underlying

relationship between the amplitude of the mfVEP and the sensitivity loss of the HVF. The results, as we will see, suggest a surprisingly simple relationship.

10.2. Interpolated field

The first step in the study of the relationship between mfVEP amplitudes and HVF sensitivities is to develop a method for comparing the results. The stimuli differ and the field is sampled differently by the two techniques (see Fig. 10D). This makes region-by-region comparisons difficult. To compare the HVF to the mfVEP results on a region-by-region basis, we developed a technique for estimating the HVF values for the regions of the visual field corresponding to each sector of the mfVEP display (Hood and Zhang, 2000; Hood et al., 2000a). Fig. 13 illustrates the technique. Based upon the total deviation scores from the HVF, we interpolate an estimated sensitivity loss for the region corresponding to each sector of the mfVEP display. Inside the black box of Fig. 13A are the HVF probability plots and total deviation values for the patient whose HVF records were shown in Figs. 9 and 10B. The monocular interpolated field for each eye of the patient is shown in the lower row. Each sector corresponds to one of the 60 sectors of the mfVEP display. They are shown here as sectors of equal size so that the numbers inside the sectors can be read. The interpolated field for the comparison of the two eyes (Fig. 13E) is obtained by subtracting the interpolated values of the left eye from that of the right eye. Thus, these numbers represent the ratio of the interpolated difference in sensitivity between the right and left eyes (i.e. the difference in dB). For example, 5 means that the left eye was less sensitive than the right by 5 dB or a factor of about 3. A -5 would indicate that the right eye was less sensitive by 5 dB. If the sensitivities of the two eyes are within 1.96 SD of the control group, then the sector is shown as white. The color indicates that the left (red) or right (blue) eye is significantly less sensitive at the 5% (desaturated red or blue) or 1% (saturated red or blue) level. The norms come from a study by Johnson and Spry (1999).

The interpolated fields provide a tool for both qualitative and quantitative comparisons of HVFs and mfVEPs. Qualitatively, the interpolated field tells us where in the mfVEP array we should look for defects based upon the HVF. Quantitatively, the interpolated fields allow us to examine the relationship between mfVEP amplitudes and HVF losses.

10.3. Monocular amplitudes as a function of HVF defects

To examine the quantitative relationship between mfVEP amplitude and HVF loss, Hood et al. (2002b) selected 20 patients, 10 with glaucoma and 10 with ischemic optic neuropathy (ION). All patients were

good “field takers” (as defined by the HVF statistics) and all had unilateral damage (see Hood et al., 2002b for details). In particular, the “better” eyes had normal HVFs (mean deviations (MD) of less than -2 dB), while the affected eyes had clear visual field defects (MD ranging from -1.5 to -13.4 dB). Fig. 27 summarizes the results. In Fig. 27A the SNR of the mfVEP response for a particular sector is plotted against the interpolated HVF value of that sector. Each point represents the data for an individual sector. For example, the point indicated by the arrow represents a response from a single sector of the affected eye of a patient with glaucoma. The response to this sector had an SNR of 2.1, and that sector had an interpolated HVF value of -17.9 dB. There is considerable scatter in the data, but the general trend is clear. For the affected eye (black symbols), there is a range of field losses extending to almost -35 dB. As the field defect becomes more profound, the SNR values tend to become smaller and approach the line for an SNR = 1.0 (dashed horizontal line). (If no signal were present, then the SNR would have an average value of 1.0.) The noise-only distribution in Fig. 22A provides an estimate of the expected range of SNRs when the signal is reduced to zero. The filled large circle in Fig. 27A shows the mean and the 95% and 5% limits for this noise-only distribution. There is little or no signal in the mfVEP responses for losses of about -10 dB or more.

The trends in the results are easier to discern in Fig. 27B, where the median SNR is plotted against the mean HVF loss for all the patients. (Notice that the scales in Figs. 27A and B are different.) The SNR of the “better” eye (open squares) is approximately constant at about 4.5 for an HVF MD of -1 dB or better. The SNR of 4.5 for the better eye is close to that of the median SNR (4.2) of our 30 normal subjects (open circle). The SNRs of the affected eye (filled squares) fall below this value and decrease with increased HVF loss. The affected eye reaches an asymptotic value of 1.0 (dashed horizontal line), close to that of the noise window of the controls (filled circle). With average field losses of -5 dB or more, the median SNR (square symbols) has already been reduced to a value that is in the range of noise. With HVF losses exceeding -10 dB, the overwhelming majority of the SNRs is within the 95%/5% confidence intervals of the noise distribution.

This analysis provides one key to the success of the monocular test. With modest field losses, the signal in the mfVEP is essentially eliminated. In Section 10.6, we consider why.

10.4. Detecting unreliable visual fields with large mfVEP responses

Modest visual field losses lead to very small mfVEP responses. Thus, the presence of a good SNR indicates

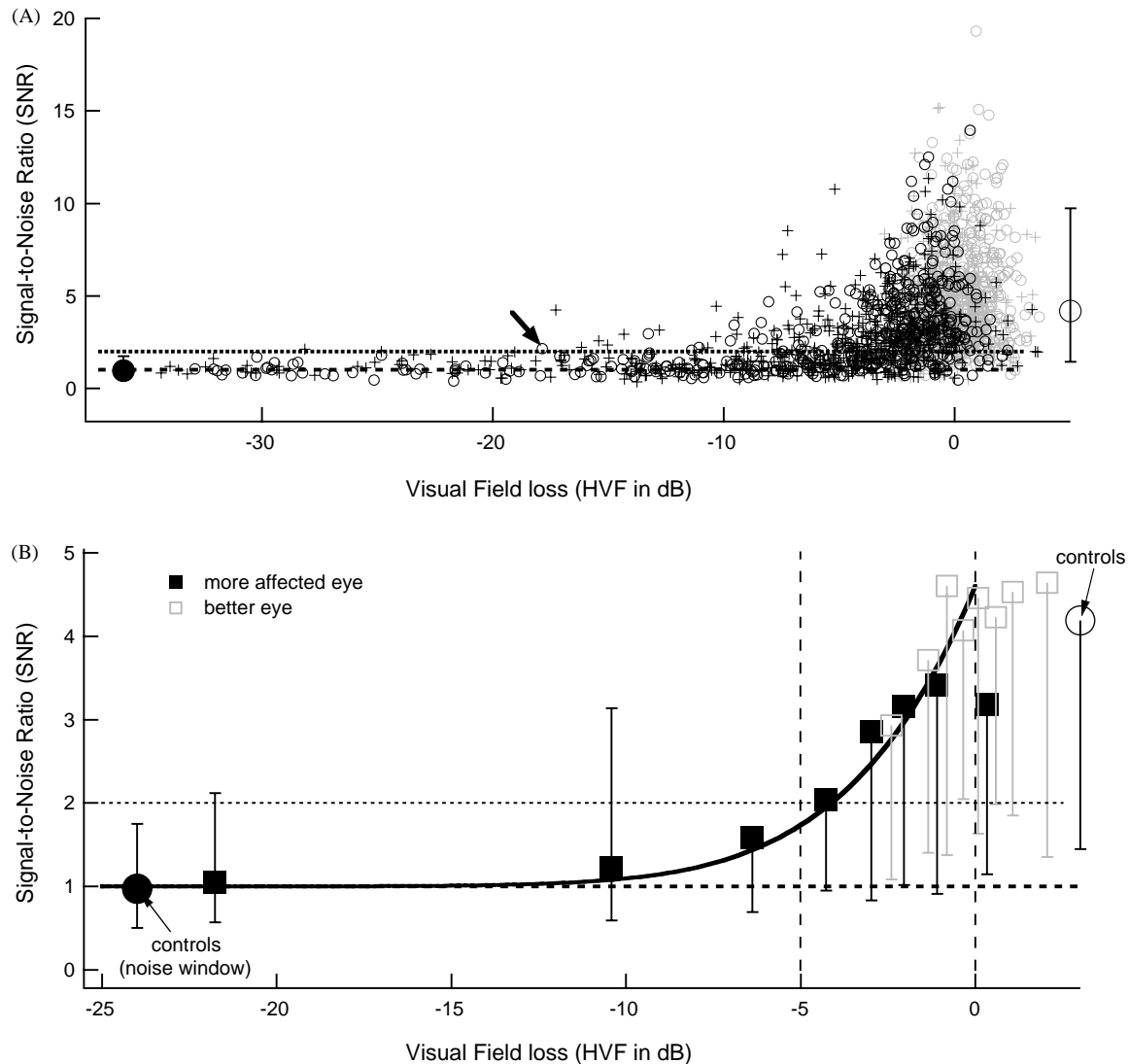


Fig. 27. (A) The SNR for the mfVEP from each sector of each of the 40 eyes of 20 patients (10 with glaucoma and 10 with ION) vs. the interpolated HVF value for that sector. The black symbols represent data for the affected eye (+ data from eyes with ION, \circ eyes with glaucoma) and the gray symbols data for the “better” eye. The dashed horizontal line represents an SNR of 1.0 and the dotted line, an SNR of 2.0. The responses for the center 12 sectors of the display were omitted as the 24-2 HVF is poorly sampled in this region (see Hood et al., 2002b). The filled and open large circles represent the mean for the noise and signal distributions from 30 control subjects shown in Fig. 22A. (B) The data for all the patients were divided into 8 bins, each with an equal number of points. The points included in the first bin were the $\frac{1}{8}$ with the largest HVF loss, those in the second bin the $\frac{1}{8}$ with the next largest HVF loss, and so on. The symbols (gray open (better eye) and filled squares (affected eye)) are the median of the SNR plotted against the mean HVF loss for that bin. (The median SNR is plotted because the SNR distribution is not normally distributed.) The error bars indicate the 95% and 5% limits. (The 95% bars are omitted for clarity when they extend off the graph.) The smooth curve is the prediction of a simple model relating mfVEP amplitudes to HVF sensitivity loss for the monocular test (see Section 10.6 for details on model) (data from Hood et al., 2002b).

that the field should be relatively good. This observation has an important clinical implication. The SNR of monocular responses can be used in situations where the clinician suspects that a large visual field defect is not “real”. An example can be seen in Fig. 17. This patient’s mfVEP response amplitudes were too large, based upon our experience, to be associated with visual field losses of -15 dB or more. Fig. 17F allows us to quantify what is meant by “our experience”. The filled black and gray symbols in Fig. 17F are the summary data from

Fig. 27B (note the change in scale of the y-axis) and the symbols in blue are the SNRs of the patient’s mfVEP from her right eye. Many of these points fall outside the 95% confidence intervals. The responses are too big given the purported visual field losses. This confirms our qualitative hunch that the HVF defects are not an accurate indication of the health of this patient’s ganglion cells. In fact, her mfVEP records are consistent with her cup-to-disc ratios, which were within the normal range. In summary, although a small mfVEP

response does not necessarily mean that there will be a visual field defect or that there is glaucomatous damage, a large response does mean that the visual field sensitivity should be reasonably good. If it is not, the visual field should be questioned.

10.5. Interocular mfVEP ratios as a function of HVF defects

To understand when the mfVEP interocular test will be better at detecting defects than the HVF, we need to know the relationship between the interocular measure of the mfVEP and HVF loss. Fig. 28 contains plots of the interocular ratio of the mfVEP (on a log scale in dB) vs. the interocular ratio of the HVF (also a log scale in dB) for the same 20 patients discussed in Section 10.3 and described in Hood et al. (2002b). These measures are comparable in two ways. First, the measures are for the same region (the sectors of the mfVEP display) of the visual field (see Section 10.2). Second, the two measures are in comparable ratio scales. For example, if the mfVEP from the right eye is 2 times larger than that of the left for a particular sector, then the log ratio of mfVEP amplitudes is 3 dB. Likewise, if the interpolated HVF sensitivity of the right eye for a particular sector is twice that of the left, then the log ratio of HVF sensitivities is 3 dB. If smaller mfVEP responses are associated with poorer fields, then the points will fall in the upper right or lower left quadrants depending upon which eye is more affected (Fig. 28A). Fig. 28B shows the results for all 20 patients. The points tend to fall into the quadrants as expected from Fig. 28A, red in the upper right and blue in the lower left. However, there is considerable variability.

The dotted line in Fig. 28B has a slope of 1.0. If the HVF and mfVEP losses (in dB) were identical, then the points should fall along this line. Scatter around this line is to be expected as each of these measures has its own independent sources of variability. However, notice that for large losses in the HVF the mfVEP points tend to fall well below the line with a slope of 1.0. There is a relatively simple explanation for these deviations. The HVF can measure losses up to -30 dB or more, while the mfVEP will be limited by the size of the signal in the better eye. Once the signal in the record is reduced well below that of the noise level, it can no longer be measured. According to this logic, the mfVEP ratio should asymptote at higher values as the SNR of the response in the better eye gets bigger. Given the range of SNRs in the better eye (see Fig. 27A), we should expect to see a range of points for large HVF losses.

Figs. 28C and D show a test of this idea. If the locations with poor responses are excluded then a clearer picture of the relationship between the mfVEP and the HVF loss emerges. Requiring one of the eyes to have an SNR better than either 3 or 6 produces the

results shown in Figs. 28C and D, respectively. (See Fig. 21C for sample responses with approximately these SNRs.) The relationship between the mfVEP and HVF ratios is now clearer. The points tend to fall near the line with a slope of 1.0 (dotted diagonal line) for relatively small field losses and tend to asymptote at a level that depends upon the SNR criterion.

This analysis also supplies a basis for understanding the relatively modest correlations that are obtained when mfVEP and HVF measures are compared. In some of the earlier studies comparable measures of the field and mfVEP similar to those described above were not obtained (Graham et al., 2000; Klistorner and Graham, 2000; Graham et al., 2000). Corresponding regions should be compared and the antilog of the HVF values should be combined (see Hood and Zhang, 2000; Greenstein et al., 2000 for a discussion). But even when care is taken to compare corresponding regions and comparable measures are used, the correlation between HVF and mfVEP is not very good ($r = 0.71$). The analysis illustrated in Fig. 28 indicates that the agreement will not be good unless one of the eyes has a reasonably good SNR. The pattern of results in Fig. 28 will be explained below in the context of a simple model.

10.6. mfVEP signal is proportional to HVF loss: a simple model

Fig. 29 illustrates a simple model that relates mfVEP amplitude to HVF sensitivity loss. We call this model “simple” because it involves only two relatively straightforward assumptions. First, it assumes that the mfVEP response (right column in Fig. 29A) is the sum of two components: signal (left column) and noise (middle column). Second, it assumes that the amplitude of the signal, but not the noise, component is proportional to the change in HVF sensitivity. In particular, we assume that if the HVF sensitivity is reduced by one half (-3 dB), then the signal portion of the mfVEP response is one half as large (-3 dB). If the mfVEP response contained only signal and no noise, then the model would predict that the point should fall at $(-3, -3)$ in Fig. 28B, on the dotted line of slope 1.0. But, the response does include noise and the noise affects the measure of the response amplitude, and thus distorts the measure of the signal. Fig. 29 illustrates two hypothetical situations in which a -3 dB loss (50% decrease) occurs in the signal amplitude. In Fig. 29A, the signal amplitude is 8 times the noise amplitude. A reduction in the signal by $\frac{1}{2}$ (-3 dB) produces, on average, an approximately 50% decrease in the response. (Note we say “on average” because in some cases it will be more, and in some cases less, depending upon how the noise reinforces or cancels local portions of the signal.) Fig. 29B shows an example where the signal is only one half (0.5) times the amplitude of the noise. Now

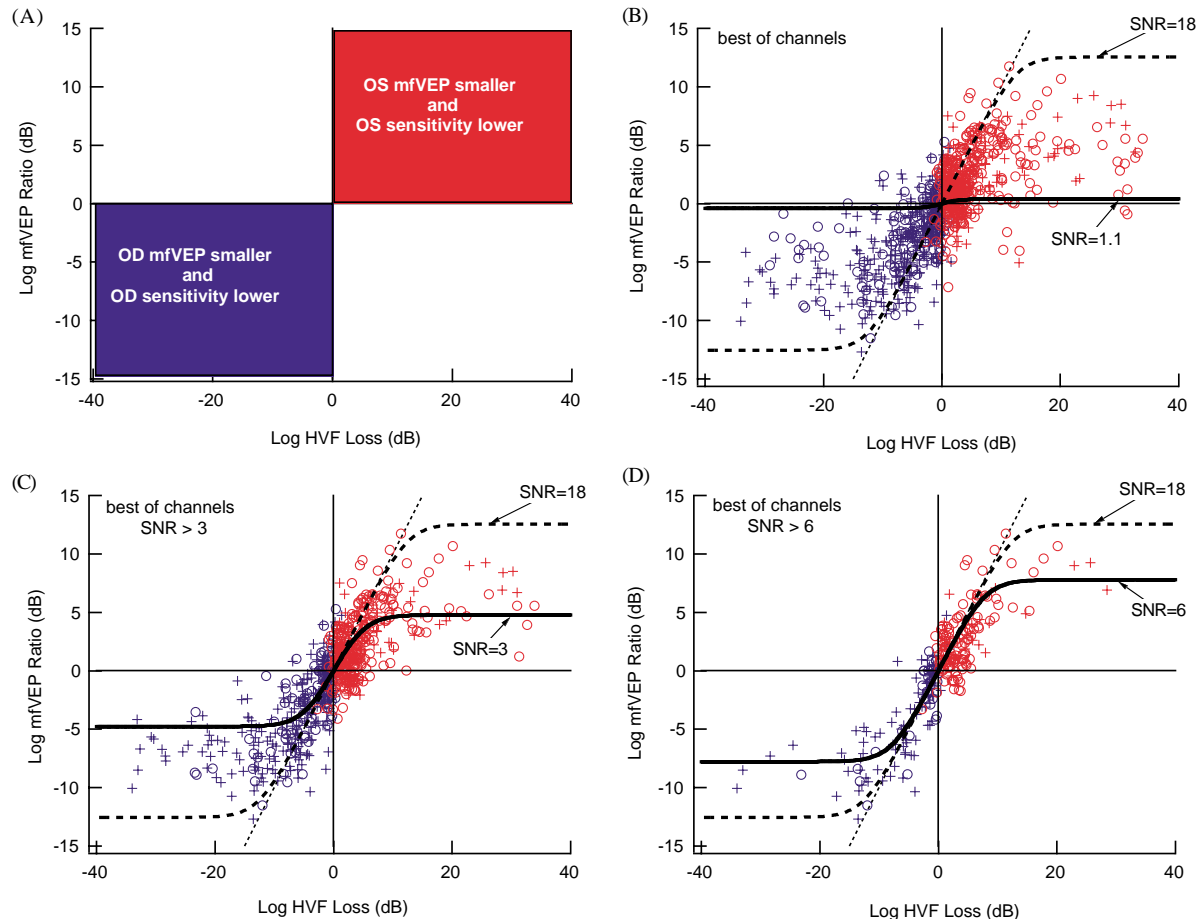


Fig. 28. (A) A key to the log mfVEP interocular ratio vs. the log HVF interocular ratio plot. (B) The relationship between the interocular measure of the mfVEP and the HVF for the 20 patients discussed in Section 10.3. Blue symbols indicate that the right eye is more affected, red symbols that the left eye is more affected. The dotted line has a slope of 1.0. (C) Results when an SNR criteria > 3.0 is required for one eye. (D) Results when an SNR criteria > 6.0 is required. The smooth curves are described in Section 10.6. Modified and reproduced with permission from Hood et al. (2002b).

reducing the signal by $\frac{1}{2}$ has very little effect on the response because the response is dominated by the noise. The smaller the signal, the smaller the change in the response amplitude associated with the -3 dB loss in the signal. In the extreme, on average there will be no change (0 dB) in the response amplitude when the signal is near zero (i.e. the response is only noise). Thus, according to this simple model, how faithfully the loss in the mfVEP reflects the loss in the HVF will depend upon the SNR before damage takes place.

Fig. 30 shows the model's predictions for monocular and interocular test data. Consider the monocular test first. The curves in Fig. 30A show the predicted decrease in SNR of the monocular mfVEP as the HVF sensitivity is decreased. All curves decrease from their initial SNR value for a 0 dB loss in HVF and asymptote at an SNR of 1.0, the average SNR for a response with no signal. According to this model, the range of results seen in Fig. 27A is to be expected as the SNR associated with a given HVF loss will depend upon the SNR before the damage took place. The model predicts that the SNR

should decrease with increased HVF sensitivity loss reaching an asymptote around the horizontal line at 1.0. A stronger test of the model can be seen in Fig. 27B. Here the smooth curve is the prediction of the model. To obtain this predicted curve we need only specify the average SNR of the affected eye before damage took place. This value is set at the SNR of the better eye (see Hood et al., 2002b for the equation). The model does a reasonable job of fitting the results for both the affected and better eyes. The exception is the solid symbol plotted at around 0 dB loss that falls below the curve. The deviation of this point from the curve suggests that the loss in signal of the affected eye may be slightly greater than predicted by the model for very small HVF losses. That is, the mfVEP maybe more sensitive for picking up very early losses than the simple model suggests.

The family of curves in Fig. 30B shows the predicted relationship for the interocular test for different SNRs of the better eye. As the SNR of the better eye decreases, the theoretical curve deviates from a slope of 1.0 at

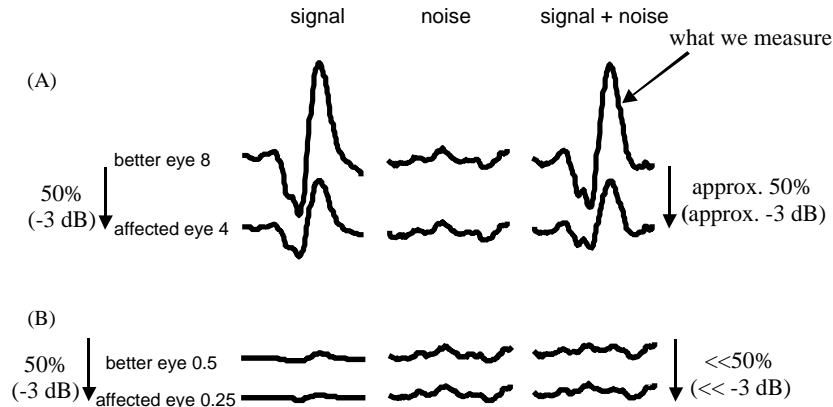


Fig. 29. (A) Features of a simple model that relates mfVEP amplitude to HVF sensitivity loss. The response in the right-hand column is the sum of two components, the signal in the left-hand column and the noise in the middle column. The amplitude of the signal is 8 times the amplitude of the noise. (B) As in A, except that the amplitude of the signal is one-half times the amplitude of the noise.

smaller HVF losses and asymptotes at a lower mfVEP ratio (see Hood et al., 2002b for equation). These predictions are also found in Fig. 28. In each panel, the prediction for the smallest SNR and for an SNR of 18 are shown. (The SNR of 18 is roughly the largest seen in the better eye.) The simple model predicts that the points should fall around and between the predicted curves. For example, in Fig. 28D if all the responses from the better eye had an SNR of 6, then the model would predict that the points would scatter around the solid curve. The scatter is to be expected due to variability in both the HVF and mfVEP (e.g. the noise components are random). Since the points in Fig. 28D have SNRs greater than 6 as well, the model predicts that the points should fall both around and between the solid and dashed curves.

The agreement with the model is good. According to the model, the signal in the mfVEP is proportional to the loss in HVF in linear, not dB units

10.7. Are mfVEP signals and HVF sensitivity losses proportional to ganglion cell loss?

The success of the simple model implies that the same relationship exists between the reduction of the mfVEP signal amplitude and ganglion cell loss, on the one hand, and linear visual sensitivity loss (antilog of dB loss) and ganglion cell loss, on the other. One simple interpretation is that each is proportional to ganglion cell loss. Hood et al. (2002b) suggested, for example, that a local loss of 50% of the ganglion cells leads to a halving of visual field sensitivity (a 50% reduction or 3 dB loss in sensitivity) and a halving of the mfVEP signal (a 50% reduction or 3 dB decrease in signal amplitude). Is it possible that each measure is linearly related to the loss in ganglion cells?

A recent study suggested that HVF loss is linearly related to ganglion cell loss (Garway-Heath et al., 2002). To support this suggestion, Garway-Heath et al. argue

that the amplitude of the pattern ERG (PERG) is linearly related to HVF loss. However, if the HVF loss is linearly related to ganglion cell loss, then the amplitude of the PERG should not be linearly related to HVF loss. There are two reasons. First, as described above for the mfVEP, it is the amplitude of the signal in the PERG that should be considered, not the amplitude of the response. Second, the PERG has contributions from cells distal to the ganglion cells (Holder, 2001). Consequently, although the Garway-Heath et al. (2002) suggested relationship between HVF loss and ganglion cell loss may be correct, it does not follow from their analysis.

In any case, the relationship between the loss in local visual field sensitivity and the local loss of human ganglion cells has yet to be established. The only direct measures of this relationship in humans can be found in post-mortem ganglion cell counts by Quigley and colleagues (e.g. Quigley et al., 1982, 1989; Kerrigan-Baumrind et al., 2000; see Quigley, 1999 for a review). In particular, they conclude that at least 25–35% of the ganglion cells are lost before defects are detected on the HVF. While this seminal work is often taken as evidence that the relationship between local field loss and local ganglion cell loss is not simple, it is, however, not inconsistent with a simple, linear relationship. Assuming the linear relationship suggested here and an SD of about 2.5 dB for the HVF, it would take, on average, a local loss of nearly 70% of the ganglion cells for a single point on the HVF to reach the 5% level (1.96 SD cutoff). Given the uncertainties involved in these estimates, the estimate based upon a linear relationship is consistent with the conclusion by Quigley and colleagues that ‘at least 25–35% of the ganglion cells are lost before defects are detected’.

Other evidence against a simple linear relationship comes from local ganglion cell counts and HVF measures from monkeys with experimentally induced glaucoma (Harwerth et al., 1999, 2002). For example,

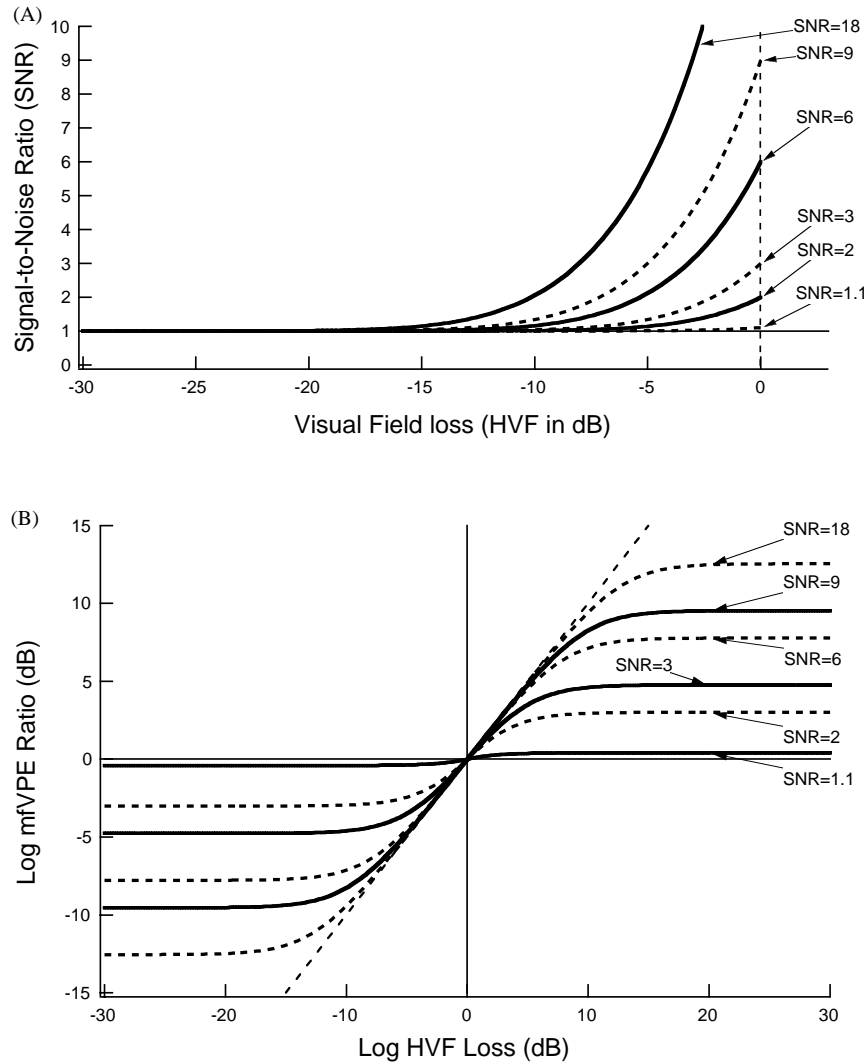


Fig. 30. (A) The simple model's prediction for monocular test data. The family of curves shows the decrease in SNR of the monocular mfVEP as a function of the decrease in HVF sensitivity. (B) The simple model's prediction for interocular test data. The family of curves shows the relationship between the log mfVEP interocular ratio and log HVF sensitivity loss for different SNRs for the better eye. Modified and reproduced with permission from Hood et al. (2002b).

for the monkeys, there are field losses of about -6 dB before ganglion cell losses are detected. This finding contradicts the finding of significant ganglion cell loss prior to HVF loss in the human post-mortem studies discussed above. Harwerth et al. (1999) suggest that either the high-pressure model for experimentally induced glaucoma is not exactly mimicking human glaucomatous damage or that the ganglion cells are damaged, but have yet to die in their monkeys. Recent electrophysiological and anatomical evidence in the monkey supports the latter conjecture (Weber, 2002).

Thus, there is no compelling evidence against a simple linear relationship between mfVEP signal amplitude, or HVF sensitivity loss, and ganglion cell loss proposed by Hood et al. (2002b). In fact, a recent attempt at modeling human HVF sensitivity loss due to ganglion cell loss concluded that there was an approximately

linear relationship between the two (Swanson et al., 2002).

11. Will the mfVEP or the HVF be better at detecting damage? A theoretical approach (advanced topic)

11.1. Detecting damage with interocular mfVEP comparisons

Will the mfVEP interocular test be better than the 24-2 HVF at detecting early damage? The model presented in Section 10.6 can be used to help answer this question. The analysis in Fig. 30B suggests that the relative effectiveness of the mfVEP and HVF in detecting glaucomatous damage will depend upon the SNR in the better eye. In fact, the answer depends both on the

SNR of the mfVEP response and on the variability in the mfVEP and HVF measures.

If the SD of the mfVEP is equal to, or greater than, the SD of the HVF, then the mfVEP, on average, cannot be superior to the HVF in detecting damage. The reason for this can be seen in Fig. 30B. Theoretically, the mfVEP loss in dB is equal to or less than the dB loss in HVF (i.e. slope ≤ 1.0). Therefore, if the SDs expressed in dBs were equal, then the mfVEP, on average, could not be better at detecting damage than the HVF. However, we find that the SD of the mfVEP can be smaller than the SD of the HVF. For the interocular test, the SD depends upon the SNR of the better eye. For our 30 control subjects, the SD of the mfVEP decreases from about 2 dB for an SNR of 2.0 to about 1.0 dB for an SNR greater than 6. In contrast, the median SD for the 24-2 HVF is about 2.7 dB for a 45 yr old individual. Thus, at first glance, the mfVEP compares quite favorably to the HVF in terms of variability. The fact that the SD for the mfVEP can be smaller than that of the HVF acts in favor of the mfVEP. On the other hand, the fact that the theoretical curves in Fig. 30B deviate from a slope of 1.0 favors the HVF. Thus, to compare the abilities of the HVF and mfVEP to detect damage, one must take into consideration both the differences in SD and the nonlinear relationship between mfVEP changes and HVF losses (Fig. 30B).

The relative advantage of one test over the other depends upon the SNR of the mfVEP. The smooth curves in Figs. 31A and B are the theoretical curves from Fig. 30B for an SNR of 6 (panel A) and 2 (panel B), respectively. (These theoretical curves are shown for the range from -8 to 8 dB for both log HVF loss and log mfVEP loss.) In both panels, the vertical (red) and horizontal (green) dashed lines show the 1.96 SD cutoffs

for the HVF and mfVEP, respectively. In particular, the mfVEP is significantly different than normal if the curve falls in the region with the green lines. Similarly, the HVF is significant if the curve falls in the region with the red lines. In both panels, the HVF cutoffs are set at 5.3 dB (1.96 times the median SD value of 2.7). As described above, the SD of the mfVEP interocular ratio depends upon the SNR. In Fig. 31, 1.96 times the SD is about 2.0 dB for the SNR of 6.0 and about 4.0 dB for the SNR of 2.0.

According to this analysis, the mfVEP never does better than the HVF for an SNR of 2.0 (Fig. 31B). The red region of the curve shows the range where the HVF is significantly abnormal, but the mfVEP is not. On the other hand, for an SNR of 6.0 (Fig. 31A), the green region of the curves shows that there is a range where the mfVEP is significantly abnormal, but the HVF is not. In the region indicated by the bold, black curve, both tests are abnormal. The mfVEP must have an SNR of about 3.0 or greater to do better than the HVF. Again, keep in mind, our purpose here is to introduce a technique for comparing the results from mfVEPs to automated perimetry. The particular results will depend upon the recording conditions (e.g. the length of the record). As the mfVEP technology is improved, the SNR and thus the advantage of the mfVEP over the HVF should improve. In any case, the conclusion is clear. The mfVEP interocular test will be better than the 24-2 HVF at detecting early damage when the SNR in the better eye is large.

11.2. Detecting damage with monocular mfVEP comparisons

The predictions of the simple model in Fig. 30A can be used to assess the relative merits of the HVF and the

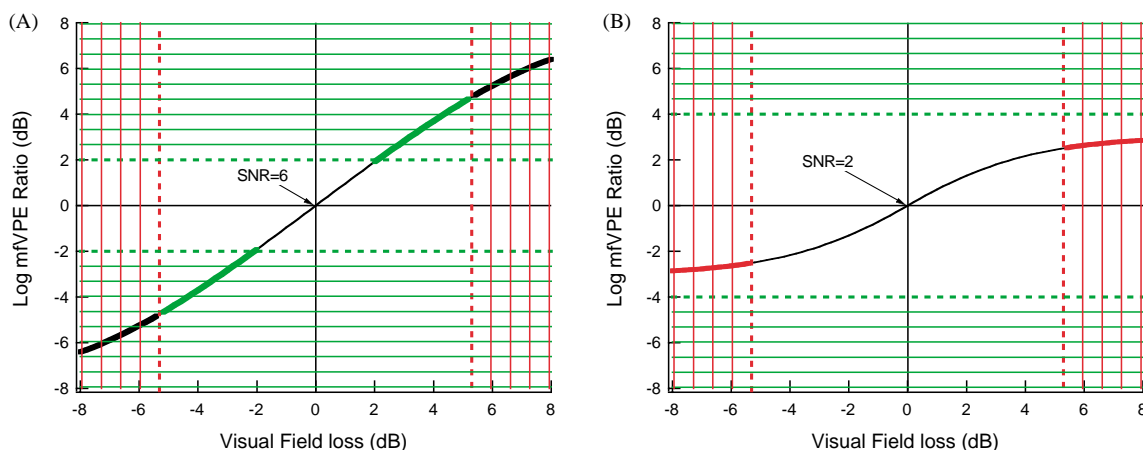


Fig. 31. The relationship between the log mfVEP interocular ratio and log HVF sensitivity loss. (A) The smooth curve is the theoretical curve from Fig. 30B for an SNR of 6. The dashed vertical (red) and horizontal (green) lines show the 1.96 SD cutoffs for the HVF and mfVEP, respectively. The green region of the curve shows where the mfVEP is significantly abnormal and the bold black region where both HVF and mfVEP tests are significantly abnormal. (B) As in panel A, but the smooth curve is the theoretical curve from Fig. 30B for an SNR of 2. The red region of the curve shows the range where the HVF is significantly abnormal.

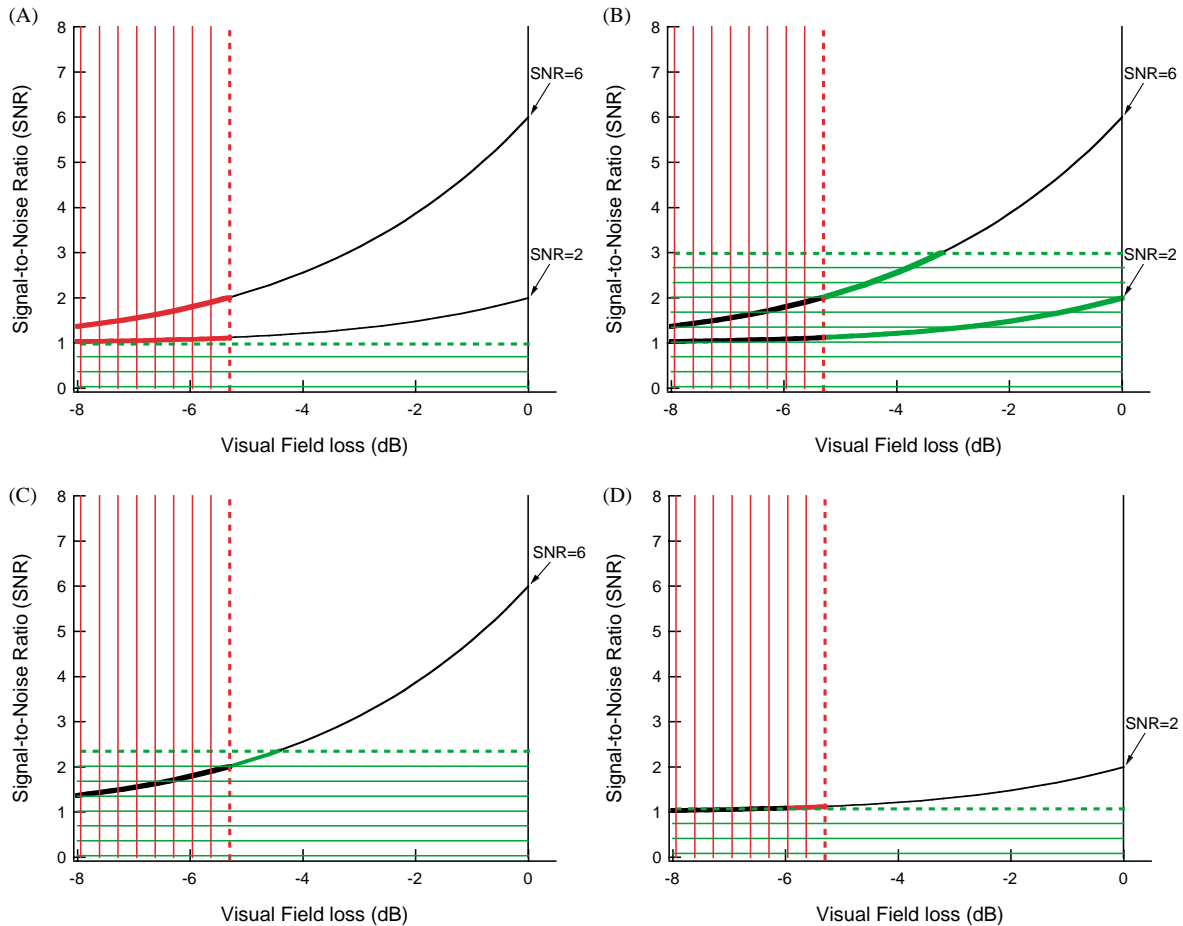


Fig. 32. The relationship between the SNR and log HVF sensitivity loss. The smooth curves are the theoretical predictions from Fig. 30A for SNRs of 6.0 and 2.0. The dashed vertical (red) line shows the -1.96 SD cutoff for the HVF. The dashed horizontal (green) lines indicate the -1.96 SD cutoffs for the mfVEP. These cutoffs for the mfVEP differ in each panel. The smallest and largest cutoffs from Fig. 23A are shown in panels A and B, respectively. In panels C and D, the dashed horizontal (green) lines indicate the cutoff associated with regions that have an SNR of 6.0 (panel C) or 2.0 (panel D). For all panels, the green region of the curve shows where the mfVEP is significantly abnormal, the red region where the HVF is abnormal, and the bold, black region where both tests are abnormal.

monocular mfVEP. Fig. 32 shows the predicted curves from Fig. 30A for SNRs of 6 and 2. As discussed above, it is necessary to take into consideration the SD of both tests. For the HVF, we use the median SD value of 2.7 dB as in Fig. 31. In all panels of Fig. 32, the points to the left of the red dashed line at -5.3 dB (-1.96 times the median SD value) are significantly abnormal on the HVF. For the monocular mfVEP test, the analysis is complicated by the fact that the -1.96 SD cutoff depends upon field location (see Fig. 23A) and not upon the SNR, as in the case of the interocular test. The dashed green lines in panels A and B show the smallest (panel A) and largest (panel B) SNR values of the -1.96 SD cutoff. Depending upon the field location of the mfVEP response in question, either the HVF or the mfVEP can be superior in detecting a defect. (The curves are color coded as in Fig. 31.) For example, suppose that a patient had a response with an SNR of 6.0 in a region where normal controls have very small responses. Under these conditions (Fig. 32A), the HVF can show a

significant defect (red portion of curve) where the mfVEP does not. On the other hand, the same mfVEP response in a region associated with very large SNRs (Fig. 32B) can show a defect when the HVF does not, in this case for an HVF value of between about -3 and -5 dB (green portion of SNR = 6 curve).

Of course, the -1.96 SD cutoffs are correlated with the SNR since the locations with the larger SNRs tend to have the larger cutoff values. The horizontal (green) dashed lines in Figs. 32C and D indicate the -1.96 SD cutoff associated with regions that have, on average, an SNR of 6 (panel C) or 2 (panel D). As above, the colored portion of the curve indicates the region where only the mfVEP (green) or HVF (red) is significantly different from normal and the bold, black portion of the curve indicates the region where both tests show significance. In these examples, the mfVEP shows an advantage for a very restricted range, about 1 dB, when the SNR equals 6 while the HVF shows an advantage over a small range when the SNR equals 2.

Thus, on average, the simple model predicts that the monocular mfVEP test and the HVF will produce fairly similar results (e.g. Figs. 32C and D). Here the operative term is “on average”. Patients who have intrinsically small mfVEP signals before ganglion cell damage will show damage earlier on the monocular mfVEP test in regions where the control eyes have large signals. The case of SNR=2 in Fig. 32B illustrates this situation. Notice, however, under these conditions there will be false positives as well. That is, the mfVEP is abnormal before damage takes place (i.e. HVF=0). The reverse will be true for patients who have mfVEP signals that are large when the retina is healthy in regions where control eyes have relatively small signals. The case of SNR=6 in Fig. 32A illustrates this point. Large decreases in the mfVEP are not showing up as significant. These examples illustrate the point made earlier. Although the monocular test will be of use, its statistical basis is not simple.

11.3. Comparison of the efficacy of the monocular and interocular mfVEP tests

Because the interocular comparison decreases the variability among the normal controls, the interocular test will be better at revealing unilateral defects than the monocular test. The probability plots for the 10 patients with unilateral defects confirm this conclusion (Figs. 25 and 26). Five defects appeared on the interocular test, but not on the monocular test. In four of these cases, the SNR was relatively high in the better eye. In Fig. 33, the difference between the total number of abnormal points detected by the interocular test, as compared to the monocular test, are shown for the better eye (open circles) and affected eye (filled circles). Overall, as

predicted by the model, more abnormal points are detected in the affected eye with the interocular test. In 8 of the 10 patients, there were more points on the interocular plot. As expected from the predictions of the simple model, the interocular test is superior to the monocular test for patients with higher SNRs in the better eye.

Although more work is needed to understand completely the relative merits of the monocular and interocular mfVEP tests, two tentative conclusions are possible. First, in general, the interocular test will be more sensitive than the monocular test in detecting early damage, and this will be especially true when the damage is unilateral. Second, the monocular test may be more sensitive when the early damage is bilateral, especially when the SNR of a region is intrinsically low.

11.4. Detecting progression and the repeat reliability of the mfVEP

Given what we have learned so far, the mfVEP will be of limited value in detecting a change in the depth of a defect. It is clear that the HVF can detect a local change in sensitivity loss of at least -30 dB, while the mfVEP, on average, cannot follow changes in the depth of a local defect that exceed approximately -6 dB (Fig. 27B). On the other hand, the mfVEP should be able to follow progression of glaucomatous damage that results in an increase in the size or extent of a defect. However, before we conclude that the mfVEP can be employed to follow an increase in the size of the scotoma, we need to know something about the repeat reliability of the mfVEP.

The ability to track progression will depend upon various factors, but it is clear that good repeat reliability is essential. Relatively little has been published thus far

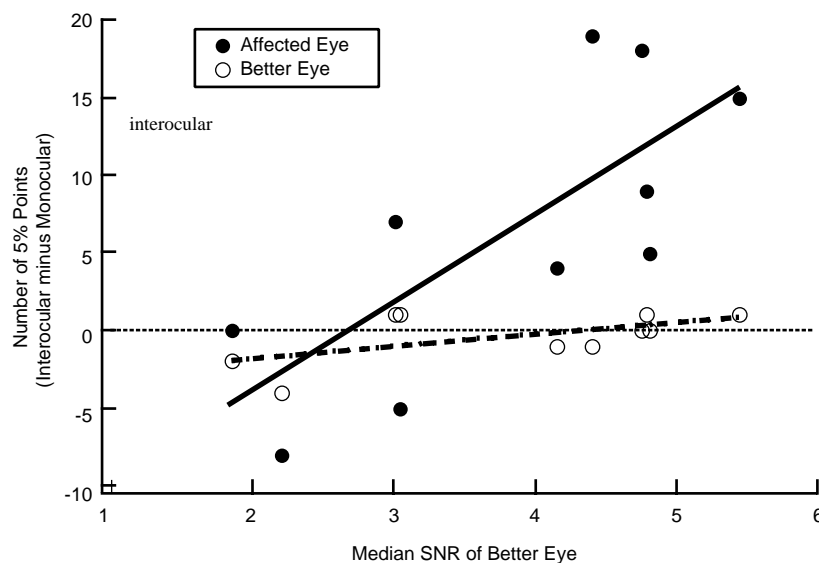


Fig. 33. The difference between the total number of abnormal points detected by the interocular test compared to the monocular test for the better eye (open circles) and affected eye (filled circles) as a function of the median SNR of the better eye. The straight lines are best fitting regression lines.

on repeat reliability, although the existing evidence suggests it is very good (Baseler et al., 1994; Graham et al., 2000; Klistorner and Graham, 1999, 2000). We (Chen et al., 2002) recently completed a study of 15 control subjects and 10 patients with glaucoma. The mfVEPs recorded on two different days from the left eye of one subject are shown in Fig. 34A. The waveforms are nearly identical, while the amplitudes show some minor variations. The mfVEP shows good repeat reliability. In particular, Chen et al. (2002) showed that the repeat reliability compared favorably to the HVF. On average, the SD for the control subjects was 1.6 dB compared to approximately 3 dB for the repeat reliability of the HVF (Johnson and Spry, 1999). Chen et al. (2002) also found that the repeat reliability of the mfVEP depends upon the amplitude or SNR of the response. The SD for reasonably large responses was less than 1.2 dB. In addition, most of the variability in the mfVEP occurred within a session. That is, the SD across days was only slightly larger (17% larger) than the SD for two recordings within a session. This was surprising as one might expect conditions to vary much more over days, especially since the electrode positions may differ.

Although the repeat reliability of the mfVEP across days is very good, this does not mean that the position of the electrodes is not important. Fig. 34B shows two runs from the same subject, but on different days. There are large differences here. See, for example, the responses inside the ellipses. The electrode placements on the 2 days were different. We determined that two different locations, about 1 cm apart, were identified on different days as the inion in this individual. That is, there were two “bumps” that could be interpreted as the location of the inion. An MRI confirmed the correct location of the inion. The mfVEP was recorded again on two different days with the electrodes correctly placed. The results for the 2 days are now similar (Fig. 34A).

The message is clear. In some individuals the inion may be hard to localize and the failure to replace the electrodes in approximately the same place can have a serious consequence. In particular, it is possible to conclude that a defect is present when, in fact, the problem was that the electrodes were not placed in the same location. To circumvent this difficulty, we measure the distance from the nasion (easier to identify than the inion) to the inion on the first testing day. For prospective studies where repeat reliability is critical, a way should be found to mark the location of the inion on the scalp. In sum, the repeat reliability of the mfVEP is very good, although in a few individuals the position of the electrodes can be critical.

12. Summary of the relative advantages of the mfVEP and HVF

Section 11 provided a theoretical consideration of the advantages of either the mfVEP or the HVF in detecting damage. Assuming reliable HVFs, this theoretical analysis suggests that the two tests will often, but not always, agree. Section 8 summarized our experience with the mfVEP in the clinic. Here we use the information from Sections 8 and 11 to provide a provisional answer to the question: Under what conditions will the mfVEP or the HVF have the advantage in detecting glaucomatous damage? To answer this question, we need to define what we mean by “each test”. By the HVF we mean achromatic 24-2 visual fields with foveal thresholds obtained using the full threshold or SITA standard strategy. By the mfVEP we mean the results of either the interocular or monocular test of mfVEP responses obtained with 14 min of recording time per eye. This section summarizes the conditions under which either the HVF or the mfVEP should have the advantage (Table 1).

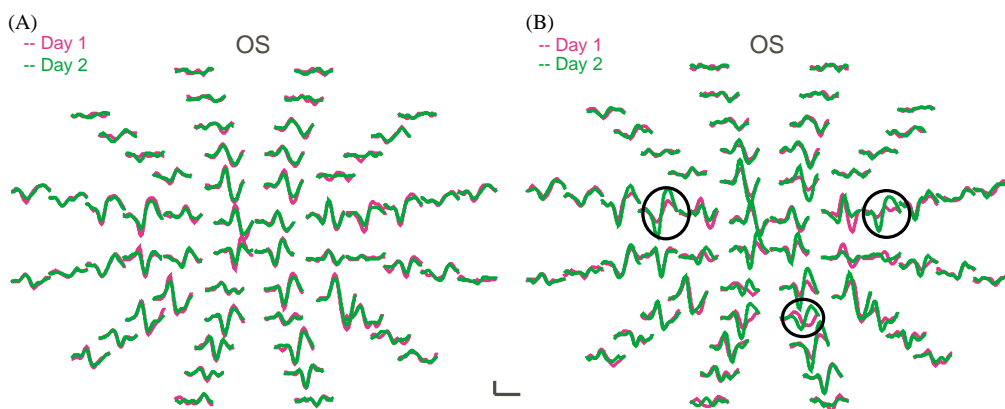


Fig. 34. mfVEP responses recorded on 2 days from the left eye of a control subject. (A) The electrodes were placed in the same location on both days. (B) The electrodes were placed in slightly different locations on different days (see text for details) The calibration bar indicates 200 nV and 100 ms.

Table 1
Relative advantages of the mfVEP and HVF tests

	Advantage mfVEP	Advantage 24-2 HVF
Confidence in test	Unreliable or questionable HVF	Poor mfVEPs (small, alpha, noise)
Size of mfVEP	Very large mfVEPs (high SNR)	Very small mfVEPs (low SNR)
Type of damage	Mild unilateral damage	Extensive and/or bilateral damage
Defect size/location	Small defect in center of field	Relatively small defect in periphery
Latency	Large latency changes	Latency not affected
Testing time	Testing time not limited	testing time limited

12.1. Confidence in test

12.1.1. Unreliable or questionable HVFs

The mfVEP offers a valuable alternative to the HVF for those patients who produce unreliable or questionable HVFs (see Sections 8.1 and 8.2). The mfVEP will usually offer a viable alternative for following unreliable field takers. Occasionally a poor HVF taker is also difficult to test with the mfVEP because he or she is sleepy, tense or uncooperative. Results obtained from a patient who was chronically sleepy are shown in Fig. 16. An example of a patient who was uncooperative is discussed in Section 8.1. This patient was so upset by the electrode paste in her hair that she refused to finish the second run of the mfVEP test. She also refused to return for any field test including the mfVEP, the HVF and the Goldmann visual field. However, our experience is that the overwhelming majority of poor HVF takers are easily tested with the mfVEP. Most patients with unreliable fields produce reliable mfVEPs.

Perhaps an even more important group of patients includes those with HVFs that we called questionable in Section 8.2. In these cases, the fields, despite having reliability indices within the normal range, do not match other clinical findings (e.g. disc appearance, cup-to-disc ratios). The mfVEP can be very helpful in the case of these questionable HVFs.

12.1.2. Poor mfVEP producers

Just as there are poor visual field takers, there are patients who are poor mfVEP producers. For example, there are patients who generate extensive alpha EEG waves and who cannot be taught to suppress them. Although this tends to be common in younger subjects, it is much less of a problem in the older glaucoma population. We do see the occasional patient whose alpha contribution to the mfVEP is so large that it is difficult to detect a defect.

There are also patients who produce more noise than others. In general, high frequency noise can be eliminated by assuring that the electrode resistance is low (at least below 5 K but preferably below 2 K). However, even with an electrode resistance below 2 K, the records can still be very noisy due to muscle tension.

This can occasionally be eliminated through biofeedback (i.e. telling the patient when the record is good). In addition, some of this noise can be removed with low pass filtering, preferably offline with a software filter. This is illustrated in Fig. 6. There are cases, however, when the records are too noisy to be of use even after filtering. This is relatively rare and poses a problem only when the patients also have small signals.

12.2. Size of mfVEP signal

The larger the mfVEP signal, the more likely the mfVEP will have an advantage over the HVF. As discussed in Section 11, the mfVEP will be most sensitive when the interocular test is employed and the better eye has a reasonably large mfVEP response, i.e. a high SNR. Although the monocular test can be used to detect damage, it is less likely than the interocular test to outperform a reliable HVF.

12.3. Type of damage

The mfVEP is more likely to detect damage missed on the HVF if the damage is unilateral and relatively mild. The theoretical analysis in Figs. 30B and 31 suggests that early damage missed on the HVF can be detected with the mfVEP if the SNR of the mfVEP is good. The purple ellipses in Fig. 25 illustrate four examples where the SNR was large and where the mfVEP showed damage missed on the HVF. Under these conditions (i.e. good SNR and unilateral damage), the mfVEP should outperform the HVF in detecting early damage.

The HVF, on the other hand, is more likely to detect damage that is extensive and/or bilateral. More extensive damage tends to produce deeper field defects up to -30 dB or more but, as seen in Section 10, the mfVEP can only decrease to the noise level. Consequently, the mfVEP can rarely decrease by more than a factor of 1/10 or -10 dB. Extensive bilateral damage in corresponding portions of the visual field is easily detected by the HVF but is difficult to detect with the interocular mfVEP test. As is clear in the examples in Figs. 14 and 26, the monocular mfVEP test can be useful in these situations. Although as we have argued above, it is

unlikely to be superior to the HVF for following the progression of extensive damage.

12.4. Size and location of defect

The mfVEP and HVF differ in the size and location of the defects each will detect. Some of these differences are a consequence of the spatial aspects of the test stimuli, while others are due to the nature of each measure. The manner in which the two tests sample the field is very different. While the 24-2 HVF is limited in its resolution by the spacing of the test points (see Fig. 12C), the HVF, in general, can detect very localized defects if the test spots are more closely spaced as in the case of the 10-2 program. On the other hand, the spatial resolution of the mfVEP is limited by the sector area needed to obtain a response of sufficient amplitude (SNR). The sectors of the mfVEP display, as originally designed by Baseler et al. (1994), were scaled to take into consideration the relative number of cells in V1 devoted to different parts of the visual field. The consequence is that the central sectors subtend a width of about 1° , while the width of the peripheral sectors exceeds 7° . The resolution is very good in the central 12 sectors. The mfVEP is clearly better than the 24-2 HVF for this central region where it rivals the 10-2 in resolution (see Figs. 12B, D and 19). Although a comparison with the 10-2 has not been made, our data suggest that the mfVEP will be useful in detecting defects in the macular and perimacular regions. Of the 10 patients with unilateral damage (Figs. 24 and 25), 6 of these showed defects in the central 2.6° on the mfVEP while only 1 of these had abnormal thresholds for the central/foveal test spot of the HVF 24-2.

In the periphery, the resolution of the mfVEP will be quite poor. The outer sectors subtend a width of more than 7° , and we need a significant change in 2 or more sectors to reliably detect damage (see Section 6.2). As seen in Fig. 35, the resolution cannot be improved in the periphery unless a way to improve the overall SNR is found. The responses in Fig. 35C were obtained with the display in Fig. 35A and the midline recording channel. To obtain this display, the sectors of the outer ring were divided into four separate regions. The purpose of this study (Hong et al., 2001) was to determine why the blind spot did not show up in most mfVEP records. The reason is apparent in Fig. 35. The area of the blind spot is shown as the circle in Fig. 35A and on the fundus view in Fig. 35B. On average, a little more than a quarter of one of the outer segments covers the blind spot. In the modified display of Fig. 35A, one of the smaller segments falls within the blind spot. There is little or no response to the segment falling within the blind spot. In Fig. 35C, the red response in the red circle, and the blue response in the blue circle, are essentially noise. However, the response to this segment from the corresponding region of the temporal retina is very

small as well. This response is small because peripheral responses for regions the size of the blind spot are small, especially along the horizontal midline.

This finding has important implications for mfVEP tests of glaucomatous damage. First, in the periphery, large defects can be missed with the mfVEP, especially if they lie in the peripheral ring near the horizontal midline and/or in the midline of the upper field. For example, the defect in the black ellipse is missed in Fig. 12B. Second, the results in Fig. 35C suggest that the spatial resolution of the mfVEP test cannot be improved by using smaller test regions, unless a way is found to increase the SNR. The responses in many of the smaller regions of the outer ring in Fig. 35C are too small to allow for a reliable detection of a change.

12.5. Latency

Thus far we have reduced the mfVEP response to a single number, the SNR in the case of the monocular test and the ratio of the RMS amplitudes in the case of the interocular test. While in the case of the HVF we are restricted to a single number based upon local sensitivity, the mfVEP response waveform can be analyzed. For example, the latency of the mfVEP response can be measured. Demyelinating diseases produce large increases in the latency of local mfVEP responses (Hood et al., 2000a; Kardon et al., 2001). In fact, it is possible to see local regions of delayed mfVEPs contiguous with regions of normal latency (Hood et al., 2000a). Since the HVF can be normal in both regions, the mfVEP has a unique advantage in detecting and tracking changes in demyelination. Glaucoma, on the other hand, appears to produce, at most, very small changes in latency (Klistorner et al., 2002). On one hand, this is not surprising since, as we have seen, relatively small field changes produce markedly reduced mfVEP signals. Thus, most of the signal in the mfVEP, even mfVEPs reduced by glaucomatous damage, will be coming from relatively healthy portions of the field. However, glaucoma has been reported to produce relatively large increases in latency of the traditionally recorded VEP (e.g. Towle et al., 1983; Atkin et al., 1983). Given the mfVEP results, these increases in latency cannot be due to changes in conduction time at or before V1. Either they are artificially produced by the summing of VEP signals from normal and abnormal regions or, more interestingly, represent delays introduced beyond V1. (Recall from Section 4.2 that the conventional VEP probably has a larger extrastriate contribution than does the mfVEP.)

12.6. Testing time

Although patients, in general, prefer the mfVEP to the HVF, the test in its current form is long. It takes 28 min of recording to obtain the data shown in this

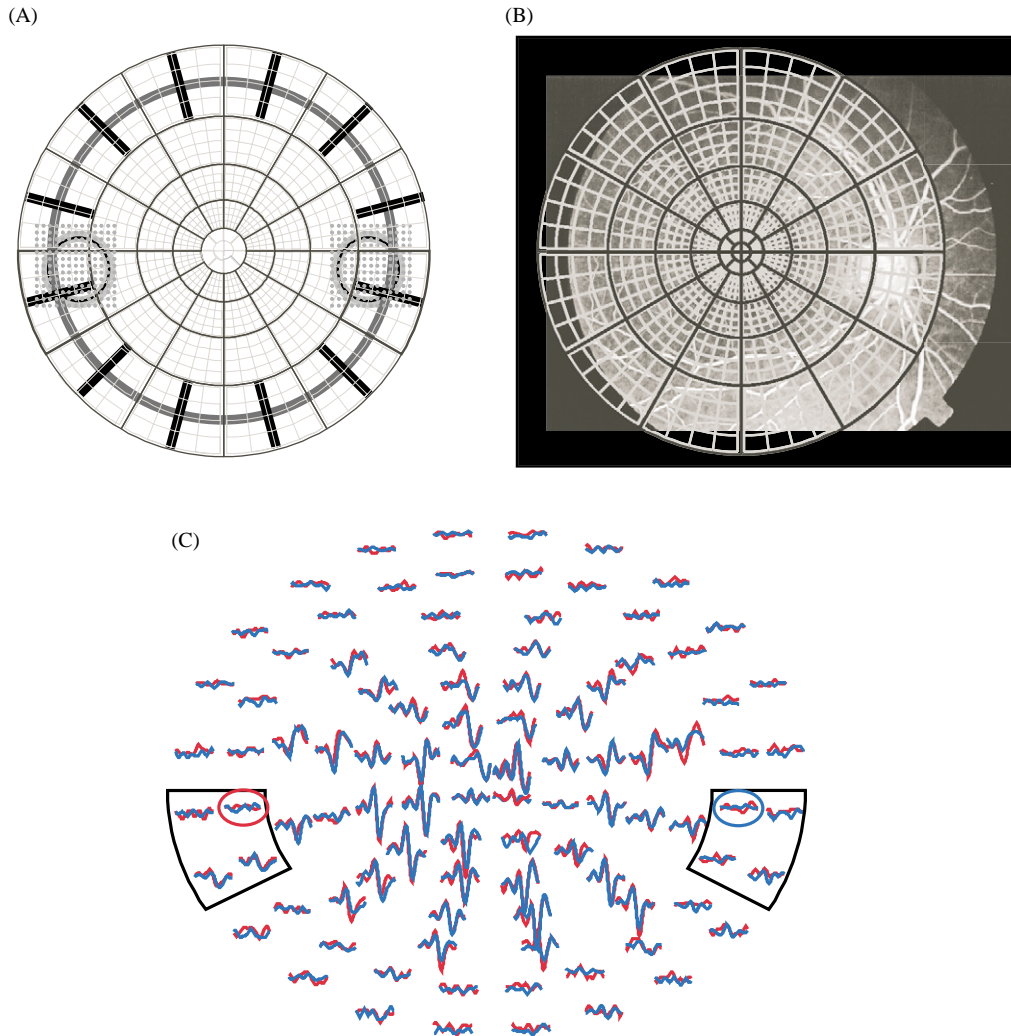


Fig. 35. The stimulus display used to determine why the blind spot is not apparent in mfVEP records. The sectors in the outer ring of the display in Fig. 1A were divided into four regions. (B) The standard display (Fig. 1A) superimposed upon the fundus. (C) mfVEP responses for the right (blue) and left (red) eyes of a control subject.

article from both eyes. For clinical purposes, we agree with Klistorner, Graham and colleagues that the time taken for recording can be reduced to 14 min or less, however the SNR will be reduced, and the mfVEP will not be as successful at detecting deficits. In either case, if we include the time it takes to prepare the patient, total testing time will take anywhere from 30 to 60 min.

12.7. Problems in common

Table 1 summarizes the relative advantages of the HVF and mfVEP discussed thus far. In addition, there are some factors that will affect the mfVEP and HVF tests in similar ways. For example, the eye lid can obscure part of the field of view and lead to an apparent defect on both the mfVEP and HVF. As in the case of the HVF, this is best avoided by monitoring the patient's eye during testing. Other factors may not have the same effects on the results of the two tests.

12.7.1. Poor fixation

Patients with nystagmus or fixation problems will not do well on the mfVEP test. The problem with nystagmus is obvious and easily identified. Eccentric fixation, or a problem with maintaining steady central fixation, may be more difficult to identify and could corrupt the results. Fig. 36 shows how apparently abnormal mfVEP responses and probability plots can be produced with eccentric fixation. A control subject was instructed to either maintain steady fixation that was down and to the left by 3° (Figs. 36C and D) or to move his fixation around a circle with a radius of 3° (Figs. 36E and F). Compared to the control condition of steady central fixation (Figs. 36A and B), the abnormal fixation condition produced apparent defects. Both the 3° eccentric fixation and the condition where fixation was moved around a circle with a radius of 3° produced abnormalities in the probability plots. Similarly, Menz et al. (2002) reported

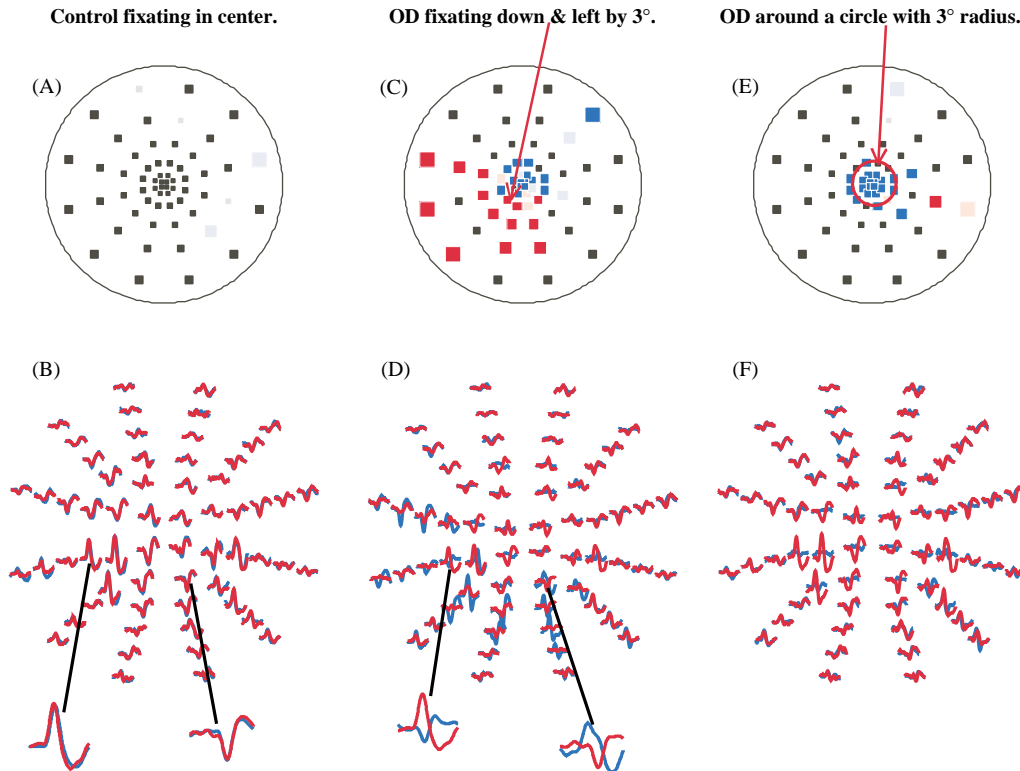


Fig. 36. The mfVEP interocular probability plot (A) and the mfVEP responses (B) for the right (blue) and left (red) eyes of a control subject who is maintaining steady central fixation. The mfVEP interocular probability plot (C) and the mfVEP responses (D) for the right (blue) and left (red) eyes of a control subject who is fixating eccentrically with the right eye down and to the left by 3° . The mfVEP interocular probability plot (E) and the mfVEP responses (F) for the right (blue) and left (red) eyes of a control subject whose fixation with the right eye was moved around a circle with a radius of 3° . Modified from Hood et al. (2003a).

decreases in the central responses with fixation errors of 1° or larger.

The eccentric fixation error is relatively easy to detect (Figs. 36C and D) (Hood et al., 2003a). The probability plot shows smaller responses in opposite parts of the field. Further, the responses from near the midline show a polarity reversal between the two eyes (see inset Figs. 36B and D). There is an important lesson here. If defects with the pattern shown in Fig. 36C are seen, then the waveforms above and below the midline should be carefully scrutinized. Further, these patients should be re-tested with equipment that either incorporates a fundus camera or a task that requires central fixation (e.g. Goldberg et al., 2002). Unsteady fixation can produce polarity reversals as well, but sometimes, as seen in Figs. 36E and F, reversals are not seen. The best way to avoid the problem of unsteady fixation is to continuously monitor the eye position during testing.

12.7.2. Pupil size, refractive error and cataracts

Pupil size, refractive error and scattered light due to cataracts have all been shown to affect the HVF (e.g. Weinreb and Perlman, 1986; Atchinson, 1987; Wood et al., 1989; Fujimoto, 1990; Budenz et al., 1993; Edgar et al., 1999). These same factors need to be explored

carefully in the case of the mfVEP. To a first approximation, decreasing the pupil size is like decreasing the overall illumination of the display. The mfVEP shows relatively small changes in amplitude and latency with large changes in illumination (unpublished observations). On the other hand, degrading the retinal image with either scattered light or defocusing may lead to depressed mfVEP amplitudes, especially in the central portion of the field. More work is required here to specify the extent to which these factors affect the mfVEP probability plots.

12.7.3. "Reliability" indices

The HVF provides three reliability indices to alert the tester to possible unreliable fields. It should be possible to develop indices for the mfVEP to help in the interpretation. For example, Hood et al. (2003c) suggested a "noise index" to indicate whether the level of noise is high relative to a group of normals. In particular, they defined a "noise index" in terms of the z -score (significance level) of the mean noise of the individual's mfVEP. The noise index is shown for each eye in Figs. 24–26. Notice that the two control subjects with the most significant points in Fig. 24 have large, and significant, noise indices. We also use measures of

SNR and alpha to help detect poor, and potentially unreliable, mfVEP recordings. This is another area in which considerable work is needed before the mfVEP technique is fully refined.

13. Conclusion and future directions

To what extent will the mfVEP replace or augment static automated achromatic perimetry? Before answering this question, it is worth emphasizing that the results from all new tests, including the new structural measures (e.g. HRT and OCT), need to be compared to the results from static automated perimetry. In this context, many of the techniques developed in this article for validating the mfVEP and for comparing it to automated perimetry can be extended to other measures as well. Concerning the mfVEP, with the currently available techniques, the mfVEP test takes longer to perform than the HVF test and it will not necessarily outperform that test. On the other hand, there are clearly many conditions under which the mfVEP will be superior to the HVF in detecting damage (see Table 1 in Section 12). In addition, there are also circumstances where patient management is improved by adding the topographical information provided by the mfVEP (see Section 8). Thus, the mfVEP does have a place in the clinical management of glaucoma. However, with current technology, the recording and interpretation of the mfVEP is not trivial and is best done by competent and experienced electrophysiologists.

It must be emphasized that the mfVEP is an evolving technology and that the future will undoubtedly see major advances. We envision that these advances will be in three general areas. First, innovations in the presentation of the stimuli will lead to improvement in the SNR of the records and to a reduction in the testing time. Relatively little has been done to optimize the stimulus parameters or to match the display to known regions of defects. Second, improvement in the positioning of the electrodes and the recording methods are also possible. Third, the analysis of the records will undoubtedly be improved, for example through the use of “neural nets” and algorithms based upon templates of the underlying response.

With these advances, we predict that the mfVEP test will become a powerful tool for the detection, management, and study of glaucoma, but it will not replace automated perimetry.

Acknowledgements

Supported by grants from the National Eye Institute R01-EY-02115 and R01-EY-09076. The authors gratefully acknowledge the help of all their collaborators at

all stages of the work reviewed here. This work would have been impossible without the help, advice, and encouragement of the ophthalmologists with whom we work, Drs. Myles Behrens, Jeffrey Liebmann, Jeffrey Odel, Robert Ritch, and Phamornsak Thienprasiddhi. Our undergraduate, graduate and medical students, Candice Chen, Annemarie Gallagher, Jenny Hong, Nitin Ohri, and Bryan Winn helped at all stages from data collection to editing. In addition, we thank Drs. Mitch Brigell, Brad Fortune, Joy Hirsch, Karen Holopigian, and Michael Wall for their comments on an earlier version of the manuscript. Finally, a special thanks is extended to Xian Zhang who has been our valued collaborator on this work from its conception.

References

- Aine, C.J., Supek, S., George, J.S., Ranken, D., Lewine, J., Sanders, J., Best, E., Tjee, W., Flynn, E.R., Wood, C.C., 1996. Retinotopic organization of human visual cortex: departures from the classical model. *Cereb. Cortex*. 6, 354–361.
- Atkin, A., Bodis-Wollner, I., Podos, S.M., Wolkstein, M., Mylin, L., Nitzberg, S., 1983. Flicker threshold and pattern VEP latency in ocular hypertension and glaucoma. *Invest. Ophthalmol. Vis. Sci.* 24, 1524–1528.
- Atchinson, D.A., 1987. Effect of defocus on visual field measurement. *Ophthalm. Physiol. Opt.* 7, 259–265.
- Barber, C., 1998. The multifocal ERG and VEP. In: Stalberg, E., de Weerd, A., Zidar, J. (Eds.), *Proceedings of the Ninth European Congress of Clinical Neurophysiology*. Monduzzi Editore, Bologna, Italy, pp. 209–216.
- Baseler, H.A., Sutter, E.E., 1997. M and P components of the VEP and their visual field distribution. *Vis. Res.* 37, 675–690.
- Baseler, H.A., Sutter, E.E., Klein, S.A., Carney, T., 1994. The topography of visual evoked response properties across the visual field. *Electroencephal. Clin. Neurophysiol.* 90, 65–81.
- Betsuin, Y., Mashima, Y., Ohde, H., Inoue, R., Oguchi, Y., 2001. Clinical application of the multifocal VEPs. *Curr. Eye Res.* 22, 54–63.
- Brenton, R.S., Phelps, C.D., 1986. The normal visual field on the Humphrey field analyzer. *Ophthalmologica* 193, 56–74.
- Brigell, M.G., 2001. The visual evoked potential. In: Fishman, G.A., Birch, D.G., Holder, G.E., Brigell, M.G. (Eds.), *Electrophysiologic Testing in Disorders of the Retina, Optic Nerve, and Visual Pathway (Ophthalmology Monographs)*, 2nd Edition. The Foundation of the American Academy of Ophthalmology, San Francisco, pp. 237–278.
- Brindley, G.S., 1972. The variability of the human striate cortex. *Proc. Physiol. Soc.* 225, 1P–3P.
- Budenz, D.L., Feuer, W.J., Anderson, D.R., 1993. The effect of simulated cataract on the glaucomatous visual field. *Ophthalmology* 100, 511–517.
- Chauhan, B.C., Henson, D.B., Hopley, A.J., 1988. Cluster analysis in visual field quantification. *Doc. Ophthalmol.* 69, 25–39.
- Chen, C.S., Hood, D.C., Zhang, X., Karam, E.Z., Liebmann, J.M., Thienprasiddhi, P., Ritch, R., 2002. Repeat reliability of the multifocal visual evoked potential in normal and glaucomatous eyes [abstract]. Annual Meeting Abstract and Program Planner [on CD-ROM]. Association for Research in Vision and Ophthalmology. Abstract 2135.
- Di Russo, F., Martinez, A., Sereno, M.I., Pitzalis, S., Hillyard, S.A., 2002. Cortical sources of the early components of the visual evoked potential. *Hum. Brain Mapp.* 15, 95–111.

- Edgar, D.F., Crabb, D.P., Rudnicka, A.R., Lawrenson, J.G., Guttridge, N.M., O'Brien, C.J., 1999. Effects of diprivenin and pilocarpine on pupil diameter, automated perimetry and log mar acuity. *Graefes Arch. Clin. Exp. Ophthalmol.* 237, 117–124.
- Fortune, B., Hood, D.C., 2003. Conventional pattern-reversal VEPs are not equivalent to summed multifocal VEPs. *Invest. Ophthalmol. Vis. Sci.*, in press.
- Fortune, B., Goh, K., Demirel, S., Novitsky, K., Mansberger, S.L., Johnson, C.A., Cioffi, G.A., 2003. Detection of glaucomatous visual field loss using multifocal VEP. In: Wall, M., Mills, R.P. (Eds.), *Perimetry Update 2003*, in press.
- Fujimoto, N., 1990. Variation of sensitivity in the central visual field by the range of measurement. *Nippon Ganka Gakkai Zasshi-Acta Soc. Ophthalm. Japonicae.* 94, 404–407.
- Gallagher, A.E., Chen, C.S., Hood, D.C., 2002. A comparison of multifocal visual evoked potentials (mfVEP) recorded with different electrode positions [abstract]. Annual Meeting Abstract and Program Planner [on CD-ROM]. Association for Research in Vision and Ophthalmology. Abstract 2172.
- Garway-Heath, D.F., Holder G., E., Fitzke F., W., Hitchings, R.A., 2002. Relationship between electrophysiological, psychophysical, and anatomical measurements in glaucoma. *Invest. Ophthalmol. Vis. Sci.* 43, 2213–2220.
- Goldberg, I., Graham, S.L., Klistorner, A.I., 2002. Multifocal objective perimetry in the detection of glaucomatous field loss. *Am. J. Ophthalmol.* 133, 29–39.
- Graham, S.L., Klistorner, A.I., Grigg, J.R., Billson, F.A., 2000. Objective VEP perimetry in glaucoma: asymmetry analysis to identify early deficits. *J. Glau.* 9, 10–19.
- Greenstein, V.C., Zhang, X., Hood, D.C., Miele, D., Liebman, J.M., Ritch, R., 2000. The multifocal VEP technique and detection of early damage to the ganglion cell/optic nerve. *Invest. Ophthalmol. Vis. Sci.* 41, S821 (Abstract No. 2775).
- Harding, G.F., Odom, J.V., Spileers, W., Spekreijse, H., 1996. Standard for visual evoked potentials 1995. The international society for clinical electrophysiology of vision. *Vis. Res.* 36, 3567–3572.
- Harwerth, R.S., Carter-Dawson, L., Shen, F., Smith 3rd, E.L., Crawford, M.L., 1999. Ganglion cell losses underlying visual field defects from experimental glaucoma. *Invest. Ophthalmol. Vis. Sci.* 40, 2242–2250.
- Harwerth, R.S., Crawford, M.L., Frishman, L.J., Viswanathan, S., Smith rd, E.L., Carter-Dawson, L., 2002. Visual field defects and neural losses from experimental glaucoma. *Prog. Retin. Eye Res.* 21, 91–125.
- Hasegawa, S., Abe, H., 2001. Mapping of glaucomatous visual field defects by multifocal veps. *Invest. Ophthalmol. Vis. Sci.* 42, 3341–3348.
- Heijl, A., Lindgren, G., Olsson, J., 1987. Normal variability of static perimetric threshold values across the central visual field. *Arch. Ophthalmol.* 105, 1544–1549.
- Holder, G.E., 2001. Pattern electroretinography (PERG) and an integrated approach to visual pathway diagnosis. *Prog Retin. Eye Res.* 20, 531–561.
- Hong, J.E., Gallagher, A.E., Zhang, X., Shady, S., Hood, D.C., 2001. The multifocal vep: lessons from the blind spot. *Invest. Ophthalmol. Vis. Sci.* 42, S828 Abstract 4443.
- Hood, D.C., 2000. Assessing retinal function with the multifocal ERG technique. *Prog. Retin. Eye Res.* 19, 607–646.
- Hood, D.C., Zhang, X., 2000. Multifocal ERG and VEP responses and visual fields: comparing disease-related changes. *Doc. Ophthalmol.* 100, 115–137.
- Hood, D.C., Odel, J.G., Zhang, X., 2000a. Tracking the recovery of local optic nerve function after optic neuritis: a multifocal VEP study. *Invest. Ophthalmol. Vis. Sci.* 41, 4032–4038.
- Hood, D.C., Zhang, X., Greenstein, V.C., Kangovi, S., Odel, J.G., Liebmann, J.M., Ritch, R., 2000b. An interocular comparison of the multifocal VEP: a possible technique for detecting local damage to the optic nerve. *Invest. Ophthalmol. Vis. Sci.* 41, 1580–1587.
- Hood, D.C., Zhang, X., Hong, J.E., Chen, C.S., 2002a. Quantifying the benefits of additional channels of multifocal VEP recording. *Doc. Ophthalmol.* 104, 303–320.
- Hood, D.C., Greenstein, V.C., Odel, J.G., Zhang, X., Ritch, R., Liebmann, J.M., Hong, J.E., Chen, C.S., Thienprasiddhi, P., 2002b. Visual field defects and multifocal visual evoked potentials: evidence for a linear relationship. *Arch. Ophthalmol.* 120, 1672–1681.
- Hood, D.C., Odel, J.G., Winn, B.J., 2003a. The mfVEP: applications and limitations in neuro-ophthalmology. *J. Neuro-Ophthalmol.*, in press.
- Hood, D.C., Odel, J.G., Chen, C.S., Winn, B.J., 2003b. The mfERG: applications and limitations in neuro-ophthalmology. *J. Neuro-Ophthalmol.*, accepted for publication.
- Hood, D.C., Zhang, X., Winn, B.J., 2003c. Detecting glaucomatous damage with the mfVEP: how can a monocular test work? *J. Glau.*, in press.
- Horton, J.C., Hoyt, W.F., 1991. Quadrantic visual field defects. A hallmark of lesions in extrastriate (V2/V3) cortex. *Brain* 114 (Part 4), 1703–1718.
- James, A.C., 2003. The pattern-pulse multifocal visual evoked potential. *Invest. Ophthalmol. Vis. Sci.* in press.
- Johnson, C.A., Spry, P.G.D., 1999. Normal age-related sensitivity loss for perimetry tests that evaluate a variety of different visual functions [ARVO abstract]. *Invest. Ophthalmol. Vis. Sci.* 40, S67. Abstract 357.
- Kardon, R.H., Givre, S.J., Wall, M., Hood, D., 2001. Comparison of threshold and multifocal-VEP perimetry in recovered optic neuritis. In: Wall, M., Mills, R.P. (Eds.), *Perimetry Update 2000/2001: Proceedings of the XVIIth International Perimetric Society Meeting, September 6–9, 2000*. Kugler Publications, New York, NY, pp. 19–28.
- Katz, J., Sommer, A., Gaasterland, D.E., Anderson, D.R., 1991. Comparison of analytic algorithms for detecting glaucomatous visual field loss. *Arch. Ophthalmol.* 109, 1684–1689.
- Kerrigan-Baumrind, L.A., Quigley, H.A., Pease, M.E., Kerrigan, D.F., Mitchell, R.S., 2000. Number of ganglion cells in glaucoma eyes compared with threshold visual field tests in the same persons. *Invest. Ophthalmol. Vis. Sci.* 41, 741–748.
- Klistorner, A.I., Graham, S.L., 1999. Multifocal pattern VEP perimetry: analysis of sectoral waveforms. *Doc. Ophthalmol.* 98, 183–196.
- Klistorner, A.I., Graham, S.L., 2000. Objective perimetry in glaucoma. *Ophthalmology* 107, 2283–2299.
- Klistorner, A.I., Graham, S.L., 2001. Electroencephalogram-based scaling of multifocal visual evoked potentials: effect on intersubject amplitude variability. *Invest. Ophthalmol. Vis. Sci.* 42, 2145–2152.
- Klistorner, A.I., Graham, S.L., Grigg, J.R., Billson, F.A., 1998. Multifocal topographic visual evoked potential: improving objective detection of local visual field defects. *Invest. Ophthalmol. Vis. Sci.* 39, 937–950.
- Klistorner, A.I., Balachandran, C., Graham, S.L., Billson F., 2002. Multifocal VEP latency in glaucoma [abstract]. Annual Meeting Abstract and Program Planner [on CD-ROM]. Association for Research in Vision and Ophthalmology. Abstract 2165.
- Kook, M.S., Sung, K., Kim, S., Park, R., Kang, W., 2001. Study of retinal nerve fibre layer thickness in eyes with high tension glaucoma and hemifield defect. *Br. J. Ophthalmol.* 85, 1167–1170.
- Kutzko, K.E., Brito, C.F., Wall, M., 2000. Effect of instructions on conventional automated perimetry. *Invest. Ophthalmol. Vis. Sci.* 41, 2006–2013.
- Menz, M.D., Poloschek, C.M., Menz, M.K., Wang, M., Penrose, P., Sutter, E.E., 2002. The effect of fixation error on the multifocal VEP. Annual Meeting Abstract and Program Planner [on CD-ROM].

- Association for Research in Vision and Ophthalmology. Abstract 4740.
- Miele, D.L., Odel, J.G., Behrens, M., Zhang, X., Hood, D.C., 2000. Functional bitemporal quadrantopia and the multifocal visual evoked potential. *J. Neuro-Ophthalmol.* 20, 159–162.
- Quigley, H.A., 1999. Neuronal death in glaucoma. *Prog. Retin. Eye Res.* 18, 39–57.
- Quigley, H.A., Addicks, E.M., Green, W.R., 1982. Optic nerve damage in human glaucoma. III. Quantitative correlation of nerve fiber loss and visual field defect in glaucoma, ischemic neuropathy, papilledema, and toxic neuropathy. *Arch. Ophthalmol.* 100, 135–146.
- Quigley, H.A., Dunkelberger, G.R., Green, W.R., 1989. Retinal ganglion cell atrophy correlated with automated perimetry in human eyes with glaucoma. *Am. J. Ophthalmol.* 107, 453–464.
- Rademacher, J., Caviness Jr., V.S., Steinmetz, H., Galaburda, A.M., 1993. Topographical variation of the human primary cortices: implications for neuroimaging, brain mapping, and neurobiology. *Cereb. Cortex.* 3, 313–329.
- Regan, D., 1989. *Human Brain Electrophysiology: Evoked Potentials and Evoked Magnetic Fields in Science and Medicine.* Elsevier, New York, NY.
- Reyes, R.D., Tomita, G., Kitazawa, Y., 1998. Retinal nerve fiber layer thickness within the area of apparently normal visual field in normal-tension glaucoma with hemifield defect. *J. Glau.* 7, 329–335.
- Slotnick, S.D., Klein, S.A., Carney, T., Sutter, E., Dastmalchi, S., 1999. Using multi-stimulus VEP source localization to obtain a retinotopic map of human primary visual cortex. *Clin. Neurophysiol.* 110, 1793–1800.
- Sokol, S., 1976. Visually evoked potentials: theory, techniques and clinical applications. *Surv. Ophthalmol.* 21, 18–44.
- Steinmetz, H., Furst, G., Meyer, B.U., 1989. Craniocerebral topography within the international 10–20 system. *Electroencephal. Clin. Neurophysiol.* 72, 499–506.
- Sutter, E.E., 1991. The fast m-transform: a fast computation of cross-correlations with binary m-sequences. *Soc. Ind. Appl. Math.* 20, 686–694.
- Sutter, E.E., 2001. Imaging visual function with the multifocal m-sequence technique. *Vis. Res.* 41, 1241–1255.
- Sutter, E.E., Bearnse, M.A., 1999. The optic nerve head component of the human ERG. *Vis. Res.* 39, 419–436.
- Swanson, W.H., Dul, M.W., Pan, F., 2002. Relating ganglion cell loss to perimetric defects: a neural model. *Invest. Ophthalm. Vis. Sci.* ARVO. Abstract 2123.
- Thienprasiddhi, P., Greenstein, V.C., Chen, C., Karam, E.Z., Liebmann, J.M., Ritch, R., Hood, D. C., 2002. Multifocal VEP responses in glaucoma patients with unilateral hemifield defects, under review.
- Towle, V.L., Moskowitz, A., Sokol, S., Schwartz B., 1983. The visual evoked potential in glaucoma and ocular hypertension: effects of check size, field size, and stimulation rate. *Invest. Ophthalmol. Vis. Sci.* 24, 175–183.
- Weber, A.J., 2002. Intracellular analysis of parasol cells in normal and glaucomatous eyes. Annual Meeting Abstract and Program Planner [on CD-ROM]. Association for Research in Vision and Ophthalmology. Abstract 2165.
- Weinreb, R.N., Perlman, J.P., 1986. The effect of refractive correction on automated perimetric thresholds. *Am. J. Ophthalmol.* 101, 706–709.
- Wild, J.M., Pacey, I.E., Hancock, S.A., Cunliffe, I.A., 1999. Between-algorithm, between-individual differences in normal perimetric sensitivity: full threshold, FASTPAC, and SITA. Swedish Interactive Threshold Algorithm. *Invest. Ophthalm. Vis. Sci.* 40, 1152–1161.
- Wood, J.M., Wild, J.M., Smerdon, D.L., Crews, S.J., 1989. Alterations in the shape of the automated perimetric profile arising from cataract. *Graefes Arch. Clin. Exp. Ophthalmol.* 227, 157–161.
- Wu, L.L., Suzuki, Y., Kunimatsu, S., Araie, M., Iwase, A., Tomita, G., 2001. Frequency doubling technology and confocal scanning ophthalmoscopic optic disc analysis in open-angle glaucoma with hemifield defects. *J. Glau.* 10, 256–260.
- Zhang, X., Hood, D.C., Greenstein, V.C., Odel, J.G., Kangovi, S., Liebmann, J. M., 1999. Detecting field defects with multifocal VEPs: two eyes are better than one [ARVO abstract]. *Invest. Ophthalm. Vis. Sci.* 40, S81. Abstract 430.
- Zhang, X., Hood, D.C., Chen, C.S., Hong, J.E., 2002. A signal-to-noise analysis of multifocal VEP responses: an objective definition for poor records. *Doc. Ophthalmol.* 104, 287–302.